



VIETNAM INSTITUTE OF METEOROLOGY HYDROLOGY AND CLIMATE CHANGE

ISSN 2525-2496

JOURNAL OF CLIMATE CHANGE SCIENCE

No. 9 - 2019



JOURNAL OF CLIMATE CHANGE SCIENCE

EDITOR-IN-CHIEF
Nguyen Van Thang

DEPUTY EDITOR-IN-CHIEF
Huynh Thi Lan Huong

EDITORIAL BOARD
HEAD OF EDITORIAL BOARD: Tran Thuc
MEMBERS:

Duong Hong Son
 Mai Van Khiem
 Nguyen Ky Phung
 Doan Ha Phong
 Hoang Minh Tuyen
 Truong Duc Tri
 Do Tien Anh
 Le Ngoc Cau
 Do Dinh Chien
 Bach Quang Dung
 Nguyen Xuan Hien
 Vu Van Thang

MANAGING EDITOR
 Tran Thanh Thuy
HEAD OF ADMINISTRATION
 Tran Thanh Thuy

PUBLICATION LICENCE
 No. 604/GP-BTTTT
 30th December 2016
 Ministry of Information and
 Communications

JOURNAL OFFICE
 23/62 Nguyen Chi Thanh Str.,
 Dong Da Dist., Hanoi
 Tel: +84.2437731410
 Email: tapchibdkh@imh.ac.vn
 Website: http://imh.ac.vn

PRINTED IN
 Le Giang jsc
 87/192 Le Trong Tan Str,
 Hoang Mai Dist, Ha Noi

SPECIAL VOLUME TO CELEBRATE NATIONAL SCIENCE AND TECHNOLOGY DAY

CONTENTS

No. 9 - 2019

- 1 **Huynh Thi Lan Huong, Koos Nee es, Nguyen Xuan Hien, Tran Van Tra, Dang Linh Chi, Duong Hong Nhung:** A generic framework for assessing urban flooding under climate change in Viet Nam: Synthesizing key results from Ha Tinh, Ninh Thuan, and Binh Thuan Provinces
- 11 **Le Ngoc Cau, Pham Thi Quynh, Makoto Kato:** Low carbon technology assessment for climate change mitigation in Viet Nam
- 22 **Mai Van Khiem, Tran Dinh Trong, Le Van Tuan, Do Thanh Tung, Vu Van Thang:** Assessments of vulnerability due to climate change in Ha Tinh City
- 30 **Winai Chaowiwa, Kanoksri Sarinnapakorn, Sutat Weesakul:** Future changes in extreme rainfall over Thailand using multi-bias corrected gcm rainfall data
- 54 **Mai Van Khiem, Le Anh Ngoc, Vo Thi Nguyen, Huynh Thi My Linh:** Impact assessment of climate change on industry and trade in Binh Thuan Province
- 62 **Dang Thi Ha:** Impact of ENSO on water discharge and sediment load in lower Mekong River
- 68 **Mai Van Khiem, Tran Tuan Hoang, Phan Thi Diem Quy, Huynh Thi My Linh, Ho Cong Toan, Pham Thanh Long, Nguyen Thi Thu Hang:** Flooding impacts on rice cultivation area under climate change in Tra Vinh Province
- 77 **Doan Thi Noi, Dang Quang Thinh:** Calculation of designed flood in weak data region in Viet Nam using Win-TR55 model
- 84 **Le Ngoc Anh, Nguyen Tin Van, Pham An Duc, Vo Thi Nguyen, Bao Thanh:** Greenhouse gas emissions in agriculture, buildings and waste sectors in Ho Chi Minh City
- 90 **Nguyen Thi Thanh, Nguyen Xuan Hien, Hoang Duc Cuong:** Impact of satellite observed SST on intensity and track simulation of tropical cyclone over Viet Nam east sea: A case study of typhoon Nalgae (2011)
- 99 **Nguyen Ngoc Anh, Nguyen Huu Quyen, Tran Thi Tam, Duong Hai Yen, Duong Van Kham:** Zoning agro-climatic factors and evaluating adaptation ability of arabica coffee in Muong Ang district, Dien Bien Province

A GENERIC FRAMEWORK FOR ASSESSING URBAN FLOODING UNDER CLIMATE CHANGE IN VIET NAM: SYNTHESIZING KEY RESULTS FROM HA TINH, NINH THUAN AND BINH THUAN PROVINCES

Huynh Thi Lan Huong⁽¹⁾, Koos Neefjes⁽²⁾, Nguyen Xuan Hien⁽¹⁾, Tran Van Tra⁽¹⁾,
Dang Linh Chi⁽¹⁾, Duong Hong Nhung⁽¹⁾

⁽¹⁾Viet Nam Institute of Meteorology, Hydrology, and Climate Change

⁽²⁾Climate Sense

Received: 31 January 2019; Accepted: 15 February 2019

Abstract: Viet Nam is among the nations most severely affected by climate change. In a recent effort to respond to the adverse effects of climate change on urban flooding, the Technical Support Unit (TSU), ENABLE-Belgian Development Agency, the Viet Nam Institute of Meteorology, Hydrology and Climate Change, and other institutes have studied the impacts of climate change on urban flooding in the provinces of Ha Tinh, Ninh Thuan, and Binh Thuan. Through different studies, climate change impacts on urban flooding have been determined. These three studies provide a generic framework to determine climate change impacts on urban flooding. Firstly downscaling of climate change scenarios is used to determine climate variables within each region. Hydrological and hydraulics models are then utilized to drive the simulation of the rainfall-runoff process as well as the response of water level during flood events. Based on the modelling, structural and non-structural measures are proposed to reduce the impacts of flooding. In an additional effort, flood warning systems would also be installed to provide timely warning to the authorities as well as the people. The generic framework has been agreed through consultation workshops as well as training workshops from August 2018 to March 2019.

Keywords: Climate change, flooding, urban planning, downscaling, modelling.

1. Introduction

Climate change is considered as an unprecedented global environmental challenge [7]. The impacts of climate change is felt in the changes in climate variables such as temperature, precipitation, humidity, etc. Climate change also leads to changes in climate extreme events such as heavy rain and flooding [1]. This is important because flooding is a dangerous hazard.

Flooding in the context of climate change is especially dangerous and damaging in urban areas. Urban drainage system have been constructed with conveyance capacities for extreme rainfall events at a desired frequency to prevent urban flooding. However, the design

of urban drainage systems is often based on historical precipitation statistics and return periods, without considering the potential changes in precipitation due to climate change [11]. Climate change leads to increased risks of urban flooding due to the increase of heavy rain and river floods as well as the limited capacity of urban drainage systems.

The study of climate change, extreme precipitation, and its relation to urban flooding have been well explored both in the past and more recently. Ashley et al. (2005) showed that flooding risks in four UK catchments could increase by up to 30 times in 2080 as compared to the year 2000, and effective adaptation measures are required to cope with the increased risk. Zhou et al. (2018) studied the impacts of climate change on

Corresponding author: Tran Van Tra
E-mail: tvtra@monre.gov.vn

urban flood volumes in northern China with an in-depth assessment of the effects of both climate change mitigation and adaptation on urban flooding. Miller and Hutchins (2017) studied the impacts of climate change on urban fluvial flooding for the United Kingdom and concluded that there is medium-high confidence showing increased risks of flooding. Kang et al. (2016) assessed the impacts of climate change and predicted the scale of potential future flood damage for the urban area of Gyeong-gu, Incheon, Korea. Kaspersen and Halsnæs (2017) described an integrated framework and tool, the Danish Integrated Assessment System (DIAS) to address urban flooding during extreme precipitation as a consequence of climate change.

One important feature in assessing and determining flooding due to climate change is the ability to properly translate the changes in climate variables into urban flooding levels. This includes the downscaling of climate change scenarios, hydrological modelling to determine river flow as a result of increased rainfall, and hydraulics modelling to determine water drainage by urban drainage systems. A search in the literature provided a wide range of approaches.

This paper provides a generic framework of downscaling climate change scenarios, applying hydrological and hydraulics model to determine the level of urban flooding at the local level. The work has been applied successfully at 3 locations in Viet Nam namely urban areas in Ha Tinh, Ninh Thuan, and Binh Thuan provinces as part of the "Integrated Water Resources Management and Urban Development in Relation to Climate Change in Binh Thuan, Ninh Thuan and Ha Tinh" project funded by Enabel, the Belgian Development Agency. As part of the project, consultation workshop and training workshop on the methodology were also carried out with positive results.

2. Climate Change Scenario Development

In the Fifth Assessment Report (AR5), IPCC adopted the Benchmark Emissions Scenarios

approach and Representative Concentration Pathways (RCPs) of greenhouse gas (GHG) in the atmosphere. The RCPs emphasise the concentration of gasses instead of emission processes. In other words, the RCP assume the target level of GHG concentrations, providing a range of options for socio-economic development that would lead to that concentration. To simulate the effects of these emissions levels or scenarios, Global Circulation Models (GCMs) are used. These models simulates physical, chemical, biological processes that occur in the atmosphere through approximations. GCMs have relatively coarse spatial resolution (200-300km² per grid). Therefore, in order to utilize the results from GCMs, downscaling is required. The process of downscaling should adhere to that procedure used by the Viet Nam Institute of Meteorology, Hydrology, and Climate Change in producing the official Climate Change and Sea Level Rise Scenario for Viet Nam (Figure 1).

The changes in climate variables is compared with the baseline period of 1986-2005. The change in temperature is thus expressed as:

$$\Delta T_{future} = T_{future}^* - \overline{T}_{1986-2005}^* \quad (1)$$

While the change in precipitation is expressed as:

$$\Delta R_{future} = \frac{(R_{future}^* - \overline{R}_{1986-2005}^*)}{\overline{R}_{1986-2005}^*} * 100 \quad (2)$$

Of which: ΔT_{future} = Changes of future temperature compared to the baseline period (°C), T_{future}^* = Temperature in the future (°C), $\overline{T}_{1986-2005}^*$ = Average temperature of the baseline period (1986-2005) (°C), ΔR_{future} = Changes of future rainfall as compared to the baseline period (%), R_{future}^* = Future rainfall (mm), $\overline{R}_{1986-2005}^*$ = Average rainfall of the baseline period (1986-2005) (mm).

The advantage of a dynamic model is the ability to simulate physical and chemical processes in the atmosphere, thus, the results are highly logical. However, the disadvantage of the model includes the limitation of simulating local climate since there

is limited information from the input. In addition, each model has systematic errors. Therefore, the result of the model needs to be calibrated based on observed data to reflect local conditions and reduce errors.

Quantile mapping is used to adjust

daily rainfall values based on historical data. For each percentile of the result time series, a separate transfer function is developed to eliminate the errors in the model so that calculated results closely match observed data in this percentile.

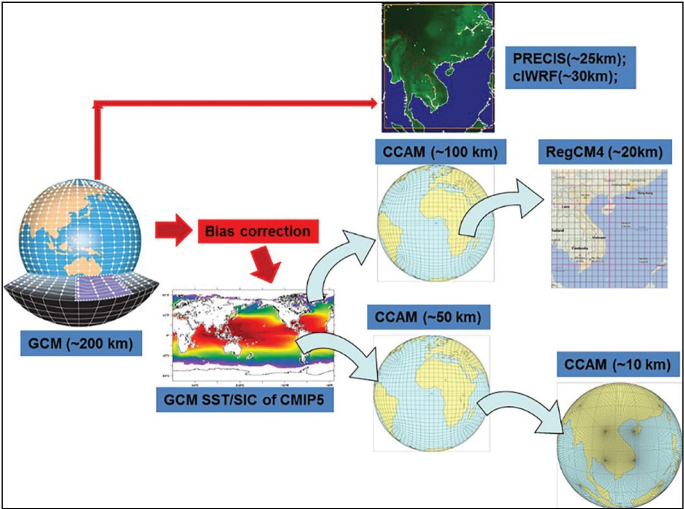


Figure 1. Dynamical downscaling procedure
(source: Viet Nam Institute of Meteorology, Hydrology and Climate Change)

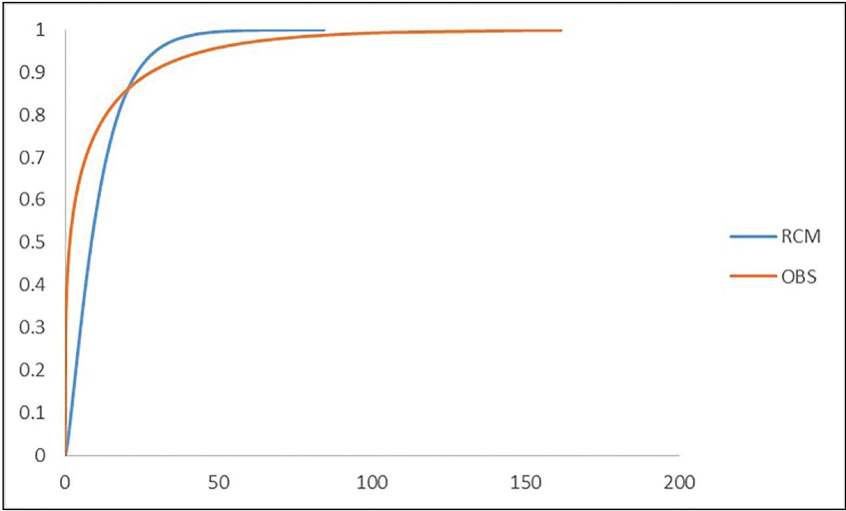


Figure 2. Rainfall cumulative distribution (red: observed, blue: simulated)

Figure 2 (x axis is the rainfall [mm]) illustrates the Cumulative Distribution Function (CDF) of the simulated and observed datasets. It is indicated that the number of wet days with daily rainfall is much higher than in reality, however, the amount of rainfall in these days is not significant. This method is applied to match CDF of a simulated dataset to CDF of the observed data in order to solve the mentioned

error following 2 main steps below:

- Wet day frequency correction;
- Matching CDF of simulated dataset to CDF of the observed one.

This method can be described in more detail, as follows:

- It is assumed that theoretical gamma distribution can be fitted into observed and simulated daily rainfall datasets. Thus, the

correction can be implemented based on gamma theory. The Probability Density Function (PDF) of gamma can be expressed by the following equation:

$$PDF: f(x) = \frac{1}{\beta^\alpha \Gamma(\alpha)} x^{\alpha-1} e^{-x/\beta} \quad (3)$$

The CDF can be found using the following equation:

$$CDF: F(x) = \int_0^x f(t) dt \quad (4)$$

Where α and β are shape and scale parameters, respectively. These parameters can be computed using Equation (5) with the mean and standard deviation determined from the data series:

$$\alpha = \left(\frac{\bar{x}}{\sigma} \right)^2; \beta = \frac{\sigma^2}{\bar{x}} \quad (5)$$

- Both two datasets are divided into 2 parts:

i) the first part consists of values, which are less than the 99th percentile of the corresponding dataset; and ii) the second part is the rest of this dataset, which are equal or greater than 99th percentile.

- To do frequency correction (the number of rainy day) for the simulated dataset, a threshold must be defined to truncate several values. Firstly, non-exceedance probability of 0.1 mm rainfall is calculated in the simulated dataset. Secondly, the threshold is obtained by taking the inverse of this probability using the shape and scale parameter of the observed dataset. Every model value, which is less than this threshold, should be truncated.

Threshold

$$= F_{\alpha, \beta-gcm}^{-1}(F_{\alpha, \beta-Obs}(0.1 \text{ mm})) \quad (6)$$

- Shape and scale parameters of truncated simulated dataset are computed again.

- The non-exceedance probability of all values in simulated dataset is calculated using new shape and scale parameters from previous step. And then, adjusted model values are derived from getting the inverse of corresponding probability using shape and scale parameters of observed dataset. This step is conducted discretely for two parts of dataset.

$$x_{base}^* = F_{obs}^{-1} \left[F_{base} \left(x_{RCM_{base}} \right) \right] \quad (7)$$

For other periods in the future, the same procedure is applied but the rain correction values are obtained by multiple rain correction values with scale factor. The scaling factor is expressed in:

$$x_{fut}^* = x_{fut} * \frac{F_{obs}^{-1} \left[F_{fut}(x_{fut}) \right]}{F_{base}^{-1} \left[F_{fut}(x_{fut}) \right]} \quad (8)$$

Calibration of temperature result is based on percentile (daily average, maximum, minimum temperatures)

+ Develop a cumulative distribution function for the observed temperature series as well as simulated temperature for the baseline and future periods

+ At each percentile, adjust the calculated temperature from the model based on observed temperature. The transfer function is defined as:

$$P_i = O_i + g\bar{\Delta} + f\bar{\Delta}_i \quad (9)$$

Of which: $i = i^{th}$ percentile from the observed and simulated temperature, O = observed temperature, P = temperature in the model after calibration, g is set to 1, $\bar{\Delta} = \bar{S}_f - \bar{S}_c$ with \bar{S}_f and \bar{S}_c correspond to uncalibrated average temperature for future and baseline period, $\bar{\Delta}_i = S_{fi} - S_{ci} - \bar{\Delta}$ with S_{fi} and S_{ci} being uncalibrated temperature for future and baseline period in the i th percentile respectively.

$$f = \frac{\sigma_0}{\sigma_{S_c}} \quad (10)$$

Of which: σ_{S_c} and σ_0 are the standard deviation of the observed and simulated temperature in the baseline period respectively.

3. Sea Level Rise Scenario Development

In terms of the sea level rise scenarios, the calculation procedure and component should adhere to that of the Viet Nam Climate Change and Sea Level Rise Scenario (Table 1). Total sea level rise, thus, is the sum of all contributing factors, including: (i) thermal

expansion, (ii) Glaciers SMB, (iii) Greenland SMB, (iv) Greenland dynamic, (v) Antarctica SMB, (vi) Antarctica dynamics, (vii) Land water, and (viii) Isometric.

Table 1. Sea level rise scenario components

No.	Contributor	Method	Data
1	Thermal expansion and dynamics	Determined from sea level rise component due to global average temperature expansion (zostoga) and sea level rise due to dynamics (zos) from AOGCM. These components are calibrated prior linear interpolation for Viet Nam’s sea region using IPCC’s method.	AOGCM models
2	Glacier SMB	Interpolated for Viet Nam’s sea region using the method prescribed in Slangen (2014) from average global data	From "glaciers" component in IPCC’s database
3	Greenland SMB	Interpolated for Viet Nam’s sea region using the method prescribed in Slangen (2014) from average global data	From "greensmb" component in IPCC’s database.
4	Antarctica SMB	Interpolated for Viet Nam’s sea region using the method prescribed in Slangen (2014) from average global data	From "antsmb" component from IPCC’s databse.
5	Greenland dynamics	Interpolated for Viet Nam’s sea region using the method prescribed in Slangen (2014) from average global data	From "greendyn" component in IPCC’s database.
6	Antarctica dynamics	Interpolated for Viet Nam’s sea region using the method prescribed in Slangen (2014) from average global data.	From "antdyn" component in IPCC’s database.
7	Land water	Interpolated for Viet Nam’s sea region using the method prescribed in Slangen (2014) from average global data	From "landwater" in IPCC’s database.
8	Isometric	Output from ICE5G model, inlcuding surface change rate geoid, vertical movement rate.	From ICE5G [8].

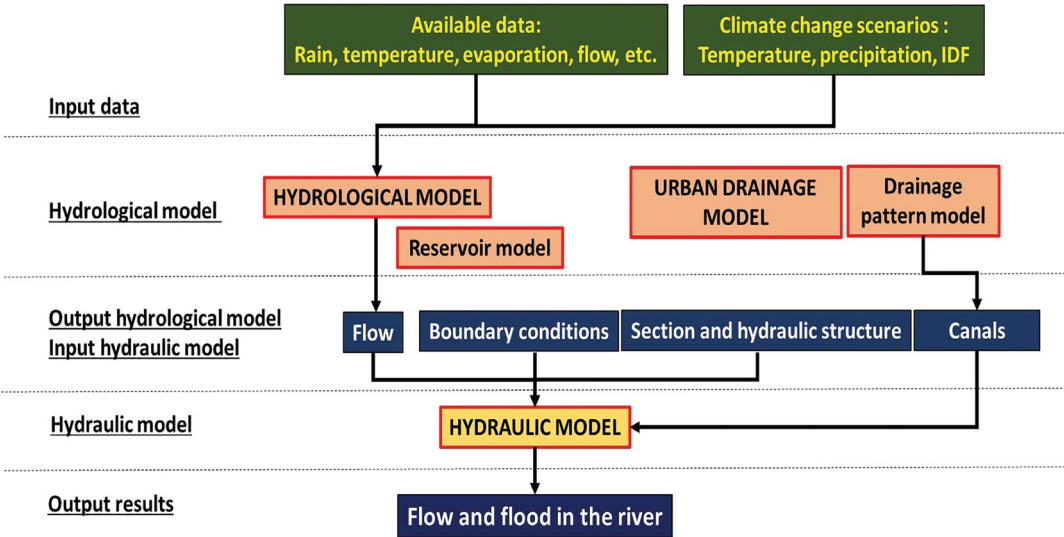


Figure 3. Overall methodology to determine the impacts of climate change on urban flooding

4. Modelling Approach

The overall modelling approach to determining climate change impacts on urban flooding is shown in Figure 3. The assessment should start with meteorological and hydrological input data, and climate change data (changes in temperature, precipitation). The input is fed into hydrological model including reservoirs as well as an urban drainage model. The output from the hydrological simulation is then the input into a hydraulic model. The output from the hydraulic model is the flow and flood in the river.

Input data for hydrological and hydraulics model include: elevation data; hydrological and meteorological data; water level; flow; and climate change scenarios. Climate change data will be used to calculate future climate change scenarios. The factors used to model input data for climate change scenarios are: rainfall and sea level rise. Rainfall of stations considering climate change according to periods is calculated according to the increase corresponding to the current status. Specific calculations are as follows:

$$R(CL) = R(BL) \times (P/100+1) \quad (11)$$

Of which:

R (CL): Rainfall with consideration of climate change relevant to frequency at time of the case

R (BL): Current rainfall correlates with the frequency at the time at present

P: Increase percentage (or decrease) of maximum daily rainfall at the time of the case

Sea level rise considering the climate change is calculated as follows:

$$H(CL) = H(BL) + A/100 \quad (6)$$

Of which:

H (CL): Water level considers climate change relevant to the frequency at time of the case

H (BL): Current water level corresponds to the frequency at the time at present

A: Value of water level at time of the case (cm)

5. Applying the generic approach for Ha Tinh, Ninh Thuan, and Binh Thuan Provinces

Future climate change and sea level rise scenarios for Ha Tinh, Ninh Thuan, and Binh

Thuan Provinces were developed using the Viet Nam Climate Change and Sea Level Rise Scenarios. This models for the RCP4.5 and RCP8.5 scenarios. 4 Regional Climate models (RCMs) were used: i) Conformal Cubic Atmospheric Model (CCAM); ii) Providing Regional Climates for Impacts Studies (PRECIS); iii) Regional Climate Model (RegCM); and iv) climate Weather Research and Forecast model (clWRF).

Sea level rise (SLR) scenarios for the coastal area were constructed on the basis of: i) guidance from AR5; ii) the findings on SLR scenariodevelopment[2,10];andiii)SLRscenarios developed for countries such as Australia, the Netherlands and Singapore. SLR scenarios for the coastal area of Binh Thuan are calculated from the components contributing to sea level in the region. They consist of 8 principal components, i.e. thermal expansion, glaciers, Greenland ice sheet, Greenland ice sheet dynamics, Antarctic ice sheet, Antarctic ice sheet dynamics, land water storage and glacial isostatic adjustment. Among those components, the thermal expansion is calculated directly from 21 AOGCMSs following AR5. The components of sea level change due to melting ice and water storage in continentare computed by a transfer function related to global projection which is based on contribution of each element to different regions [10]. Sea level change due to vertical fluctuations in the Earth's crust reacting to changes in ice volume was estimated from the ICE5G model [11].

The uncertainty of the thermal expansion component is estimated from models. The uncertainty of SLR due to the balanced with the amount of ice is assumed to be governed by the intensity of climate change, while the uncertainty in the estimation of SLR due to melting ice in glaciers, mountain peaks or at the poles is mainly due to the calculation method. Each component contributing to SLR (except glacial isostatic adjustment) has a central estimated value (based on the percentiles) with the same upper and lower bounds, determined through 5th and 95th

percentiles (IPCC 2013). The central estimated value of the various components would be added together to give the value of SLR for the coastal area. The uncertainty of the trend of total SLR will be estimated according to the methodology of the IPCC [2] with the assumption that the components with a close relationship with the air temperature are also highly correlated with each other in terms of uncertainty. Squared total uncertainty of these components is estimated by getting the sum of all squared uncertainty of every component:

$$\sigma_{tot}^2 = (\sigma_{steric/dynamic}^2 + \sigma_{smb_a}^2 + \sigma_{smb_g}^2)^2 + \sigma_{glac}^2 + \sigma_{LW}^2 + \sigma_{dyn_a}^2 + \sigma_{dyn_g}^2 \quad (6)$$

In which:

σ_{tot} : is the uncertainty of total water level components;

$\sigma_{steric/dynamic}$, σ_{smb_a} , σ_{smb_g} , σ_{glac} , σ_{LW} , σ_{dyn_a} and σ_{dyn_g} are the uncertainties of components: thermal expansion, mass balance of the

Antarctic ice sheet, mass balance of Greenland ice sheet, ice in glaciers, water storage on the continent, Antarctic ice sheet dynamics and Greenland ice sheet dynamics, respectively.

5.1. Ha Tinh

For Ha Tinh city the flood peak discharge of the Rao Cai River is critical and within the system the Ke Go reservoir plays a key role in flood mitigation. The current flood risk is very high, as a 2% design flood would lead to 80% flooding of the city. This would still be 42% of the total city area the flood management plan of the province of 2015 is implemented. Therefore, additional measures are recommended that would reduce flooding to 14.2%. These measures would also deal with the flood risks in the middle of the century, but in the longer term more flood prevention measures are needed.

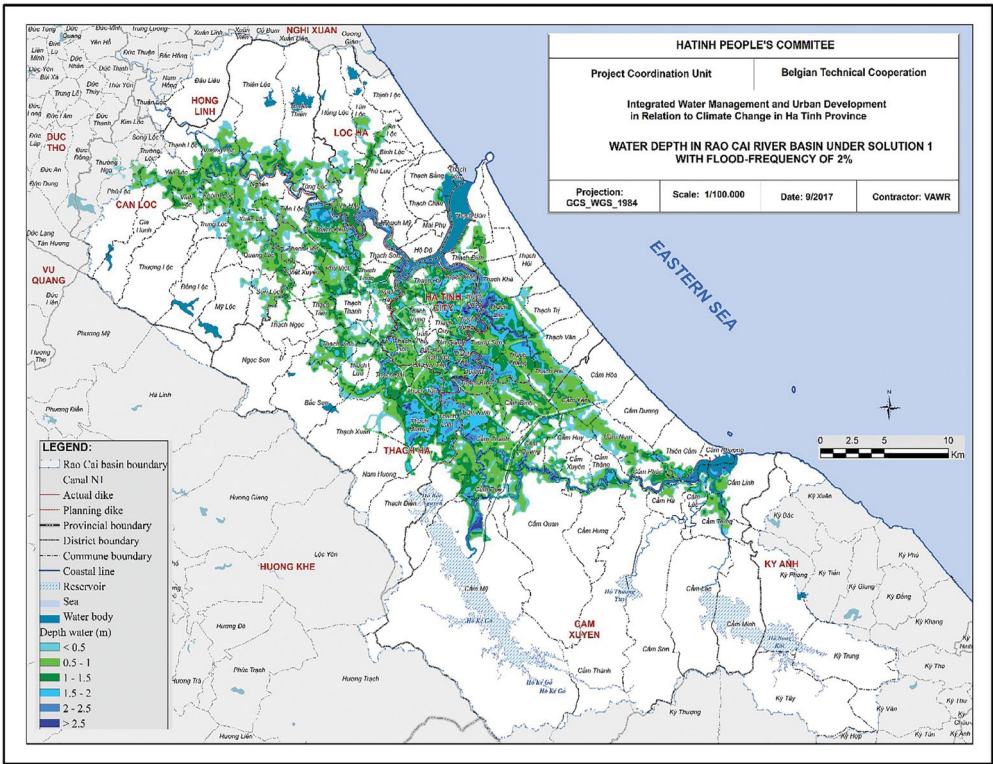


Figure 4. Flood map in Rao Cai river basin corresponding to design flood, in current situation

5.2. Binh Thuan

The current flood risks in the Luy river basin and drainage systems for Luong Son and Cho Lau towns in Binh Thuan province

were modelled. The reservoirs in the Luy river basin play an important role in the mitigation of flood risks downstream. Modelling the current situation for a design flood shows that even if

existing plans for e.g. upstream reservoirs are implemented, the flooded area in the river basin would increase by 2030 as a result of climate change. In the present situation, the inundated area of Luong Son and Cho Lau towns would be 13.6% and 10.4% of the surface areas of these towns respectively with a

design flood of 1%. The risks will increase in 2030 because of the urban drainage infrastructure planning to 2025 plus the effects of climate change, to 39.8% and 20.1% of the surface areas of these towns respectively. Additional measures would deal with current and 2030 flood risks.

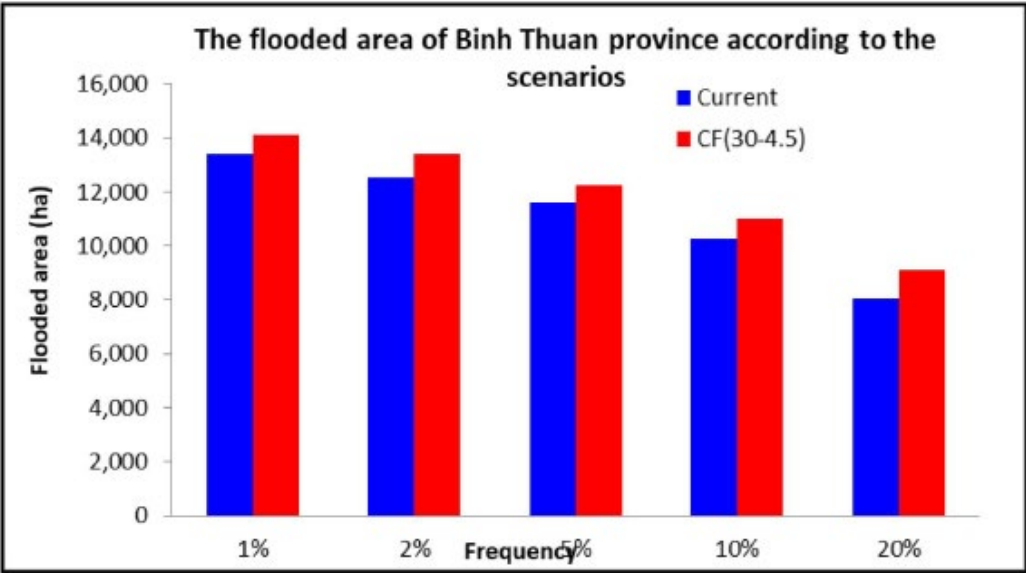


Figure 5. Comparison of flooded area in case of climate change till 2030, scenario RCP4.5 in current condition and planned topography

5.3. Ninh Thuan

The current flood risks in the Cai Phan Rang river basin in Ninh Thuan as well as the Phan Rang - Thap Cham city drainage systems province were assessed. Flooding is caused by occasional extreme rainfall. Modelling with the present topography and infrastructure shows that the Cai Phan Rang river basin inundation is 16,000 ha (1% design storm and flood), affecting especially Ninh Phuoc district. The planned measures for the period to 2025 in the river basin, Phan Rang - Thap Cham city and Ninh Phuoc district will decrease inundation in the current situation, but climate change will increase the flooded area in the river basin around 2030. Therefore, it is recommended to accelerate the construction of the Cai river reservoir, to increase flood retention capacity. The flooded areas in Phan Rang - Thap Cham city are limited in the current situation to just 1.25% of the city's land area (1% rainstorm).

If the city's residential areas and drainage system expand according to the Planning to 2025, this would be 9.7% of the city's surface area, and adding climate change would further increase the inundated area to 17.5% of the city by 2030. Flooding can be minimised by improving the city's drainage system in addition to existing plans. The ongoing northern river bank dyke upgrading will protect the city, but it could mean increasing the flood risk for Ninh Phuoc district. This district needs retention reservoirs and possibly an additional dyke along the southern river bank.

6. Conclusion

Climate change poses a significant challenge for Viet Nam. This includes the increase in severity of heavy precipitation and flooding in urban areas. The ability to accurately depict the impacts of climate change on phenomena such as urban flooding is thus important. There has been a significant amount

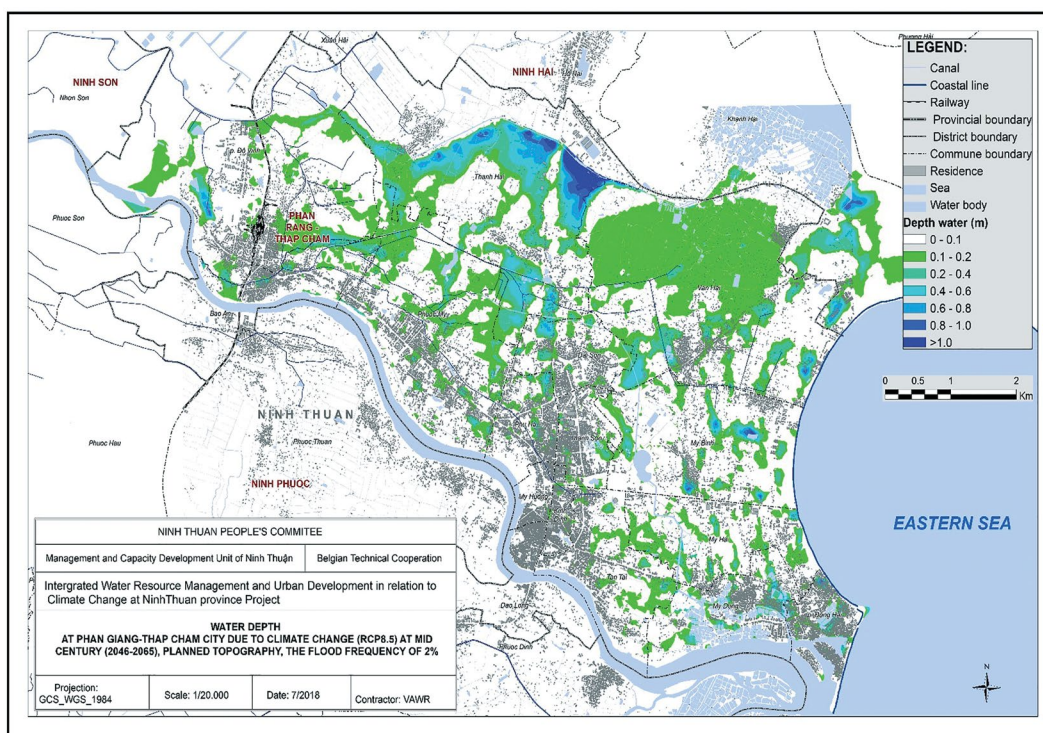


Figure 6. Flooding in Phan Rang - Thap Cham city in 2050, included Planned city expansion and drainage infrastructure, with 2% storm (once in 50 years), according to the emissions scenario RCP8.5

of effort in determining such impact, and this paper contributes to the volume of literature by providing a generic framework for urban flooding assessment within the context of climate change.

The approach described the various components and procedures that are vital in assessing the impacts of climate change on urban flooding in Viet Nam. The approach includes, firstly, to downscale climate change scenarios using GCMs to obtain changes in

climate variables. Secondly, hydrological and hydraulic models are applied to simulate future conditions using downscaled climate variables. The paper provided examples of applying the approach in the three provinces of Ha Tinh, Ninh Thuan, and Binh Thuan. Given the limited availability of space, the reader is advised to refer to IMHEN (2018) for a more detailed description of work for the three provinces of Ha Tinh, Ninh Thuan, and Binh Thuan.

Acknowledgement: The study was conducted through the funding of Enabel, the Belgian Development Agency, and the kind support from the Technical Support Unit under the Viet Nam Ministry of Planning and Investment. Without such support, the results would not have been possible.

References

1. Ashley, R.M., Balmfort, D.J., Saul, A.J., Blanskby, J.D. (2005), *Flooding in the future - Predicting climate change, risks and responses in urban areas*. *Water Sci. Technol.* 52, 265-273. <https://doi.org/10.2166/wst.2005.0142>.
2. Church, John A., Didier Monselesan, Jonathan M. Gregory, and Ben Marzeion. (2013), "Evaluating the Ability of Process Based Models to Project Sea-Level Change", *Environmental Research Letters* 8 (1): 014051. doi:10.1088/1748-9326/8/1/014051.

3. IMHEN (2018), *Synthesis Report: "Knowledge Management-Downscaling climate change scenarios, hydrological/hydraulics model, applying a 2-D model at the local level, Ha Noi.*
4. IPCC (2014), *Climate Change 2013, the Fifth Assessment Report.*
5. Kang, N., Kim, S., Kim, Y., Noh, H., Hong, S.J., Kim, H.S. (2016), *Urban drainage system improvement for climate change adaptation. Water (Switzerland) 8.* <https://doi.org/10.3390/w8070268>.
6. Kaspersen, P.S., Halsnæs, K. (2017), *Integrated climate change risk assessment: A practical application for urban flooding during extreme precipitation. Clim. Serv. 6,* 55-64. <https://doi.org/10.1016/j.cliser.2017.06.012>.
7. Makondo, C.C., Thomas, D.S.G. (2018), *Climate change adaptation: Linking indigenous knowledge with western science for effective adaptation. Environ. Sci. Policy 88,* 83-91. <https://doi.org/10.1016/j.envsci.2018.06.014>
8. Miller, J.D., Hutchins, M. (2017), *The impacts of urbanisation and climate change on urban flooding and urban water quality: A review of the evidence concerning the United Kingdom. J. Hydrol. Reg. Stud. 12,* 345-362. <https://doi.org/10.1016/j.ejrh.2017.06.006>
9. Peltier, W. R. (2004), *"GLOBAL GLACIAL ISOSTASY AND THE SURFACE OF THE ICE-AGE EARTH: The ICE-5G (VM2) Model and GRACE."* *Annual Review of Earth and Planetary Sciences* 32 (1): 111-49. doi:10.1146/annurev.earth.32.082503.144359.
10. Slangen, A. B. A., M. Carson, C. A. Katsman, R. S. W. van de Wal, A. Köhl, L. L. A. Vermeersen, and D. Stammer. (2014), *"Projecting Twenty-First Century Regional Sea-Level Changes", Climatic Change* 124 (1-2): 317-32. doi:10.1007/s10584-014-1080-9.
11. Zhou, Q., Leng, G., Huang, M. (2018), *Impacts of future climate change on urban flood volumes in Hohhot in northern China: benefits of climate change mitigation and adaptations. Hydrol. Earth Syst. Sci. 22,* 305-316. <https://doi.org/10.5194/hess-22-305-2018>.

LOW CARBON TECHNOLOGY ASSESSMENT FOR CLIMATE CHANGE MITIGATION IN VIET NAM

Le Ngoc Cau⁽¹⁾, Pham Thi Quynh⁽¹⁾, Makoto Kato⁽²⁾

⁽¹⁾Viet Nam Institute of Meteorology, Hydrology and Climate Change (IMHEN)

⁽²⁾Overseas Environmental Cooperation Center (OECC), Japan

Received: 10 January 2019; Accepted: 16 February 2019

Abstract: *This paper presents a multicriteria low carbon assessment for seven sectors identified in the Nationally Determined Contribution (NDC) of Viet Nam including energy efficiency, power generation, transport, agriculture, land use, land-use change and forestry (LULUCF), and waste, plus F-gas. Specific technologies for sectoral mitigation options identified in Viet Nam's NDC were selected and assessed. An analysis and discussion on policy and investment barriers for deploying the identified low carbon technologies for seven sectors is also presented. Key sector-specific challenges for implementation of the identified low carbon technologies for enabling Viet Nam's NDC are discussed. For future steps, the sharing of information between stakeholders prior to the planning of technology introduction would help to promote effective deployment of the technologies in Viet Nam.*

Keywords: *low carbon technology, climate change mitigation, multi-criteria assessment, nationally determined contribution.*

1. Introduction

1.1. Background

The Nationally Determined Contributions (NDC) of Viet Nam has identified 45 mitigation options for seven sectors including energy efficiency, power generation, transport, agriculture, land use, land use change and forestry (LULUCF), waste, and here F-gas is also considered. With the support of JICA's Technical Assistance Project on the Planning and Implementation of NAMAs ("SPI-NAMA"), a low carbon technology assessment project was implemented. The Ministry of Natural Resources and Environment (MONRE), the focal point for climate change, has cooperated with relevant line ministries (MOIT, MOT, MARD, MOC and MPI) on the project implementation. The aims was to identify all applicable low carbon technologies, develop the capacity of line ministries in charge of mitigation, improve

coordination among departments, and obtain sufficient inputs for future review and update of NDC [1]. The objectives are as follows:

- o Objective 1: Enhancement of Planning, Implementation and Coordination Capacity. The work aims to enhances capacities of the Government in multiple ways as (1) planning capacities of relevant line ministries (LMs) to develop and implement sector-based action plans for NDC; (2) effective coordination capability within related LMs, and also between MONRE and key stakeholders through reaching internal consensus; (3) facilitative capacity of MONRE by pointing out Viet Nam's context and clarifying policy needs, mitigation actions to enable the deployment of low carbon technologies.

- o Objective 2: Direct inputs to further review and update Viet Nam's NDC. Existing proposed mitigation options under the NDC are to be revisited to confirm legitimacy of assumptions, scope, and barriers against Viet Nam's country-specific context and

Corresponding author: Le Ngoc Cau
Email: caukttv@gmail.com

conditions. Further assessment and identification of potential options beyond the current scope, as presented in the Assessment work, will be the direct inputs to the revision process of NDC.

The technology list was identified drawing on the 45 mitigation options of the INDC Technical Report, existing relevant technology database, and collection of mitigation needs discovered through stakeholder consultations per sector. These technologies were then subjected to evaluation with universal and sector specific criteria in order to extract prioritized technologies, exploring prototype projects to find opportunities for future deployment.

These options were identified by the INDC Technical Report, and the elaboration of means of implementation through identifying all applicable low carbon technologies. The common approach for the low carbon technology assessment follows three steps: listing technologies with a view to Viet Nam’s context (Step 1); evaluation of the technologies to identify priority technologies (Step 2); and exploring opportunities for NDC

implementation (Step 3). In order to collect views from a wide range of stakeholders, private sector, and research institutes were also invited to join in the assessment work process [2].

The institutional arrangement, involving multiple stakeholders to ensure quality analysis of technology options for each mitigation options, is summarized in Figure 2. Engagement of multiple stakeholders was meant to provide balanced viewpoints over technology options while ensuring sectoral needs and priorities. MONRE and JICA jointly supervised the project through consultations and close cooperation, and provided guidance to the Assessment Team to study and evaluate the low carbon technologies. A number of dialogues, discussions and workshops were held with the participation of relevant line ministries (LMs), private sector stakeholders as well as international development partners. Besides, a Technology Advisory Committee comprising domestic and international experts was also established in order to benefit from third party expertise.

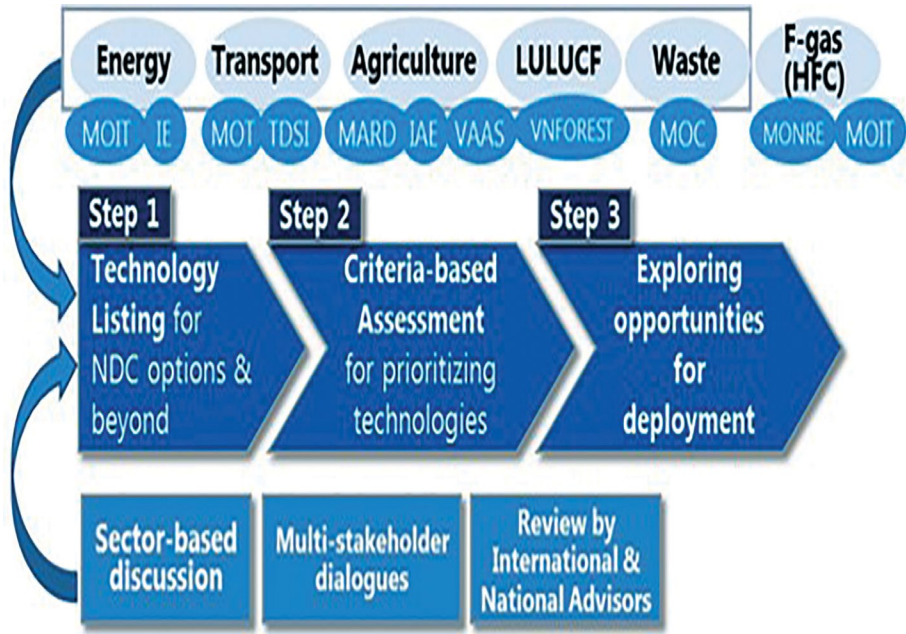


Figure 1. Modality of Low Carbon Technology Assessment
(Source: MONRE and JICA, 2018)

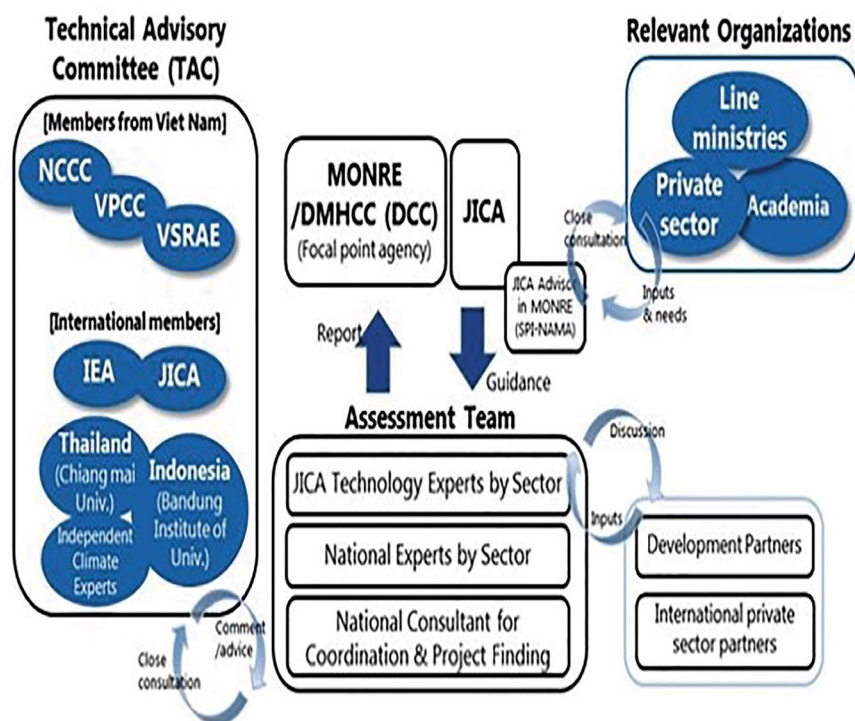


Figure 2. Institutional arrangement for Low Carbon Technology Assessment

(Source: MONRE and JICA, 2018)

1.2. Methodology

Three methods were employed for this study, namely desk-based literature review, expert consultation, and multi-criteria assessment.

The desk-based literature review included an analysis of related documents in the field of study with both qualitative or quantitative design to gain a solid theoretical foundation for the research [3]. Some important documents, scholarly articles, journal and book publications were analyzed to provide different perspectives along with the use of data collecting instruments like interview and consultation [4]. The significant sources included publications on low carbon technology development from the Ministry of Environment and Natural Resources (MONRE), Ministry of Agriculture and Rural Development (MARD), Ministry of Planning and Investment (MPI), Ministry of Trade and Industry (MOIT), World Bank, Asian Development Bank, United Nations Development Programme, EX Research Institute Ltd., Ministry of Environment - Japan, etc.,...

Climate change measures are often cross-sectoral, and the cooperation among related ministries was essential for actions that are effective timewise and also financially [6]. Furthermore, to reflect these measures in future national plans and legislations, it was vital to reach agreement not just among officials inside the leading ministry but more so between related ministries. Five joint workshops in dialogue format had been conducted by November 2017 to receive comments from related ministries and advisory committee in order to promote the effective implementation of climate change measures [1].

Multi-criteria assessment (MCA) is a decision-making tool to evaluate the current problems and identify the best option regarding different objectives, alternatives and expectations [6]. The MCA aims to deal with complicated issues which involves various environmental, social and economic problems, and different group interests in the context of environmental and natural resource

management [7,8]. In relation to the approach adopted for the prioritization of suitable technologies, it is divided into four major steps.

- + Step 1: Conduct stakeholder interviews with line ministries on 45 mitigation options.

- + Step 2: With the current situation and directions of the climate change measures in Viet Nam, technologies applicable in Viet Nam's context have been selected from existing technology lists.

- + Step 3: Determination of assessment criteria and technology prioritization. Qualitatively evaluation was divided into high, middle or low (A, B or C) for each criterion [2].

2. Low carbon technologies for 45 mitigation options in Viet Nam

2.1. Energy efficiency

Energy efficiency is one of the priority subsectors under mitigation policies through 2030, as described in the INDC. The MOIT has been developing energy benchmarks and Monitoring, Reporting, Verification (MRV) framework for major industry sub-sectors, and promoting ESCOs (Energy Service Companies) to facilitate energy efficiency.

The first choice among low carbon technologies is high efficiency residential air conditioning. An inverter is an energy saving technology that eliminates operation waste in air conditioners (AC) by efficiently controlling motor speed. In inverter ACs, temperature is adjusted by changing motor speed without turning the motor on and off. When compared with ACs without inverter, power consumption is reduced by 30% and operation noise is reduced. The mitigation potential is at $0.27\text{tCO}_2\text{eq/year/unit}$.

The second is the high efficiency residential refrigerators. Inverter technology also applied to these refrigerators (inverter-fed motor, and linear and scroll compressors), with capacities between 190 to 700 litres. This provides around 40% reduction in power consumption by a refrigerator made in 2015 compared to one of 2006, to $0.07\text{tCO}_2\text{eq/year/unit}$ (volume: 401-450L). The operation noise is also reduced.

High efficiency residential lighting is the

third technological option. LED lighting can produce more useable white light per unit of energy compared to metal halide, sodium vapor, and fluorescent and halogen light sources. Fluorescent lamps (CFL) contain mercury which causes the tube to produce light mostly in the UV region of the spectrum. There is a 50% reduction in electricity consumption by CFL and 80% reduction by LED lighting compared with incandescent bulbs. Their small size, durability, long operating lifetime, wavelength specificity, relatively cool emitting surfaces, and linear photon output with electrical input make these solid-state light sources ideal for use in places in such as plant lighting designs. The mitigation potential is at $0.04\text{tCO}_2\text{eq/year/unit}$ (incandescent to LED) and $0.02\text{tCO}_2\text{eq/year/unit}$ (incandescent to CFL).

Solar water heaters collect solar thermal energy by a solar energy absorber to warm water or air for hot water supply or air-conditioning. One type is a forced-circulation solar system and the other is the natural-circulation solar water heater. This solar system consists of a solar energy collector and a heat storage tank. Solar heaters reduce gas or power consumption. The mitigation potential is $0.46\text{tCO}_2\text{eq/year/unit}$.

Fifthly, a cement-making technology, the new suspension preheater (NSP) kiln is a dry kiln with multistage pre-heaters and a separate pre-calciner installed in suspension preheater to avoid damage inside the refractory from full combustion, which reduces specific energy consumption per unit clinker by 50-60%. The NO_x emission level is expected to reduce as well, and damage mitigation is enhanced to the refractory materials in the kiln. The mitigation potential remains at $0.01\text{tCO}_2\text{eq/t-clinker}$.

Sixth, the vertical shaft brick kiln (VSBK) technology is one of the best available options for small brick manufacturers. VSBK essentially comprises one or more rectangular vertical shafts within a kiln structure. It can be operated perennially as it is protected from the vagaries of weather by the kiln's roof; reduced suspended particulate matter emission; and less fuel consumption can be expected (0.065kg

coal/unit of brick). The mitigation potential is 0.04 tCO₂eq/t-brick (2.4 MtCO₂eq/year by 2030 (for high efficiency VSBK) [1].

Last but not least, building high efficiency commercial air conditioning composes of a single outdoor unit and multi-indoor units. This enables the operation to be controlled by individual rooms/compartments/sections, leading to improved energy efficiency, 40% reduction in power consumption compared with conventional/old central AC system.

2.2. Power generation

Viet Nam's power supply capacity must be increased because of power demand for economic growth. The government has high expectations of renewable energy (including solar PV with steady cost reductions, and biomass power), and is planning extensive introduction. On the other hand, as renewable energy alone cannot satisfy the power demand, coal power plants are planned in parallel due to its large capacity and low cost.

Firstly, bioenergy is a form of renewable energy derived from biomass to generate electricity and heat. Biomass is any organic matter, available in many forms such as agricultural/forestry products, and municipal and other waste. Biomass power plants can supply electricity in non-grid areas. For biomass power plants, the mitigation potential is 1,752-1,838ktCO₂/year by 2020 and 7,942-8,775ktCO₂/year by 2030.

Hydroelectricity is generated when falling water is channelled through turbine blades which that drive an electrical generator, converting the motion into electrical energy. Small hydropower plants have the potential of electricity access improvement in non-grid areas, and they emits no waste. The mitigation potential is 51,689-54,225ktCO₂/year and 58,622-64,771ktCO₂/year in 2020 and 2030 respectively.

Also useful is wind power plant development with domestic or international funding. There are on-shore (on land) and off-shore (on the sea) wind power potentials. Wind turbines convert the force of

the wind into a torque (rotational force), which is then used to propel an generator to create electricity. Wind power stations (wind farms) commonly aggregate the output of multiple wind turbines through a central connection point to the electricity grid. This plant is zero emission. They have the potential of electricity access improvement in non-grid areas. The mitigation potential is 1,402-1,470ktCO₂/year in 2020, and 7,942-8,775ktCO₂/year in 2030.

In biogas power plants, power is generated by burning the combustible gas from anaerobic biomass digestion. Heat and power can be supplied by using small-scale generation capacity and cogeneration. Biogas power plants do not necessarily need to be connected with the power grid have the potential of electricity access improvement in non-grid areas. The mitigation potential is similar for biomass power plants.

Ultra-supercritical (USC) coal power plants operate at temperatures and pressures above the critical point of water, i.e. above the temperature and pressure at which the liquid and gas phases of water coexist in equilibrium, at which point there is no difference between water gas and liquid water. In comparison with sub-critical (SC) coal power plants, there is up to 5.5% improvement on USC heat exchange efficiency. The mitigation potential is 38MtCO₂eq/year (in case 12,720 MW of SC technology coal power generation would be replaced by USC technology).

Lastly, solar PV power systems convert sunlight directly into electricity using photovoltaic cells. Solar PV systems can be installed on rooftops, integrated into building designs and applied in megawatt scale power plants. This technology is zero emissions and can improve access to electricity in non-grid areas. The mitigation potential is 876-919 ktCO₂/year by 2020, and 12,480-13,790ktCO₂/year by 2030 [1].

2.3. Transport

Climate change mitigation measures in the transport sector three sets of measures: Modal

shifts (passenger and freight); energy efficiency (road, railway, inland waterway, maritime and aviation); and fuel switching.

Using biofuel as alternative, such as ethanol for gasoline, can reduce fossil use. Bioethanol can be produced using feedstock containing sugar, such as sugar cane and cassava and wheat starch. Bioethanol can be blended with conventional gasoline fuel and be used for vehicles. Utilization of agricultural waste for ethanol can decrease the amount of wastes such as cassava pulp. The mitigation potential is 888gCO₂/litre of ethanol (but this is highly dependent on feedstock and technologies for waste treatment).

The passenger transport modal shift from private to public, with various measures as development of urban/inter-city railways (e.g. metro, LRT (light rail transit), tram, monorail, high-speed railway), bus/BRT, and inland waterways. Related technologies are to improve energy efficiency of vehicles, such as light weight vehicle using aluminium body, variable voltage variable frequency (VVVF) inverter, regenerative braking system, and low emission buses. It is important to introduce technologies that enhance user friendliness and safety, e.g. IC cards, automatic ticket gates, common ticketing systems, bus location system, and park & ride. There are multiple advantages such as urban railways have high transportation capacity, high speed, less travel time, traffic congestions and accidents reduction and less local air pollutants. For urban railways, the mitigation potential is 38,267tCO₂/year in Ha noi line 1; 41,579 tCO₂/year in Ha Noi line 2; and 88,678tCO₂/year in Ho Chi Minh line 1.

Freight transport switch from road to railways and waterways, can include development/improvement of railway/waterway freight terminals, renovation of railway tracks/ports, and access roads to these terminals. Accordingly, local air pollution, noise and traffic accidents caused by trucks will be reduced. The mitigation potential is 305tCO₂/year (for rubber products, shift from truck 810km to railway 859km+truck 35km), 405tCO₂/year (for miscellaneous goods, shift from truck to

railway), 3,320tCO₂/year (for chemicals, shift from truck to waterway), 2,116MtCO₂/year (for electronic parts, shift from truck to waterway) [1].

2.4. Agriculture

Profitability and food security for farmers are the first priority rather than GHG emission reduction that ensures economic sustainability of mitigation actions especially for farmers.

The first option is increased use of biogas. A small scale biogas digester consists of a tank in which the organic material is digested combined with a system to collect and store the biogas. This technology reduces groundwater contamination, needs for fuelwood, and indoor air pollution caused by fuelwood burning. This technology eliminates methane emissions created during fermentation of openly-discharged sewage. The mitigation potential is 6.4 x10⁻³kgCO₂/unit/year.

The second and third proposed options are the reuse of agricultural residue as organic fertilizer in rice and upland crops. Through using dry and green farm biomass piled in a heap in a relatively short time, biodynamic composting is an inexpensive method to produce a large amount of compost. Static pile composting can produce compost relatively quickly (within three to six months). This method is suitable for a relatively homogenous mix of organic waste except animal by-products or grease from food processing industries. These easy to prepare and low cost technologies have a reduced potential of 1.07x10⁻⁴kgCO₂/ha/year.

The fourth option is alternate wetting and drying (AWD), and improved rice cultivation system (small and large scale). Flooded rice fields are a large source of methane emission. In AWD, the rice field is drained periodically to enhance aeration of the soil, inhibiting methane-producing bacteria thereby reducing methane emissions. This technology shows other advantages such as lowering irrigation water consumption by 25%; reducing fuel consumption for pumping

water; no yield difference from continuous flooding but heavier and bigger grains; more tillers; fewer pests/diseases; and it saves time and labour. The mitigation potential is 1.46-2.93tCO₂eq/ha/season and 48% reduction of methane emission.

The fifth method is integrated crop management (ICM) in rice cultivation. Major components of ICM include site and variety selection; seed quality and health; site, crop rotation and varietal choice; soil management and crop nutrition; crop protection; wildlife and landscape management, and energy efficiency. ICM can contribute to GHG emissions reduction in particular through energy efficiency in rice cultivation with high efficiency water pumps. It can reduce a total energy usage, save cost and maximise drainage capacity. Higher pump efficiency can reduce 78-83% of fuel needs. The mitigation potential is 5.2tCO₂eq/unit/year.

The sixth and seventh technologies are biochar introduction and ICM in upland crops. Biochar is produced with low cost methods that generated less black smoke and biochar incorporation in soils improves nutrient, water and air accessibility. Size and type of equipment to produce biochar depends on stock volume and available area for installation of equipment: barrel type bio stove (small size), batch type bio stove (small to middle size) and batch kiln (brick kiln, TPI transportable metal kiln, missouri-type charcoal kiln, continuous multiple hearth kiln, small scale biochar plant) (small to large size). The mitigation potential is 50-65% reduction of CO₂ emissions (carbon sequestration).

Eighth is the substitution of urea with SA fertilizer (Ammonium Sulphate (NH₄)₂SO₄). As part of fertilizer manufacturing plants, the following production units can save energy and reduce operation cost, such as calcium silicate insulation of high pressure steam pipe line (0.78GJ/t) with the mitigation potential at 0.47MtCO₂; isothermal CO conversion reactor (0.418GJ/t) with 0.09MtCO₂, installation of variable speed drives for cooling tower fans in fertilizer (2.77kWh/ton) at 0.02MtCO₂; and steam trap management (0.0003GJ/t) at 0.01MtCO₂.

The ninth option is livestock diet improvement. A large portion of enteric methane and nitrous oxide comes from fermentation processes in ruminants. It was demonstrated that dietary lipids (e.g. fatty acids, medium to long chain) can suppress CH₄ production. For monogastric farm animals, adding lysine in feed is effective in reducing the total volume of CO₂ produced in the process from manufacture of raw materials to production (life cycle) as well as excretion of nitrogen. The results show that it is safe for the animals and does not affect other ruminal parameters. Amino acid balance and efficiency of feeds can be improved, resulting in reduction of the amount of animal waste and methane gas at 3.8% reduction of CH₄ with each 1% addition of supplemental fatty acid. The mitigation potential is 1t of life-cycle-CO₂/2.4kg of added lysine.

Tenth is the improvement of available quality and services for aquaculture such as inputs and foodstuff, purification, aerobic treatment, microbe fermentation, up-flow anaerobic blanket process and rotating biological contactor are the series of methods to remove impurities in wastewater generated from the livestock production, food and aquaculture processing. It can also recover methane gas for power generation and reduce production costs. The mitigation potential is 7,739tCO₂eq/system/year.

Eleventh is the improvement of technologies in aquaculture and waste treatment in biogas plants that capture the methane gas from the anaerobic fermentation of biomass from aquaculture waste. An industrial scale biogas digester consists of five items, including: pre-treatment system; sterilization system; methane fermentation system; gas utilization system; and post-treatment system. These high efficiency, energy saving processes have a mitigation potential of 22,806tCO₂eq/year (from the plant: one anaerobic digester with biogas production of 3,000m³/day, and one 500kW biogas generator with power generation of 3,285MWh/year).

Twelfth is improved irrigation for coffee by allowing water to drip slowly to the plant root zone. Drip irrigation has a high efficiency of over 90% and reduces water, as well as fertilizer use, fuel and other production costs. The mitigation potential is $5.3 \times 10^{-3} \text{kgCO}_2\text{eq/ha/year}$.

Finally, there are improved technologies in high efficiency cooling (chilling and freezing) facilities in cold chain process in agriculture, forestry and aquaculture. Ammonia and CO_2 are used as primary and secondary refrigerant, respectively (more than 25% reduction), no ammonia leakage on the load side, and reduced fuel cost, as well as other production costs. The mitigation potential is $165 \text{tCO}_2\text{eq/year}$ [1].

2.5. Land Use, Land-Use Change and Forestry (LULUCF)

The methods for protection of natural forest (1 and 2.2 million ha) include: reforestation; forest fire control; insect and pest control; invasive species prevention; forest degradation and deforestation prevention; restoring degraded forest ecosystems; and development of non-timber forest products. For economic benefit, sustainable timber trade increases average income. For social benefits, the number of jobs and income in local areas can increase. For environmental benefits, conservation technologies lead to sustainable forest use and management. The mitigation potential is $70.6 \text{MtCO}_2\text{eq/year}$.

The protection of coastal forest (100,000, 10,000, and 30,000 ha) is a combination of the following techniques such as conservation of existing forests; enrichment planting; reforestation; and silvo-fishery practices (e.g. a fish/shrimp pond combined with mangrove trees). For economic benefits, plants and aquaculture products are a source of income in the local economy. For social benefits, the number of jobs and income is increased through growing aquatic resources (fish, shrimp, crab etc.) by plantation and enrichment of mangrove forests in long term. For environmental benefit,

mangrove swamps are considered a low-cost, efficient “green dyke” to prevent wave or storm damage, increase sedimentation rates, and protect shrimp farms. The mitigation potential is $12.5 \text{MtCO}_2\text{eq/year}$.

The natural forest and production forest regeneration (200,000 ha) is a combination of the following: planting technique; tree selecting; proper site and suitability assessment for tree species selection; seedling production and quality. This increases carbon sinks, protection of environment, and watershed conservation. The mitigation reduction potential is $37.5 \text{MtCO}_2\text{eq/year}$.

The plantation of large timber production forest (150,000ha) is a business model for transformation and restoration of short-rotation acacia plantations (commonly 5-6 years), in which the rotation length is up to 12-15 years if used for high-value sawn log production. It not only enhances carbon storage and other environmental services (soil fertility, etc.) but also promotes sustainable forest management. The mitigation potential is $10 \text{tCO}_2\text{eq/ha/year}$ [1].

2.6. Waste

In accordance with a study conducted by the Ministry of Construction (MOC) and United States Agency for International Development (USAID), the priority for technology introduction in the waste sector is in the following order: composting, incineration, and landfill.

Organic fertilizer production composting is a method of decomposing organic solid waste. The process involves decomposition of organic waste into humus known as “compost” which can be utilized as organic fertilizer for plants or conditioners of agricultural/horticultural soil. This is low-cost and relatively simple (easy-to-apply) technologies. The mitigation reduction is $17,000 \text{MtCO}_2\text{eq/year}$ (from 200 ton/day of municipal solid waste).

Landfill Gas (LFG) recovery for electricity and heat generation is process consisting of LFG collection, refining and conversion into energy. The quality of LFG

highly depends on the composition of waste and presence of oxygen in the decomposition process of organic waste at landfills. The collected LFG can be utilized for generating power and/or heat while reducing methane that might have otherwise been released to the atmosphere. It can be applied to various landfill types (existing, closed, and newly disposal landfills). The mitigation potential is 7,000MtCO₂eq/year (the landfill of disposing 200 ton/day).

The recycling of solid waste needs proper separation of recyclable items from waste at source. A series of manual or mechanical separation technologies are required when the solid waste is collected in the mixed state. The cost of recycling can be minimized by making use of the existing recycling industry at its maximum. The mitigation potential is 3MtCO₂eq/year.

The anaerobic treatment of organic solid waste with methane recovery for power and heat generation is specifically designed to treat waste from considerably large sources (wet markets, restaurants, hotels, etc.) and wastewater treatment sludge. It treats the waste with anaerobic digestion system to produce high quality fertilizers while collecting the biogas to produce heat or electricity, depending on the amount collected. The mitigation potential is 1,680MtCO₂eq/year (from 50 ton/day of waste collected) [1].

2.7. Fluorinated greenhouse gas (F-gas)

The measures on F-gases had not yet identified, with scarce and scattered information on consumption of HFC preventing the Government of Viet Nam to plan mitigation options for these gases. However, some energy options are relevant, namely high efficiency air conditioner for households, high efficiency commercial air conditioning, and high efficiency residential refrigerators. Consumption of HFC is likely to increase over time after the ban of chlorofluorocarbons (CFC) and hydrochlorofluorocarbons (HCFC), and phasing down the use of HFCs will soon be necessary under the Kigali Amendment to the Montreal Protocol, as well

as the UNFCCC. Thus, wider options on F-gases should be considered in addition to the energy efficiency options.

There are several destruction methods for F-gas, such as the rotary kiln, waste combustion, submerged combustion, plasma, catalytic, overheated steam method, etc. In Viet Nam, there are no specific facilities and/or equipment for F-gas destruction. However, currently, LaFarge Holcim (cement factory) has a pilot project of F-gas destruction in their cement kiln. There are three steps in the destruction process of F-gas by cement kiln: recovery of refrigerant; refilling and transporting F-gas cylinders; and thermal destruction at destruction site, where recovered F-gas is injected into cement kiln and combusted at over 1,000 degrees during at least 6 seconds. The process results in over 99.9% of decomposed F-gas.

One technology is to change high global warming potential (GWP) refrigerant to low GWP refrigerant (R600a/isobutane) in household refrigerators. Low GWP refrigerant R600a (isobutene, GWP=4) is widely available in Viet Nam with the limitation at less than 100g use of R600a for household refrigerators to prevent explosion. The reduction reaches at 99.7% by changing refrigerant from R-134a (GWP=1,430) to R600a (GWP=4).

For commercial cold storage, the change in high GWP refrigerant to low GWP refrigerant (CO₂) (GWP=1) is necessary. It shows that electricity saving is approximately 2,400USD/year. Besides, freezer would be smaller in size and lightweight so that installation cost can be reduced.

Another technical approach is the change of high GWP refrigerant to low GWP refrigerant (R32) in air conditioners in the residential and commercial sector. R32 has zero ozone depletion potential and low toxicity, and 1/3 GWP compared to the R410a refrigerant. R410a is a mixed refrigerant whereas R32 is a single component refrigerant that is easy to handle and recover. 68% reduction is obtained by changing refrigerant from R410a (GWP=2,090) to R32 (GWP=675).

For automobile air conditioners (ACs), the change of high GWP refrigerant to low GWP refrigerant (HFO-1234yf) consists of re-filling the low GWP refrigerant gas into ACs and recovering the old high GWP refrigerant. It has zero ozone depletion potential, low toxicity and is easy-to-change cooler gas. It can be used with the existing standard equipment configuration and materials. The reduction reaches at 99.7% by changing from R134a refrigerant (GWP=1,430) to HFO-1234yf (GWP=4) (amount of gas in car AC: 300-1,000g/car) [1].

In addition, the proper management of refrigerants can prevent reduction of energy efficiency and save costs for refilling of lost refrigerant. There are three steps for leakage inspection: exterior check (visual inspection), indirect inspection (monitoring of gas pressure, discharge temperature, etc.) and direct inspection (using bubbling liquid, electronical gas detection machines, etc.). Based on the results of above inspections, maintenance and repairs to prevent leakage are conducted as necessary.

3. Barrier analysis and next step for low carbon technology implementation

The development of low carbon technologies is very important in order to reach the 8% greenhouse gas emission reduction target by domestic efforts and 25% reduction in case of international support. Regarding 45 mitigation options in Viet Nam's NDC, approximately 100 low carbon technologies were introduced. Of those, based on criteria and expert judgment, about 60 technologies are relatively easy to adopt [1]. The main challenges for the deployment of the identified low carbon technologies were also discussed. The challenges are sector-specific. It was pointed out that standards and policy framework are still not sufficient. Besides, various barriers related to investment were identified as 'low incentive' (energy, waste, F-gas), 'demand risk' (transport), and 'limited resource' (agriculture and LULUCF).

For equipment and industries, there are

no mandatory energy efficiency standards, labelling, and environmental standard. In industry, incentives for energy efficiency measures are still limited. However, the hydropower sector must pay small fees for forest ecosystem services.

For transport, the bioethanol standard is not yet available. In addition, the investment in this sector requires increased demand to achieve project profitability (modal shift).

For agriculture, cross-sectoral benefits between livestock and food security may be possible but require high initial investment.

For LULUCF, there are limited financial resources, and the policy barrier of land use prioritization.

For waste, the limited demand in anaerobic treatment of organic solid waste will require a more effective strategy for commercializing compost products.

For F-gas, there is no policy framework, low awareness of stakeholders, but price competitiveness of low GWP refrigerant [2].

The promotion of private sector involvement, financial incentives for investment, awareness raising on the benefits of low carbon technologies and systems, and consultations and discussions with many stakeholders including private sector businesses are essential to remove barriers to adopt the low carbon technologies in Viet Nam.

4. Conclusion

A multicriteria assessment approach was used for assessing and selecting low carbon technologies for enabling 45 mitigation options in 7 sectors identified in Viet Nam's NDC, plus F-gas. Specific low carbon technologies with their mitigation potential calculated in CO₂ emission reduction equivalent were assessed and selected. The identified low carbon technologies could help line ministries implement their sectoral mitigation options and also to inform the NDC review.

The main challenges for deployment of the identified low carbon technologies were also discussed. The challenges are sector-specific and on both policy and investment aspects.

Necessary steps for effective deployment of the low carbon technologies enabling NDC implementation include removing barriers,

promoting coordination with relevant stakeholders, and support from international cooperation.

References

1. MONRE and JICA. (2018), *Low carbon technology assessment facilitating effectiveness of Viet Nam's Nationally Determined Contributions. Volume 1: Low carbon technologies for 45 mitigation options.*
2. MONRE and JICA. (2018), *Low carbon technology assessment facilitating effectiveness of Viet Nam's NDC. Volume 2: Multi-criteria Assessment to Identify Prioritized Technologies and Essential Steps to Build Consensus Among Key Stakeholders.*
3. Bowen, G. A., (2009), *Document Analysis as a Qualitative Research Method, Qualitative Research Journal, Vol. 9, No. 2.*
4. Hefferman, C., (2013), *Qualitative Research Approach. Available: <http://www.explorable.com>.*
5. Antunes, P., et al. (2006), *Participatory decision making for sustainable development - the use of mediated modelling techniques, Land Use Policy, 23, 44-52.*
6. Gerber, J.F., et al. (2012), *Guide to Multicriteria Evaluation for Environmental Justice Organisations. EJOLT Report No. 8, 45 p.*
7. Munda, G. (1995), *Multicriteria evaluation in a fuzzy environment. Theory and applications in ecological economics, Physica-Verlag, Heidelberg.*
8. Munda, G. (2008), *Social Multi-Criteria Evaluation for a Sustainable Economy, Berlin Heidelberg: Springer-Verlag.*

ASSESSMENTS OF VULNERABILITY DUE TO CLIMATE CHANGE IN HA TINH CITY

Mai Van Khiem, Tran Dinh Trong, Le Van Tuan, Do Thanh Tung, Vu Van Thang
Viet Nam Institute of Meteorology, Hydrology and Climate Change

Received: 1 February 2019; Accepted: 15 March 2019

Abstract: *Climate change is one of the most serious challenges to Ha Tinh City in the coming time, affecting the natural environment, socio-economic development, and especially people's lives. This paper assesses the vulnerability due to climate change in Ha Tinh City by the ADB/NDF/ICEM and UNDP/GEF toolkits through investigating the exposure, sensitivity, and adaptive capacity data of Ha Tinh City. The result shows that most communes and wards have moderate levels of vulnerability, particularly, Dai Nai ward is at a high level and Bac Ha at a low level. In the future, due to the increased risk of climate change, the vulnerability tends to increase, especially at the end of the century. The level of vulnerability of 13/16 wards/communes may increase by 1 or 2 levels, particularly, the Dai Nai, Nguyen Du, Tan Giang and Thach Hung communes/wards would have very high vulnerability. On the contrary, 4 out of 16 communes/wards (accounting for 25%) would be at average level of vulnerability, in which, vulnerability level of three communes (Thach Linh, Tran Phu, Ha Huy Tap) would be unchanged compared to the current situation.*

Keywords: *Exposure, sensitivity, adaptive capacity, vulnerability, climate change impacts.*

1. Introduction

Ha Tinh is one of the localities affected by natural disasters and climate change. Natural disasters and climate change undermine natural resources, negatively impacting the production system and food security [1, 2, 5]. Within the framework of bilateral cooperation between Viet Nam and Belgium, the provincial project: "Integrated water resources management and urban development related to climate change in Ha Tinh Province" has been implemented to support the Ha Tinh provincial government to increase its ability to adapt to water-related impacts, through strengthening knowledge and capacity development.

To implement this project, SRDP-IWMC Ha Tinh and IMHEN jointly signed a consulting contract named "Assessing vulnerability related to climate change and developing climate change action plan in Ha Tinh City",

with two goals: (i) Support Ha Tinh Province in assessing vulnerability due to climate change impacts on water management and urban development in Ha Tinh City, and (ii) Develop an action plan to respond to climate change for Ha Tinh City.

This paper, based on the research, aims to assess vulnerability due to climate change impacts in Ha Tinh City, including investigate the exposure, sensitivity, and adaptive capacity of Ha Tinh City.

2. Data and methodology

2.1. Data

(1) Data of exposure

The exposure of climate change, based on a set of criteria including 22 factors: Location, distance to the floodplain/riverbank; flood frequency; impacts of floods, droughts, heat wave, and storms; proportion of houses affected by natural disasters; proportion of houses affected by floods; percentage of population affected by natural disasters;

Corresponding author: Tran Van Tra
E-mail: tvtra@monre.gov.vn

proportion of population affected by floods; percentage of areas affected by natural disasters; the extent of damage caused by natural disasters; inundated medical, educational, rural, urban, market, agriculture, land; inundated national highway, provincial roads; deep inundated area.

(2) Data of sensitivity

A set of criteria to assess the sensitivity of climate change consists of four factors: Integrity of design of housing; proportion of children; proportion of the elderly; poverty rate.

(3) Data of adaptive capacity

Adaptive capacity is assessed based on factors such as: Average income of the household; proportion of people in working age, the rate of swimming, skill, literacy rate; flood awareness; disaster support budget.

The above figures are calculated based on the results of socio-economic surveys. Data for the inundated area were inherited from the project “Technical Consultancy of Hydraulic/ Hydrological Model of Rao Cai River Basin and Modelling of Drainage System for Ha Tinh City, related to climate change” [4].

2.2. Methodology

The vulnerability assessment is based on the documents of the ADB/NDF/ICEM and UNDP/GEF toolkits, which are widely used by international and domestic organizations in assessing vulnerability.

The vulnerability can be expressed as a function of the level of exposure (E), sensitivity (S) and adaptive capacity (AC) [1,3]. The impact (I) will be the function of the exposure and sensitivity. The general formula is as follows:

$$V = \frac{E \times S}{AC} = \frac{1}{AC} \quad (1)$$

The elements in the formula (1) are defined as follows:

The exposure of climate change (E)

Exposure is the extent to which a system is exposed to the climate change threat. After identifying the factors, standardising the data for the rational factors, and then decomposing the factors, make the ranking from very low (VL),

low (L), medium (M), high (H), to very high (VH) in accordance with the value of <0.2, 0.2-0.4, 0.4-0.6, 0.6-0.8, 0.8-1.0 [1,3].

Sensitivity to climate change (S)

Sensitivity is the degree to which a system will be affected by, or responsive to the exposure. The potential impact is a function of the level of exposure to climate change threats, and the sensitivity of the target assets or system to that exposure. This includes changes in average climate and frequency as well as extreme weather. Impact may be direct (such as crop change due to temperature changes), or indirect (damage caused by increased coastal flooding frequency) due to sea level rise, and intensity of climate change and the likelihood that the system will be affected by these changes.

After defining the factors, normalizing the data for the quiz factors, and then averaging the factors, performs the rankings from very low (VL), low (L), medium (M), high (H), to very high (VH) in accordance with the value of <0.2, 0.2-0.4, 0.4-0.6, 0.6-0.8, ≥0.8 [1,3].

Impacts of climate change (AC)

Impact assessment is the most important stage in the assessment of vulnerability. Use the impact ranking matrix to rank and carefully record the results in the impact column of the vulnerability matrix. The impact was calculated by the function below:

$$\text{Impact} = \text{Exposure} \times \text{Sensitivity} \quad (2)$$

Adaptability to the threats of climate change

Adaptive capacity is the adaptation of the natural and human systems to respond to current and future climate impacts, such as reducing damage or utilizing beneficial opportunities.

After the adaptive capacity assessment factors for each commune and ward have been identified, the adaptive capacity and allocation of the competencies will be determined at the different levels from very low (VL), low (L), medium (M), high (H), to very high (VH) in accordance with the value of <0.2, 0.2-0.4, 0.4-0.6, 0.6-0.8, 0.8-1.0 [1,5].

Finally, after decentralizing factors of exposure, sensitivity and adaptive capacity, then to score the vulnerability calculation

according to the ranking matrix for each administrative unit in Ha Tinh City [1, 3].

It should be noted that this is a relatively simple ranking method for the purpose of giving a “vulnerability” comparison between communes and wards in the study area. It is based on assumption that current vulnerability is a reliable in predicting vulnerability to future conditions.

3. Results and discussion

The following shows the calculation of vulnerability through ratings with criteria for each factor: exposure, sensitivity, impact, adaptive capacity and vulnerability.

3.1. Exposure

The exposure in Ha Tinh City was calculated in Table 1. It can be seen that, the exposures of Tran Phu and Bac Ha currently are very low, despite the increasing of flooded area in the future. Moreover, 4 wards and communes (accounting for 25%) have low exposure, 8 regions have medium exposure. Especially, Dai Nai and Nam Ha have high exposure to climate

change.

At the beginning of 21 century, 7 wards and communes have similar exposure with current state. The exposures of other regions are increased one rank, such as: Bac Ha, Tan Giang, Thach Ha, Thach Mon, Thach Quy, Thach Trung, and Tran Phu.

By mid of century, the exposure is projected increasing one level in Bac Ha, Nguyen Du, Thach Ha, and Thach Mon. The regions with high exposure increase from 2 (at the current) to 8 (at the middle) as: Dai Nai, Nam Ha, Nguyen Du, Tan Giang, Thach Binh, Thach Ha, Thach Hung, Thach Mon.

By the end of 21 century, the exposure is significantly increased. It increases one rank in 13 ward and communes. The exposures of Thach Binh, Thach Ha, Thach Mon are similar to the middle of century. The exposures of Dai Nai, Nam Ha, Nguyen Du, Tan Giang, Thach Hung are increased to the rank of very high (VH) by the end of century.

Thus, comparing with current, the exposure in Ha Tinh City is significantly increased in the future.

Table 1. Table of hierarchy of exposure levels corresponding to the periods [1,2]

Administrative units	Current	2016-2035	2046-2065	2080-2099
Bac Ha	VL	VL	L	M
Dai Nai	H	H	H	VH
Ha Huy Tap	M	M	M	H
Nam Ha	H	H	H	VH
Nguyen Du	M	M	H	VH
Tan Giang	M	H	H	VH
Thach Binh	M	M	H	H
Thach Dong	M	M	M	H
Thach Ha	L	M	H	H
Thach Hang	M	H	H	VH
Thach Linh	M	M	M	H
Thach Mon	L	M	H	H
Thach Quy	L	M	M	H
Thach Trung	L	M	M	H
Tran Phu	VL	L	L	M
Van Yen	M	M	M	H

3.2 Sensitivity

The current sensitivity was calculated and mapped in Figure 1. The high sensitivity is seen in Ha Huy Tap, Thach Binh, Thach Dong, Thach Quy, Thach Mon because of the high rate of four-level houses, the old, children and the poor in these regions. The sensitivity of Bac Ha, Nam Ha, Tran Phu is low; these wards have low

sensitivity because of urban area, invested strongly in infrastructure, so the ability to withstand the risks of climate change in the future. Seven wards and communes (accounting for 43,75%) have medium sensitivity. Since there is no future sensitivity data, in this study, we use the current sensitivity data, combined with other factors to calculate vulnerability levels.

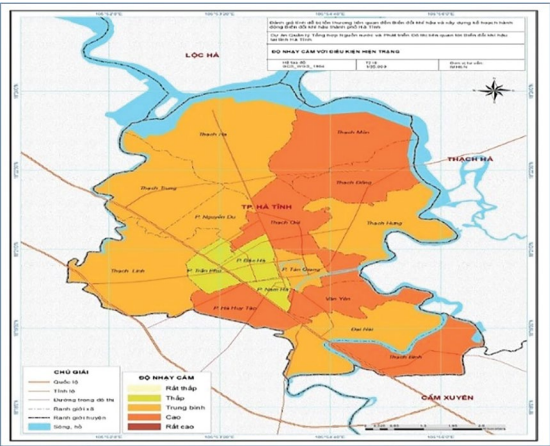


Figure 1. Sensitivity map for Ha Tinh City [1]

3.3. Impacts

The ranking of exposure and sensitivity were combined to determine impact in accordance with the impact scoring matrix. Table 2 shows impact ranking for Ha Tinh City.

Under the current climate conditions, the impacts of climate change on most of wards and communes in Ha Tinh City are at medium level (M). The impact on Tran Phu and Bac Ha are low due to the low sensitivity and low exposure. The high exposure and sensitivity of Dai Nai cause high impact.

In the early part of the 21st century (2016-2035), the impact of climate change is projected to increase one rank, such as in Thach Hung and Tan Giang. The impacts of other regions are similar to current.

At the middle of century, the impacts of 4 wards and communes (Thach Mon, Thach Ha, Thach Binh, Nguyen Du) increase one rank from medium to high compared with the beginning of century.

By the end of 21st century, the impact of climate change is significantly increased due to the increasing of exposure with on rank higher

in most of wards and communes.

3.4. Adaptive capacity

The adaptive capacity for Ha Tinh City was calculated and mapped in Figure 2. Similar to sensitivity, the adaptive capacity in the future is assumed to be similar as that in the current situation. This may not be strictly correct as continued economic development in the region is likely to change many factors that will give rise to changes in adaptive capacity. There is however no way to predict how this adaptive capacity may change. For example, on the one hand the impact of climate change may restrict development in a location while on the other hand economic improvement related to external factors may improve living conditions and therefore improve adaptive capacity.

The adaptive capacity of Bac Ha, Ha Huy Tap and Thach Linh are high due to the high income (more than 38 million per year) and high awareness of climate change impact. Whereas, the adaptive capacity of Dai Nai, Thach Mon, Thach Dong, Thach Quy, Van Yen are low due to the low rate of swimming skills (under 40%), low income, and low awareness of climate change.

Table 2. Impact ranking based on exposure and sensitivity level [1]

Administrative units	Current	2016-2035	2046-2065	2080-2099
Bac Ha	L	L	L	M
Dai Nai	H	H	H	VH
Ha Huy Tap	M	M	M	H
Nam Ha	M	M	M	H
Nguyen Du	M	M	H	VH
Tan Giang	M	H	H	VH
Thach Binh	M	M	H	H
Thach Dong	M	M	M	H
Thach Ha	M	M	H	H
Thach Hang	M	H	H	VH
Thach Linh	M	M	M	H
Thach Mon	M	M	H	H
Thach Quy	M	M	M	H
Thach Trung	M	M	M	H
Tran Phu	L	L	L	M
Van Yen	M	M	M	H

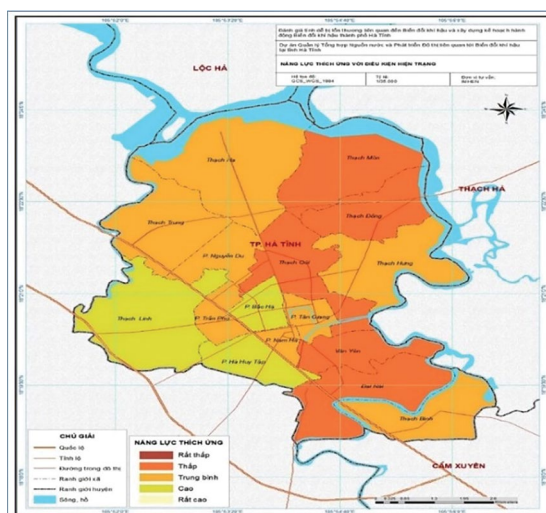


Figure 2. Adaptive capacity map of Ha Tinh City [1]

3.5. Vulnerability assessment

The final vulnerability score is determined by considering the impact and adaptation capacity together. To do so, we the impact and adaptive capacity of each of threat and plot them on the vulnerability scoring matrix.

An important point is that with increasing severity of impact, vulnerability of the target infrastructure system increases.

Adaptation capacity has the opposite effect: with increasing adaptive capacity an infrastructure system would have reduced vulnerability.

In the future, the vulnerability of wards and communes in Ha Tinh City is projected to increase, especially by the end of 21 century (Figure 3).

Bac Ha ward: This ward is located in the

centre of the city with the smallest natural land surface area (1.71% of the total). However, the population of this ward is highest, 11.62%. The vulnerability of Bac Ha is low due to the low exposure and high adaptive capacity. By the end of 21 century, human life and business in Bac Ha are seriously affected by climate change, and caused medium vulnerability.

Dai Nai ward: The vulnerability is high due to many reasons as nearing Rao Cai river, low topography, high influence of flood, high rate of the old (30%) and poor (4%), low rate of swimmer (30%). In the future, the impact of climate change increases, especially the influence of flood (100% land use types are flooded) caused the increasing of vulnerability.

Nam Ha ward: The vulnerability is medium due to the high rate of solid house and high income (50 million/year). By the end of 21 century, the vulnerability increases from medium to high because of the increasing of exposure and the decreasing of adaptive capacity.

Nguyen Du ward: Similar to Nam Ha, the vulnerability in Nguyen Du ward is medium at the current. In the future, the vulnerability increases significantly, can reach to high rank at the middle and very high rank at the end of 21 century. The increasing of vulnerability due to the increasing of flooded area, medium adaptive capacity and low budget for natural disasters prevention (30 million/year).

Tan Giang ward: This ward has high exposure to climate change, it can reach to very high rank by the end of century. The vulnerability is very high due to the medium adaptive capacity, low awareness of climate change, low budget for natural disasters prevention (20 million/year).

Thach Binh commune: The vulnerability of Thach Binh is medium at the current and the beginning of century. At the middle and the end, the vulnerability is high because of the increasing influence of flood, low income (31.2 million/year), high rate of the old (15%) and children (30%).

Thach Dong commune: The vulnerability of Thach Dong is medium at the current, the beginning and the middle of century. By the end

of 21 century, the vulnerability of this region is projected to be high.

Thach Ha commune: At current and the beginning of century, the vulnerability of this region is medium. At the middle and the end of century, the vulnerability is high due to the location next to Ke Go lake, the increasing of flooded area, low adaptive capacity and low income (30 million/year).

Thach Hung commune: At current, the vulnerability is medium. In the future, the vulnerability of this commune increases; at the beginning and middle of century, the vulnerability is high; by the end of 21 century, the vulnerability is very high due to the location next to river, low budget for natural disasters prevention (10 million per year), serious influence of flood on agriculture, health, transport, education.

Thach Linh commune: The vulnerability of this commune is medium and not changes much in the future because of low influence of flood and high adaptive capacity.

Thach Mon commune: This commune has the highest rate of four-level house (50%), high exposure to flood, low budget for natural disasters prevention (17 million per year), low income (31.88 million per year). The vulnerability increases in the future; it will be high at the middle and the end of 21 century.

Thach Quy commune: This commune has high sensitivity due to the high rate of four-level house (50%), low adaptive capacity caused medium vulnerability at the middle of century. Be the end of 21 century, the vulnerability is high due to the seriously influence of flood on business.

Thach Trung commune: In the future, the vulnerability of Thach Trung is high by the end of century, because of the increasing impact of climate change on economic structure, livelihood and infrastructure.

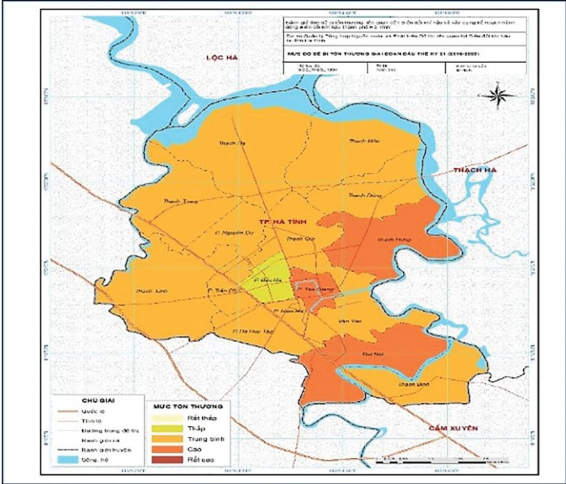
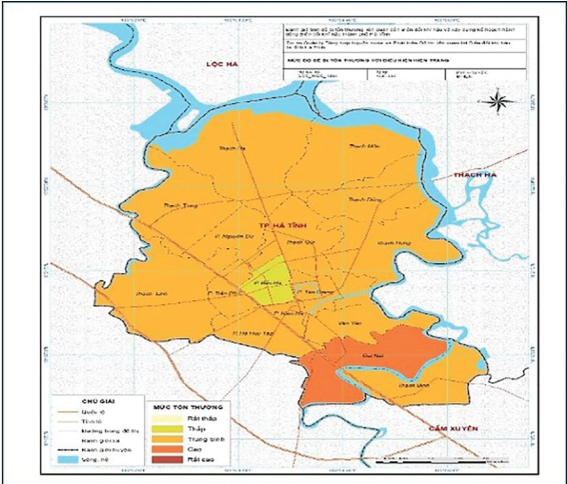
Tran Phu ward: Although the exposure of this ward increases in the future, the vulnerability of Tran Phu is medium and likely similar in the future due to the large annual budget for natural disasters prevention (100 million per year), high resilient infrastructure.

Van Yen ward: The vulnerability of this ward increases in the future; by the end of century, the vulnerability is high. This ward is vulnerable

to flood due to the location next to Rao Cai river, low income (25 million per year), the low rate of swimmer (20%) and low adaptive capacity.

Current

Period of 2016-2035



Period of 2046-2065

Period of 2080-2099

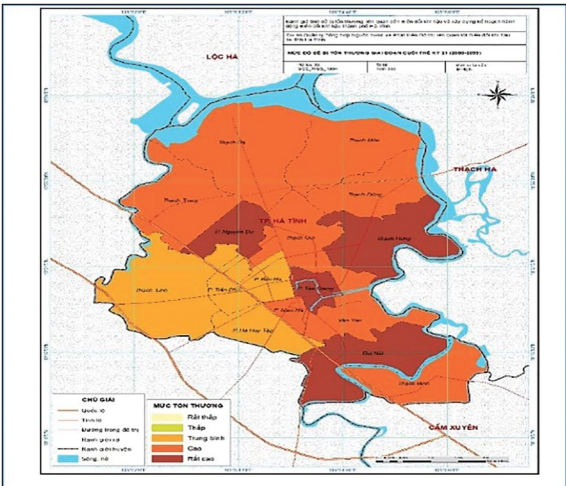
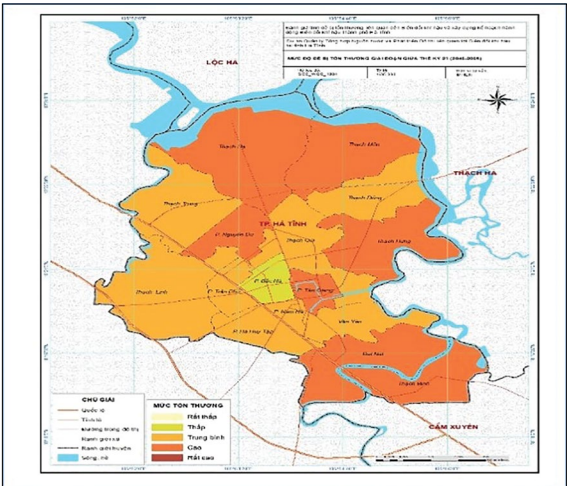


Figure 3. Vulnerability map for Ha Tinh City [1]

4. Conclusions

Ha Tinh is one of the localities affected by natural disasters and climate change which causes natural resources undermined, negatively impacting the production system, food security, people's lives and other vulnerable objects. For assessing vulnerability to climate change in Ha Tinh City according to ADB/NDF method, a set of evaluation criteria includes 3 components: exposure, sensitivity, adaptive capacity was developed and analysed.

At present status, most communes and wards have medium levels of vulnerability, particularly Dai Nai ward at a high level and Bac Ha at a low level. In the future, due to the risk increase of climate change, the vulnerability tends to increase especially at the end of the century. There are 13/16 wards, commune vulnerability increases by 1 or 2 levels. Particularly, communes and wards such as Dai Nai, Nguyen Du, Tan Giang and Thach Hung have a very high vulnerability, consistent with the assessment of the initial increase in

exposure. In contrast, 4/16 communes, wards are at a medium level of vulnerability, in which 3 communes do not change compared to the current level.

Acknowledgements: *This paper is part of a research contract entitled: “Assessing vulnerability related to climate change and developing climate change action plan in Ha Tinh City” jointly signed by SRDP-IWMC Hà Tĩnh and IMHEN. Authors acknowledge the support and contribution of SRDP-IWMC Hà Tĩnh. Also, special thanks to the research team at IMHEN for participating in research, supporting and contributing to the completion of the paper.*

References

1. IMHEN (2019), *Assessing vulnerability related to climate change and developing climate change action plan in Ha Tinh City, Final report of consulting contract 2019.*
2. IMHEN (2015), *Technical advice and analysis of current and future climate for water resource management in Ha Tinh.*
3. International Centre for Environmental Management submit Asian Development Bank and Nordic Development Fund (2015), *Building resilience and sustainability in urban areas of Mekong River region.*
4. Irrigation Planning Institute (2015), *Technical Consultancy of Hydraulic/Hydrological Model of Rao Cai River Basin and Modelling of Drainage System for Ha Tinh City, related to climate change*
5. People’s Committee of Ha Tinh City (2017), *Report on statistics of natural disasters and disaster support in the period of 2010-2016 in Ha Tinh City.*

FUTURE CHANGES IN EXTREME RAINFALL OVER THAILAND USING MULTI-BIAS CORRECTED GCM RAINFALL DATA

Winai Chaowiwat, Kanoksri Sarinnapakorn, Sutat Weesakul
Hydro-Informatics Institute, Bangkok, Thailand

Received: 1 March 2019; Accepted: 21 March 2019

Abstract: Climate change is a controversial issue presented in the media. Obviously, global climate change affects local climate significantly, especially extreme rainfall frequently causes more flood and drought problem. The impact results in loss of life, resources and agriculture products interrupting the national economic progress. Even though many institutes have predicted the future climate under the Representative Concentration Pathway scenario using Global Circulation Model, the predicted climate results depend on the initial conditions and modelled assumptions. Several predicted climate results might confuse audiences because they provide high uncertainty of climate prediction. Coping with the uncertainty of climate prediction requires an understanding of the future extreme rainfall possibility, so the consistency of extreme rainfall analysis is used to investigate the extreme rainfall in the aspect of duration, frequency, and intensity in the national scale. This study aimed to analyse the consistency index of future extreme rainfall using multi-bias corrected GCM under the CMIP5 Project. Extreme rainfall indices were calculated using 20 bias-corrected GCM climate data sets under the Representative Concentration Pathway (RCP4.5 and RCP8.5). Furthermore consistency analysis and statistical hypothesis testing were used to explore the extreme rainfall possibility areas. The focused extreme rainfall indices comprised CWD, CDD, Rx1D, Rx3D, Rx5D, R10mm, R20mm, R95PT, SDII and PRCPTOT indices. The new approach of consistency analysis in this study used hypothesis test for comparing 2 means to enhance a greater reliability of extreme rainfall indices. The results revealed significant changes of extreme rainfall indices including mean CWD increased 28 to 41% in RCP4.5 and 26 to 37% in RCP8.5. Mean R20mm increased 5 to 53% in RCP4.5 and 3 to 61% in RCP8.5. Finally, mean Rx5D increased 38 to 54% in RCP4.5 and 26 to 53% in RCP8.5. The resulting consistency indices could be used to identify areas where extreme rainfall indices have changed.

Keywords: Climate change, extreme rainfall indices, bias correction technique, consistency analysis.

1. Introduction

Recently, Thailand faced extreme climates more frequency caused by global climate change especially flooding and drought events. The flooding and drought problems have created obstacles to economic development, causing damage to housing and public infrastructure and affecting the usual lifestyle of people. Even though weather is forecasted weekly and seasonally; however, long term planning is need to use the climate information

to prepare adaptive measures to cope with the changing climate. These expected extreme events are a challenge that water managers need to understand including their characteristics in terms of severity and spatial profile.

Much related literature involves applied climate indices to investigate the precipitation extreme. Pao-Shin et al. (2013) analysed trends in precipitation extremes during the typhoon season in Taiwan from 21 stations. The extreme precipitation induced by typhoons and monsoon systems has increased over the last 60 years and these two components contribute to strong upward trends in

Corresponding author: Winai Chaowiwat
E-mail: winai@haii.or.th

precipitation intensity. Furthermore, much research employed the extreme precipitation indices to study the trends, changes and variability in temperature and precipitation extreme events, e.g., Kektev et al. (2003), Kamiguchi et al. (2006), Kharin et al. (2007), Rusticucci et al (2010), and Atsamon and Patama, (2016). The R95PT and maximum 1-day 3-day and 5-day precipitation amount (Rx1day, Rx3day and Rx5day) indices characterize the magnitude of intense rainfall events, whereas, simple daily intensity index (SDII) constitutes a measure of the mean total precipitation that falls on a wet day in a given year. Wang et al. (2014) employed R95PT to analyse the long term changing characteristics of extreme precipitation and their links to SST/TS and atmospheric patterns from annual and seasonal time scales for China and the USA. Furthermore, R95pT represents the contribution from very wet days to annual precipitation totals [6]. This research is aimed to investigate the future extreme rainfall in Thailand using daily bias-corrected GCM rainfall data under the changing climate.

2. Study area

Thailand is located in the tropical zone of the Southeast area of the continent between latitude 5°37’N-20°27’N and longitude 97°22’E-105°37’E covering 511,376 square kilometres. The climate of Thailand is under the influence of monsoon winds of seasonal character, i.e., southwest monsoon and northeast monsoon. The southwest monsoon, starting in May, brings a stream of warm moist air from the Indian Ocean towards Thailand causing abundant rain over the country, especially on the windward side of the mountains. Rainfall during this period is caused not only by the southwest monsoon, but also by the Inter-Tropical Convergence Zone (ITCZ) and tropical cyclones, producing a large amount of rainfall. The onset of monsoons varies to some extent. The southwest monsoon usually starts in mid-May and ends in mid-October, while northeast monsoon normally starts in mid-October and ends in mid-February. The river basins have been divided in 9 group basins shown in Table 1 and Figure 1.

Table 1. Coverage area of group river basins

Group River Basin	Area, Km ²
1. Mae Khong River Basin Group (GB1)	188,645
2. Salawin River Basin Group (GB2)	17,918
3. Chao Phraya - Thachin River Basin Group (GB3)	157,927
4. Mae Khlong River Basin Group (GB4)	30,836
5. Bang Prakong River Basin Group (GB5)	18,459
6. Eastern Coast River Basin Group (GB6)	13,829
7. Western Coast River Basin Group (GB7)	12,347
8. Eastern South River Basin Group (GB8)	50,942
9. Western South River Basin Group (GB9)	20,473
Total	511,376

3. Data

Observed rainfall data from 1,029 rain gauge stations shown in Figure 1 were obtained from Thai Meteorological Department (TMD). We collected daily rainfall in the period 1979 to 2005. For the 20 general circulation models (GCM), precipitation was downloaded

from the APEC Climate Center using Climate Information ToolKit, Version 1.0 (CLIK3.0) (Lee and Kim, 2014) shown in Table 2. The concerned time period was divided in 4 periods: present (1979 to 2005), near future (NF: 2006 to 2039), mid future (MF: 2040 to 2069), and far future (FF: 2070 to 2099). The selected climate scenarios

are Representative Concentration Pathways (RCPs) 4.5 and 8.5 which were presented in the fifth assessment report (AR5) of IPCC. RCP 8.5 exhibits high emissions consistent with the future of no policy changes to reduce

emissions. RCP 4.5 is exhibits intermediate emissions for which the radiative force is stabilized shortly after year 2100, consistent with the future of relatively ambitious emissions reductions [12].

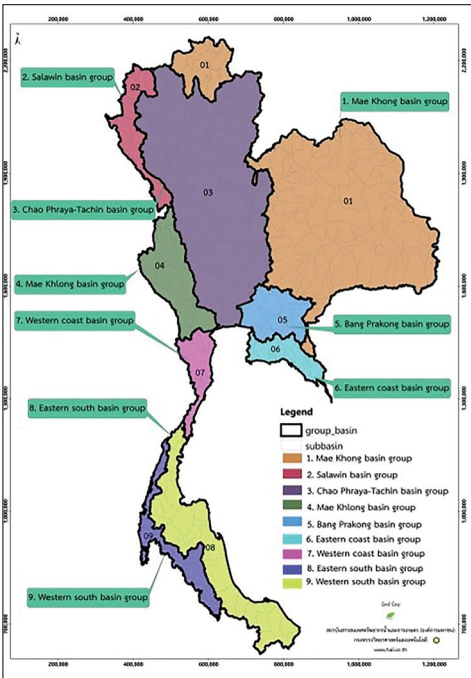


Figure 1. Division of group river basins of Thailand

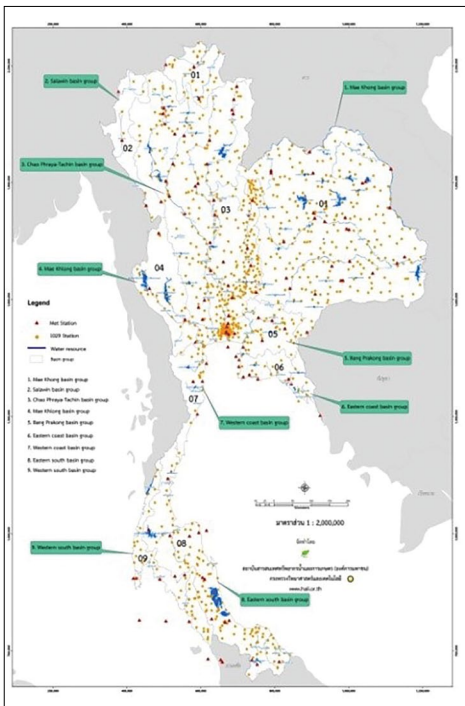


Figure 2. Rain gauges stations in study area

Table 2. Description of GCM climate data used

Modeling group	Model designation	Horizontal/vertical resolution	
		AGCM	OGCM
Beijing Climate Center, China Meteorological Administration	BCC-CSM1.1	T42 L26	1°lon x 1.33°lat L40
Beijing Normal University - Earth System Model	BNU-ESM	2.8125 lon 2.7906 lat	1 lon 0.3344 lat
Canadian Center for Climate Modelling and Analysis	CanESM2	T63 L35	256 x 192 L40
National Center for Atmospheric Research	CCSM4	1.25lon x 0.9 lat L26	1.1°lon x 0.27° -0.54°lat L60
The Community Earth System Model, version 1-Biogeochemistry	CESM1_BGC	1.25 lon 0.9424 lat	
The Community Earth System Model, version 1-Community Atmospheric Model version 5	CESM1_CAM5	1.25 lon 0.9424 lat	
Centre National de Recherches Meteorologiques	CNRM-CM5	TL127 L31	1°lon x 1°lat L42
Commonwealth Scientific and Industrial Research Organization in collaboration with Queensland Climate Change Centre of Excellence	CSIRO-Mk3.6.0	T63 L18	1.875°lon x 0.9375°lat L31
The EC-Earth consortium	EC_EARTH	1.125 lon 1.1215 lat	1 lon x 0.3 –1.0 lat
LASG, Institute of Atmospheric Physics, Chinese Academy of Sciences and CESS, Tsinghua University	FGOALS-g2	128 x 60 L26	360 x 196 L30
	FGOALS-s2	R42 L26	0.5 –1 lon x 0.5 –1 lat L
NOAA Geophysical Fluid Dynamics Laboratory	GFDL-CM3	C48 L48	360 x 200 L50
Institut Pierre-Simon Laplace	IPSL-CM5A-LR	96 x 95 L39	2 lon x 2 lat L31
	IPSL-CM5A-MR	144 x 143 L39	2 lon x 2 lat L31
Japan Agency for Marine-Earth Science and Technology, Atmosphere and Ocean Research Institute, and National Institute for Environmental Studies	MIROC-ESM	T42 L80	256 x 192 L44
Atmosphere and Ocean Research Institute, National Institute for Environmental Studies, and Japan Agency for Marine-Earth Science and Technology	MIROC5	T85 L40	256 x 224 L50
Max Planck Institute for Meteorology	MPI-ESM-LR	T63 L47	GR15 L40
	MPI-ESM-MR	T63 L47	GR15 L40
Meteorological Research Institute	MRI-CGCM3	TL15x L48	1 lon x 0.5 lat L51
Norwegian Climate Centre	NorESM1-M	144 x 96 L26	384 x 320 L53

4. Method

4.1 Gamma-gamma transformation

We modified the Gamma-gamma transformation bias correction method proposed by Mishra and Herath (2008; 2011). The daily rainfall data were defined as the independent variables. The distribution of daily rainfall obtained each month can be approximated by the gamma distribution. The following represent the major steps employed to correct the rainfall data. First, a gamma distribution for daily observed rainfall data series – Fobs(xobs) was considered fit. Second, a gamma distribution for daily GCM rainfall data of the same period was considered fit – FGCM20(xGCM20). Third, a gamma distribution for the 21st century GCM rainfall data was considered fit – FGCM21(xGCM21). Fourth, the inverse of the GCM rainfall data was taken with observed rainfall data and GCM rainfall data was corrected using Eq.1.,

$$X_{GCM20CORR} = F_{obs}^{-1}(F_{GCM20}(X_{GCM20})) \quad (1)$$

where $X_{GCM20CORR}$ represents the corrected GCM rainfall data in each month during the present period and X_{GCM20} represents the raw rainfall during the present period.

For the future period, the future GCM corrected the daily rainfall data in each month using Eq.2.,

$$X_{GCM21CORR} = X_{GCM21} \frac{F_{obs}^{-1}(F_{GCM21}(X_{GCM21}))}{F_{GCM20}^{-1}(F_{GCM21}(X_{GCM21}))} \quad (2)$$

where $X_{GCM21CORR}$ is the daily corrected GCM rainfall data in each month in the future period and X_{GCM21} is the daily raw rainfall data in each month in future period.

4.2. Extreme rainfall indices

In this study, we adopted the concept of extreme rainfall indices [9, 15] to calculate the extreme rainfall indicators focusing on different aspects such as duration, frequency and intensity. The duration indices included consecutive wet day (CWD and dry day (CDD). The frequency indices included heavy rainfall days (R10mm) and very heavy rainfall days (R20mm). The intensity indices included max 1-day rainfall (Rx1D), max 3-day rainfall (Rx3D), max 5-day rainfall (Rx5D), annual contribution from very wet days (R95pT), simple daily intensity index (SDII), and annual contribution from wet days (PRCPTOT), respectively. The description of extreme rainfall indices recommended by the ETCCDI are shown in Table 3.

Table 3. Definition of the ten extreme rainfall indices

Index	Name	Definition
CWD	Consecutive wet days	Maximum number of consecutive days with RR ≥ 1mm, days
CDD	Consecutive dry days	Maximum number of consecutive days with RR < 1mm, days
R10mm	Heavy rainfall days	Annual count of days where rainfall > 10mm, days
R20mm	Very heavy rainfall days	Annual count of days where rainfall > 20mm, days
Rx1D	Max 1-day rainfall	Seasonal maximum 1-day rainfall, mm
Rx3D	Max 3-day rainfall	Seasonal maximum 3-day rainfall, mm
Rx5D	Max 5-day rainfall	Seasonal maximum 5-day rainfall, mm
R95pT	Annual contribution from very wet days	Total annual rainfall from wet days (≥ 1 mm) with rainfall above the 95th percentile for wet days, divided by the annual rainfall
SDII	Simple daily intensity index	The ratio of annual total rainfall to the number of wet days (≥1 mm)
PRCPTOT	Annual contribution from wet days	Annual total precipitation from days ≥1 mm, mm/year

4.3. Changes in extreme rainfall index

Assuming data follow normal distribution, the procedure for testing the changes in mean is as described below. First, the homogeneity of variance is tested for present and future index series. The F test statistic [16] for comparing two population variances is the ratio of the two sample variances,

$$F = \frac{S_1^2}{S_2^2} \quad (3)$$

where S_1 and S_2 are the sample standard deviations of the two series. The more this ratio deviates from 1, the more likely the 2 variances differ, and we will reject the null hypothesis of equal variances when the ratio differs too much from 1. Under the null hypothesis, the test statistic F has an F-distribution with numerator degrees of freedom equal to n_1-1 and denominator degrees of freedom equal to n_2-1 , where n_1 and n_2 are the sample sizes of the two data sets.

Second, the means of present and future index series are compared using 2-independent samples t test. The selection of the t test statistics is based on the result of the equality test of variances in step 1. When the test in step 1 indicates unequal variances, the t test assuming unequal variances will be applied. On the other hand, when the test indicates equal variances, the t test assuming equal variances will be applied. In step 2, the null hypothesis $H_0: \mu_1 = \mu_2$ is tested against the alternative hypothesis $H_1: \mu_1 \neq \mu_2$. The t test statistic in the equal variances case [17], t_{cal} is calculated as:

$$t_{cal} = \frac{\bar{x}_1 - \bar{x}_2}{\sqrt{\left[\frac{(n_1-1)S_1^2 + (n_2-1)S_2^2}{n_1+n_2-2} \right] * \left(\frac{1}{n_1} + \frac{1}{n_2} \right)}} \quad (4)$$

where \bar{x}_1 and \bar{x}_2 are the means of the two time series. Under the null hypothesis, tcal has a t distribution with degrees of freedom n_1+n_2-2 . A difference between two means is significant at $\alpha = 0.05$ when p-value of the calculated t test statistic (t_{cal}) is less than 0.05. When variances are unequal, the t test statistic [17], tcal, is calculated as:

$$t_{cal} = \frac{\bar{x}_1 - \bar{x}_2}{\sqrt{\frac{S_1^2}{n_1} + \frac{S_2^2}{n_2}}} \quad (5)$$

The degrees of freedom of t_{cal} for this case is

$$d.f. = \frac{\left(\frac{S_1^2}{n_1} + \frac{S_2^2}{n_2} \right)^2}{\frac{\left(\frac{S_1^2}{n_1} \right)^2}{n_1-1} + \frac{\left(\frac{S_2^2}{n_2} \right)^2}{n_2-1}} \quad (6)$$

When the null hypothesis is rejected based on the t test result, the change in mean extreme rainfall indices will be calculated as the percentage of the difference between future and present mean extreme rainfall indices in each grid using Eq.7,

$$\% \Delta_m = \left(\frac{\bar{X}_{FU} - \bar{X}_{PR}}{\bar{X}_{PR}} \right) \times 100 \quad (7)$$

where $\% \Delta_m$ represents the percentage of change between future (\bar{X}_{FU}) and present (\bar{X}_{PR}) mean extreme indices.

Moreover, when the F test is rejected, the change in standard deviation can also be calculated. The change in standard deviation of extreme rainfall indices is the percentage of the difference between future and present standard deviations of extreme rainfall indices in Eq.8,

$$\% \Delta_{std} = \left(\frac{S_{FU} - S_{PR}}{S_{PR}} \right) \times 100 \quad (8)$$

where $\% \Delta_{std}$ represents the percentage of change between future (S_{FU}) and present (S_{PR}) standard deviations of extreme indices.

The consistency index for change in means (CI_m) can be computed in Eq.9.

$$CI_m = \begin{cases} \frac{NM_p}{NM_p + NM_o + NM_n}; & \text{Different means, } NM_p > NM_n \\ \frac{NM_o}{NM_p + NM_o + NM_n}; & \text{No change in means,} \\ \frac{NM_p}{NM_p + NM_o + NM_n}; & \text{Different means, } NM_n > NM_p \end{cases} \quad (9)$$

where NM_p is the number of BC GCMs that predict an increase in mean extreme rainfall indices, NM_n is the number of BC GCMs that predict a decrease, and NM_o is the number of BC GCMs that predict no change. Therefore, the sign of the index denotes the direction of changes projected by the majority of the BC GCMs.

The consistency index for change in variances (CI_v) can be computed similarly as in Eq.10.

$$CI_v = \begin{cases} \frac{NV_p}{NV_p + NV_o + NV_m}; \text{Different variances, } NV_p > NV_o, \\ \frac{NV_o}{NV_p + NV_o + NV_m}; \text{No change in variances,} \\ \frac{NV_p}{NV_p + NV_o + NV_m}; \text{Different variances, } NV_n > NV_p \end{cases} \quad (10)$$

where NV_p is the number of BC GCMs that predict an increase in variance of extreme rainfall indices, NV_n is the number of BC GCMs that predict a decrease, and NV_o is the number of BC GCMs that predict no change.

4.5. Performance evaluation

The goodness of fit tests are used to evaluate the performance of daily BC rainfall data and extreme rainfall indices including Pearson's correlation (r), root mean square error (RMSE) [20-22], mean absolute error (MAE), percent bias (PBIAS) [23,24], skill score (SS) [25,26] and difference in mean and standard deviation. The formulas used to calculate the performance are:

$$r = \frac{n(\sum x_0 x_{bc}) - (\sum x_0)(\sum x_{bc})}{\sqrt{[n\sum x_0^2 - (\sum x_0)^2][n\sum x_{bc}^2 - (\sum x_{bc})^2]}} \quad (11)$$

$$RMSE = \sqrt{\frac{\sum_{i=1}^n (x_{bc} - x_0)^2}{n}} \quad (12)$$

$$MAE = \frac{1}{2} \sum_{i=1}^n |x_{bc} - x_0| \quad (13)$$

$$SS = 1 - \frac{MSE_{bc}}{MSE_{GCM}} \quad (14)$$

$$MSE = \frac{\sum_{i=1}^n (x_{bc} - x_0)^2}{n} \quad (15)$$

$$PBIAS = \frac{\sum (x_0 - x_{bc})}{\sum x_0} \quad (16)$$

where x_{bc} represents BC data, x_0 represents observed data, MSE_{bc} represents mean square error between BC and observed data, and MSE_o represents mean square error between raw GCM and observed data.

5. Results

5.1. Evaluation of daily BC rainfall

The daily BC rainfall data of each GCM was verified using the correlation (r), percent biases (PBIAS), root mean square error (RMSE), and mean absolute error (MAE) shown in Table 4. The average correlation of daily BC rainfall data varied from 0.14 to 0.19, RMSE varied from 9.52 to 10.72, and MAE varied from 4.21 to 4.97. The percent biases produced a better result which varied from -1.29 to 1.13%. The evaluation of BC rainfall data implied that these BC data are able to help investigate the changes of future extreme rainfall.

Table 4. Performance of daily BC rainfall

GCM	r	PBIAS, %	RMSE	MAE
BCC_ESM	0.17	-0.50	9.92	4.52
BNU	0.16	-0.21	10.29	4.69
CanESM2	0.18	-0.20	10.24	4.42
CCSM4	0.17	-0.41	10.21	4.52
CESM1_BGC	0.17	-0.35	10.22	4.54
CESM1_CAM5	0.16	-0.32	10.32	4.56
CNRM	0.19	-0.29	9.52	4.21
CSIRO	0.15	1.13	10.53	4.78
EC_EARTH	0.15	-0.20	10.43	4.75
FGOALS_g2	0.17	-1.29	10.15	4.64
FGOALS_s2	0.15	-0.24	10.31	4.67
GFDL	0.16	-0.02	10.18	4.50

GCM	r	PBIAS, %	RMSE	MAE
IPSL_CM5A_LR	0.17	-0.22	10.14	4.53
IPSL_CM5A_MR	0.16	-0.19	10.35	4.56
MIROC5	0.17	-0.32	10.18	4.62
MIROC_ESM	0.15	-0.18	10.51	4.84
MPI_ESM_LR	0.15	-0.25	10.69	4.97
MPI_ESM_MR	0.14	0.70	10.72	4.94
MRI_CGCM3	0.15	-0.26	10.51	4.70
NorESM	0.16	-0.31	10.27	4.65
Average	0.16	-0.20	10.28	4.63
Max	0.19	1.13	10.72	4.97
Min	0.14	-1.29	9.52	4.21

5.2. Verification of extreme rainfall indices

The performance of 20 BC GCM extreme rainfall indices is verified by using the RMSE, skill score and percentage of difference in mean and standard deviation as shown in Tables 5 and 6. The comparison of CWD, R20mm and Rx5D between observed and BC extreme indices is shown as in Figure 3, revealing that the spatial profile of BC extreme indices corresponded to the observed extreme indices. Especially the BCR20mm showed similar means to the observed R20mm, whereas the observed

Rx5D showed a higher mean than the BC Rx5D. The average RMSE of BCGCM extreme rainfall indices varied from 0.04 to 259.03, while the skill score varied from -0.14 to 0.44. The R20mm showed a better result in skill score (0.44). The difference in mean produced better results varying from -4.97 to 16.62%, whereas the difference in standard deviation produced higher biases varying from -24.59 to 82.02%. The verified result implied that these extreme indices could represent the extreme events in the Thai boundary.

Table 5. RMSE and skill score of extreme rainfall indices

Extreme index	RMSE			Skill score		
	Max	Mean	Min	Max	Mean	Min
CDD	39.55	30.67	26.19	0.65	0.37	0.10
CWD	38.27	19.56	13.29	0.78	0.22	-0.92
R10mm	14.12	10.24	7.65	0.87	0.38	-0.60
R20mm	7.86	5.49	4.44	0.88	0.44	-0.44
Rx1D	46.32	25.21	17.66	0.90	0.19	-0.76
Rx3D	61.67	46.91	36.54	0.95	-0.14	-1.03
Rx5D	76.61	55.49	41.36	0.95	-0.11	-1.24
R95PT	0.05	0.04	0.03	0.90	0.33	-0.50
SDII	3.29	2.17	1.68	0.61	0.14	-1.72
PRCPTOT	316.11	259.03	221.83	0.91	0.40	-0.13

Table 6. Difference in mean and standard deviation of extreme rainfall indices

Extreme index	Difference in mean, %			Difference in std, %		
	Max	Mean	Min	Max	Mean	Min
CDD	22.61	-4.00	-17.90	46.15	13.33	-23.85
CWD	87.84	-3.61	-66.07	73.16	-24.59	-76.02
R10mm	23.59	1.79	-31.35	85.21	38.93	-10.77
R20mm	29.18	-4.83	-49.66	60.56	32.33	-20.65
Rx1D	25.27	6.04	-9.21	225.09	63.91	0.00
Rx3D	29.57	16.62	0.00	159.97	77.10	0.00
Rx5D	36.11	16.18	-1.97	172.78	82.02	0.00
R95PT	11.07	1.37	-16.46	129.49	54.28	0.00
SDII	26.93	-4.97	-30.25	41.45	7.74	-36.78
PRCPTOT	1.27	0.19	-1.07	78.50	38.16	0.00

5.3 Changes of extreme rainfall indices

Figures 4 and 5 showed the extreme rainfall changes in all mean and standard deviation of CWD, R20mm and Rx5D indices for the NF, MF, and FF periods against the present period under two RCPs scenarios. The changes of mean and standard deviation of extreme indices were analysed in terms of portion of increased and decreased area to total area, regional increase and decreased percentage and change of whole area as shown in Tables 7 and 8. The results showed that the mean CWD was projected to consistently increase over the upper part of Thailand. A significant increase in mean CWD, greater than 40% was observed over the same region and was significant at the 95% confidence level, whereas mean CDD increased 5 to 25%. The change in mean of frequency indices (R10mm and R20mm) tended to significantly increase higher than 20% except for R20mm in the NF period which increased less than 6%. The sign of intensity extreme indices tended to increase higher than 20% in both RCP4.5 and RCP8.5 (see Tables 5 and 6).

Regarding the changes of spatial distribution analysis, the changes in mean CWD and Rx5D indices in the NF, MF and FF periods under RCP4.5 and RCP8.5 were analysed and compared among the 9 group river basins shown in Figure 6. The CWD index tended to significantly increase higher than 15%

in all periods under RCP4.5, while also tending to increase higher than 15% under RCP8.5 except for GB5 (Bang Prakong River Basin Group) and GB7 (Western Coast River Basin Group) in the NF period and GB8 (Eastern South River Basin Group) in the FF period. Further, Rx5D tended to significantly increase higher than 30% in all periods under RCP4.5 except GB6 (Eastern Coast River Basin Group) in the MF period, whereas Rx5D tended to increase higher than 15% in all periods under RCP8.5 except GB6 (Eastern Coast River Basin Group) in the NF period.

5.4 Consistency of extreme rainfall indices

Figures 7 and 8 showed the extreme rainfall consistencies in all mean and standard deviation of CWD, R20mm and Rx5D indices for the NF, MF, and FF periods against the present period under two RCPs scenarios. The consistency of duration, frequency and intensity of extreme rainfall indices were analysed in the same terms as the change analysis as shown in Tables 9 and 10. The consistency results revealed that the CDD index tended to significantly increase 3 to 19% in the majority of areas (more than 50%), whereas the CWD index tended to significantly increase more than 20% in the majority of areas (more than 70%). The consistency of frequency indices (R10mm and R20mm) of all periods and scenarios tended to significantly increase higher than 20% in the majority of areas except R20mm

in the NF period which tended to decrease less than 4% under RCP4.5 and RCP8.5. In addition, the consistency of intensity indices tended to significantly increase higher than 20% in all periods and RCP scenarios. However, some indices increased less than 20% such as Rx1D in the NF period and R95PT in the NF and MF periods under RCP4.5, Rx1D, Rx3D and Rx5D in the NF period and R95PT in the NF and MF periods under RCP8.5.

Concerning the consistency of spatial distribution analysis, the changes in mean CWD and Rx5D indices in the NF, MF and FF periods under RCP4.5 and RCP8.5 were analysed and compared among the 9 group river basins shown in Figure 9. The CWD index tended to increase higher than 10% in all periods under RCP4.5 except GB5 (Bang Prakong River Basin Group) in the MF period and GB8 (Eastern South River Basin Group) in the FF period. It also tended to increase higher than 10% under RCP8.5 except GB5 (Bang Prakong River Basin Group) and GB7 (Western Coast River Basin Group) which decreased in the NF period and GB8 (Eastern South River Basin Group), which decreased in the MF and FF periods. Furthermore, Rx5D tended to increase higher than 10% in all periods under RCP4.5, whereas Rx5D tended to increase higher than 7% in all periods under RCP8.5 except GB6 (Eastern Coast River Basin Group) and GB9 (Western South River Basin Group) which decreased in the NF period.

6. Conclusion

In this study, the prediction of future extreme rainfall indices was estimated over Thailand based on multiple BC GCM rainfall data under RCP4.5 and RCP8.5 scenarios. The 20 daily BC GCM models of precipitation were used to calculate the extreme rainfall indices around Thailand and analysed the changes and consistency associated with these indices. The horizontal resolution of each BC GCM is 0.1 degree and these BC datasets are available for present (PR:1979 to 2005), near future (NF:2006 to 2039), middle future (MF:2040 to 2069), and far future (FF:2070 to 2099) periods under force from RCP4.5 and RCP8.5 scenarios.

The performance of the 20 BC GCM in

correcting the biases of raw GCM precipitation in the present period is evaluated against observations across Thailand. The results show the BC GCM could perform the proper spatial distribution of precipitation with lower PBIAS values (-0.20%). For the performance of extreme rainfall indices, the goodness of fit tests was used to evaluate, and the results of evaluation showed the difference in mean produced better results less than 17%.

In future scenarios, the changes of mean and standard deviation of extreme indices are predicted to remain consistently over the upper part of Thailand, whereas the sign of projected extreme indices changes differs depending on the periods and RCP scenarios. In particular, mean intensity indices over the upper part of Thailand (GB1 to GB5) were projected to increase higher than 20% during the NF period in RCP4.5, whereas they would increase higher than 20% during the MF and FF periods in RCP8.5.

The change of standard deviation of extreme indices results (Rx3D, Rx5D, R95PT, SDII, and PRCPOT) revealed that the variation of these indices tended to increase higher than 100% except PRCPOT in the NF period under RCP8.5.

In addition, concerning consistency analysis in changes in mean, the result revealed that the trend of extreme indices would be increasing in all periods and all scenarios except R20mm, which tended to decrease less than 4% in the NF period under RCP4.5 and RCP8.5 scenarios. Furthermore, regarding the consistency of changes in variation, the results revealed that the trend of the intensity extreme indices would be increasing more than 10% in all periods and all RCP scenarios except Rx1D and PRCPOT.

Concerning the overall future changes and consistency results, it could be implied that future extreme rainfall event might cause more flood events than drought events in the NF period (2006 to 2039), because the intensity indices values produced higher mean and standard deviations compared with the present period under all RCP scenarios.

Table 7. Changes of mean extreme rainfall indices

Index	Period	RCP4.5						RCP8.5					
		Portion of increased areas	Regional increase, %	Portion of decreased areas	Regional decrease, %	No change areas	Difference in whole area	Portion of increase areas	Regional increase, %	Portion of decreased areas	Regional decrease, %	No change areas	Difference in whole area
CDD	NF	0.526	19.11	0.126	-16.40	0.348	7.68	0.518	19.91	0.048	-16.33	0.434	9.48
	MF	0.480	21.02	0.283	-16.16	0.237	4.80	0.736	22.62	0.223	-15.24	0.041	12.28
	FF	0.636	22.08	0.182	-17.20	0.182	10.22	0.936	28.67	0.063	-19.73	0.001	25.20
CWD	NF	0.821	40.37	0.179	-26.16	0.000	27.91	0.729	45.04	0.271	-25.43	0.000	26.33
	MF	0.852	44.46	0.148	-27.27	0.000	33.13	0.849	47.74	0.151	-27.55	0.000	37.13
	FF	0.873	50.11	0.127	-25.95	0.000	40.57	0.718	48.43	0.282	-31.32	0.000	27.60
R10mm	NF	0.949	31.64	0.051	-15.48	0.000	28.20	0.956	34.19	0.044	-15.29	0.000	31.06
	MF	0.998	31.14	0.002	-18.75	0.000	30.27	0.997	28.71	0.003	-20.28	0.000	27.93
	FF	0.999	33.52	0.001	-18.40	0.000	32.97	0.998	34.60	0.002	-22.74	0.000	34.11
R20mm	NF	0.415	51.88	0.585	-24.04	0.000	5.21	0.429	46.46	0.570	-24.91	0.001	3.24
	MF	0.922	50.53	0.078	-24.12	0.000	43.51	0.973	46.80	0.027	-26.84	0.000	44.34
	FF	0.983	54.57	0.017	-28.32	0.000	53.16	0.996	61.73	0.004	-27.99	0.000	61.24
Rx1D	NF	0.717	38.65	0.282	-22.86	0.000	20.72	0.624	38.13	0.374	-22.86	0.001	15.40
	MF	0.833	36.06	0.167	-21.00	0.000	25.89	0.931	37.42	0.069	-22.35	0.000	33.07
	FF	0.962	41.41	0.038	-24.56	0.000	39.11	0.996	44.25	0.004	-28.11	0.000	44.18
Rx3D	NF	0.885	43.34	0.115	-19.91	0.000	35.51	0.671	39.23	0.328	-19.48	0.001	20.08
	MF	0.882	40.46	0.118	-18.93	0.000	32.65	0.970	42.60	0.030	-21.47	0.000	40.76
	FF	0.978	49.75	0.022	-20.72	0.000	48.86	0.998	50.33	0.002	-23.69	0.000	50.80

Index	Period	RCP4.5						RCP8.5					
		Portion of increased areas	Regional increase, %	Portion of decreased areas	Regional decrease, %	No change areas	Difference in whole area	Portion of increase areas	Regional increase, %	Portion of decreased areas	Regional decrease, %	No change areas	Difference in whole area
Rx5D	NF	0.941	45.27	0.059	-18.50	0.000	40.82	0.761	39.67	0.238	-17.38	0.001	26.39
	MF	0.939	42.00	0.060	-17.54	0.000	37.76	0.984	43.82	0.016	-20.72	0.000	42.82
	FF	0.987	53.69	0.013	-19.46	0.000	53.50	0.997	52.30	0.003	-24.18	0.000	52.68
R95PT	NF	0.556	20.48	0.444	-12.16	0.000	6.18	0.524	19.88	0.476	-12.84	0.000	4.66
	MF	0.564	19.79	0.436	-10.98	0.000	6.42	0.734	20.38	0.266	-11.27	0.000	12.08
	FF	0.742	21.45	0.258	-10.85	0.000	13.53	0.987	21.34	0.013	-14.35	0.000	21.37
SDII	NF	0.857	23.12	0.143	-11.19	0.000	17.22	0.981	27.74	0.019	-11.66	0.000	14.06
	MF	0.986	22.86	0.014	-11.44	0.000	21.57	0.999	27.19	0.001	-18.19	0.000	22.66
	FF	0.995	26.79	0.005	-12.71	0.000	26.32	0.997	32.31	0.003	-19.37	0.000	30.29
PRCPTOT	NF	0.992	28.48	0.008	-12.40	0.000	27.10	0.849	18.88	0.151	-11.35	0.000	25.49
	MF	0.992	27.85	0.008	-16.12	0.000	26.21	0.996	23.45	0.004	-13.36	0.000	26.22
		0.998	34.90	0.002	-19.00	0.000	34.34	1.000	30.50	0.000	0.00	0.000	31.65

Remark: NF: near future, MF: middle future, FF: far future

Table 8. Changes of standard deviation extreme rainfall indices

Index	Period	RCP4.5						RCP8.5					
		Portion of increased areas	Regional increase, %	Portion of decreased areas	Regional decrease, %	No change areas	Difference in whole area	Portion of increase areas	Regional increase, %	Portion of decreased areas	Regional decrease, %	No change areas	Difference in whole area
CDD	NF	0.504	173.61	0.256	-57.72	0.240	67.13	0.424	144.04	0.042	-57.01	0.535	56.85
	MF	0.495	184.45	0.276	-57.20	0.229	65.78	0.776	163.36	0.177	-59.65	0.047	115.18
	FF	0.780	182.36	0.137	-59.22	0.083	126.65	0.829	173.98	0.100	-61.53	0.072	134.36
CWD	NF	0.792	265.74	0.208	-65.72	0.000	191.11	0.879	269.42	0.121	-64.88	0.000	226.08
	MF	0.871	268.05	0.129	-68.87	0.000	220.38	0.901	321.26	0.099	-69.21	0.000	279.45
	FF	0.895	340.97	0.104	-65.36	0.000	295.60	0.764	326.77	0.236	-69.55	0.000	237.76
R10mm	NF	0.575	146.79	0.268	-56.59	0.157	71.55	0.260	139.52	0.433	-60.22	0.307	15.08
	MF	0.303	145.74	0.520	-58.74	0.177	17.89	0.506	155.96	0.184	-60.81	0.310	67.89
	FF	0.509	152.14	0.346	-58.78	0.145	63.82	0.595	182.54	0.355	-60.68	0.050	93.16
R20mm	NF	0.578	175.11	0.236	-57.90	0.186	84.93	0.399	157.18	0.313	-58.90	0.288	43.93
	MF	0.634	191.53	0.298	-61.39	0.069	110.60	0.655	187.68	0.271	-58.97	0.074	109.24
	FF	0.827	185.48	0.154	-60.38	0.019	150.54	0.897	193.45	0.076	-61.62	0.027	174.12
Rx1D	NF	0.188	253.68	0.812	-66.29	0.000	-3.95	0.183	245.11	0.817	-65.40	0.000	-3.21
	MF	0.222	246.91	0.778	-67.02	0.000	6.97	0.365	241.81	0.635	-67.64	0.000	51.87
	FF	0.136	256.05	0.862	-69.92	0.001	-23.90	0.680	252.00	0.320	-67.62	0.000	158.93
Rx3D	NF	0.677	249.25	0.321	-66.21	0.002	151.60	0.540	244.60	0.460	-66.25	0.000	108.26
	MF	0.707	233.56	0.291	-66.39	0.002	148.99	0.755	261.22	0.245	-66.19	0.000	186.76
	FF	0.674	279.04	0.326	-67.81	0.000	172.85	0.929	284.53	0.071	-68.85	0.000	264.66

Index	Period	RCP4.5						RCP8.5					
		Portion of increased areas	Regional increase, %	Portion of decreased areas	Regional decrease, %	No change areas	Difference in whole area	Portion of increase areas	Regional increase, %	Portion of decreased areas	Regional decrease, %	No change areas	Difference in whole area
Rx5D	NF	0.834	275.84	0.166	-68.03	0.000	220.73	0.776	249.07	0.224	-67.01	0.000	179.90
	MF	0.886	253.24	0.113	-66.76	0.001	218.29	0.918	283.44	0.082	-66.61	0.000	258.08
	FF	0.871	315.40	0.129	-66.41	0.000	270.27	0.966	333.19	0.034	-67.55	0.000	325.47
R95PT	NF	0.775	226.96	0.219	-61.94	0.006	164.07	0.717	219.37	0.275	-62.13	0.007	145.84
	MF	0.778	215.10	0.216	-62.85	0.006	159.32	0.780	227.69	0.217	-64.02	0.003	171.04
	FF	0.727	239.45	0.265	-62.39	0.008	163.19	0.914	238.68	0.084	-62.58	0.002	216.46
SDII	NF	0.818	214.51	0.102	-56.87	0.079	206.18	0.358	162.13	0.438	-58.62	0.204	141.48
	MF	0.635	196.06	0.281	-59.00	0.084	236.09	0.795	188.38	0.071	-57.43	0.134	259.99
	FF	0.883	203.73	0.114	-58.77	0.003	266.73	0.970	200.93	0.016	-68.69	0.014	320.98
PRCPTOT	NF	0.782	277.95	0.217	-64.72	0.001	170.43	0.738	215.78	0.254	-64.43	0.007	31.45
	MF	0.885	271.85	0.112	-62.89	0.004	115.35	0.915	289.32	0.085	-65.21	0.000	145.81
	FF	0.918	294.46	0.082	-64.45	0.000	174.17	0.995	320.02	0.005	-61.93	0.000	195.29

Remark: NF: near future, MF: middle future, FF: far future

Table 9. Consistency of mean extreme rainfall indices

Index	Period	RCP4.5						RCP8.5					
		Portion of increased areas	Regional increase, %	Portion of decreased areas	Regional decrease, %	No change areas	Difference in whole area	Portion of increase areas	Regional increase, %	Portion of decreased areas	Regional decrease, %	No change areas	Difference in whole area
CDD	NF	0.526	8.72	0.126	-5.95	0.348	3.68	0.518	7.94	0.048	-6.23	0.434	3.78
	MF	0.480	11.95	0.283	-6.32	0.237	3.35	0.736	15.04	0.223	-7.33	0.041	8.56
	FF	0.636	9.01	0.182	-8.20	0.182	3.84	0.936	21.75	0.063	-9.42	0.001	18.95
CWD	NF	0.821	40.93	0.179	-34.90	0.000	26.90	0.729	41.59	0.271	-36.93	0.000	21.15
	MF	0.852	43.66	0.148	-34.66	0.000	31.44	0.849	44.54	0.151	-34.59	0.000	33.48
	FF	0.873	46.33	0.127	-35.08	0.000	36.22	0.718	45.53	0.282	-38.21	0.000	24.04
R10mm	NF	0.949	25.76	0.051	-18.87	0.000	23.06	0.956	25.30	0.044	-21.21	0.000	22.82
	MF	0.998	42.08	0.002	-22.22	0.000	41.68	0.997	53.27	0.003	-21.54	0.000	53.16
	FF	0.999	56.96	0.001	-23.57	0.000	57.12	0.998	60.18	0.002	-26.88	0.000	60.18
R20mm	NF	0.415	24.61	0.585	-25.16	0.000	-5.24	0.429	22.69	0.570	-22.55	0.001	-4.39
	MF	0.922	37.89	0.078	-24.89	0.000	32.44	0.973	47.16	0.027	-25.94	0.000	45.02
	FF	0.983	53.45	0.017	-28.98	0.000	51.78	0.996	61.84	0.004	-23.86	0.000	61.70
Rx1D	NF	0.717	26.44	0.282	-20.69	0.000	12.64	0.624	26.00	0.374	-23.47	0.001	7.44
	MF	0.833	33.81	0.167	-20.61	0.000	23.67	0.931	40.53	0.069	-20.67	0.000	35.59
	FF	0.962	43.44	0.038	-22.04	0.000	40.31	0.996	63.54	0.004	-22.05	0.000	63.29
Rx3D	NF	0.885	30.09	0.115	-22.34	0.000	23.44	0.671	27.13	0.328	-23.20	0.001	10.55
	MF	0.882	35.42	0.118	-17.92	0.000	28.04	0.970	43.94	0.030	-20.62	0.000	41.47
	FF	0.978	45.53	0.022	-23.11	0.000	43.37	0.998	65.29	0.002	-22.00	0.000	65.03

Index	Period	RCP4.5						RCP8.5					
		Portion of increased areas	Regional increase, %	Portion of decreased areas	Regional decrease, %	No change areas	Difference in whole area	Portion of increase areas	Regional increase, %	Portion of decreased areas	Regional decrease, %	No change areas	Difference in whole area
Rx5D	NF	0.941	29.89	0.059	-19.62	0.000	26.43	0.761	25.88	0.238	-20.70	0.001	14.88
	MF	0.939	35.64	0.060	-15.29	0.000	31.84	0.984	45.84	0.016	-20.31	0.000	44.50
	FF	0.987	47.00	0.013	-23.86	0.000	45.58	0.997	66.24	0.003	-22.67	0.000	66.00
R95PT	NF	0.556	31.38	0.444	-25.81	0.000	5.66	0.524	27.86	0.476	-27.01	0.000	2.16
	MF	0.564	32.19	0.436	-26.42	0.000	5.93	0.734	36.67	0.266	-29.97	0.000	18.14
	FF	0.742	36.75	0.258	-27.42	0.000	19.55	0.987	53.45	0.013	-29.08	0.000	51.80
SDII	NF	0.857	38.37	0.143	-30.63	0.000	27.96	0.981	23.94	0.019	-13.81	0.000	26.28
	MF	0.986	53.06	0.014	-34.93	0.000	52.03	0.999	48.46	0.001	-17.14	0.000	60.42
	FF	0.995	62.70	0.005	-35.00	0.000	62.44	0.997	66.25	0.003	-21.00	0.000	69.72
PRCPTOT	NF	0.992	25.36	0.008	-15.60	0.000	24.51	0.849	36.10	0.151	-31.34	0.000	23.27
	MF	0.992	40.33	0.008	-15.37	0.000	39.77	0.996	60.34	0.004	-30.50	0.000	48.55
	FF	0.998	53.63	0.002	-21.25	0.000	53.63	1.000	69.73	0.000	0.00	0.000	66.42

Remark: NF: near future, MF: middle future, FF: far future

Table 10. Consistency of standard deviation extreme rainfall indices

Index	Period	RCP4.5						RCP8.5					
		Portion of increased areas	Regional increase, %	Portion of decreased areas	Regional decrease, %	No change areas	Difference in whole area	Portion of increase areas	Regional increase, %	Portion of decreased areas	Regional decrease, %	No change areas	Difference in whole area
CDD	NF	0.504	9.03	0.256	-7.86	0.240	2.28	0.424	7.50	0.042	-6.10	0.535	2.81
	MF	0.495	8.61	0.276	-6.75	0.229	2.08	0.776	11.43	0.177	-7.06	0.047	7.27
	FF	0.780	10.15	0.137	-6.62	0.083	6.65	0.829	11.11	0.100	-9.90	0.072	7.91
CWD	NF	0.792	25.78	0.208	-18.73	0.000	15.91	0.879	30.14	0.121	-21.88	0.000	23.78
	MF	0.871	30.71	0.129	-23.12	0.000	23.61	0.901	33.38	0.099	-19.74	0.000	27.58
	FF	0.895	30.72	0.104	-21.53	0.000	25.23	0.764	28.73	0.236	-21.50	0.000	17.83
R10mm	NF	0.575	7.84	0.268	-6.48	0.157	3.02	0.260	5.99	0.433	-6.84	0.307	-1.07
	MF	0.303	7.07	0.520	-6.72	0.177	-0.93	0.506	7.15	0.184	-7.14	0.310	2.30
	FF	0.509	7.41	0.346	-7.03	0.145	1.91	0.595	8.36	0.355	-8.88	0.050	2.60
R20mm	NF	0.578	11.50	0.236	-7.77	0.186	4.31	0.399	10.42	0.313	-7.85	0.288	1.77
	MF	0.634	12.96	0.298	-7.68	0.069	6.62	0.655	14.98	0.271	-8.76	0.074	7.33
	FF	0.827	16.94	0.154	-9.86	0.019	13.49	0.897	20.25	0.076	-12.64	0.027	17.90
Rx1D	NF	0.188	21.32	0.812	-23.20	0.000	-14.73	0.183	22.20	0.817	-24.55	0.000	-15.60
	MF	0.222	19.38	0.778	-21.34	0.000	-11.95	0.365	22.27	0.635	-21.19	0.000	-4.61
	FF	0.136	25.16	0.862	-22.62	0.001	-15.85	0.680	26.60	0.320	-20.79	0.000	12.44
Rx3D	NF	0.677	21.82	0.321	-17.80	0.002	9.54	0.540	22.60	0.460	-18.08	0.000	4.62
	MF	0.707	22.44	0.291	-17.56	0.002	11.26	0.755	24.93	0.245	-16.26	0.000	15.33
	FF	0.674	24.18	0.326	-15.85	0.000	11.80	0.929	36.36	0.071	-17.20	0.000	33.33

Index	Period	RCP4.5						RCP8.5					
		Portion of increased areas	Regional increase, %	Portion of decreased areas	Regional decrease, %	No change areas	Difference in whole area	Portion of increase areas	Regional increase, %	Portion of decreased areas	Regional decrease, %	No change areas	Difference in whole area
Rx5D	NF	0.834	24.24	0.166	-17.70	0.000	17.40	0.776	24.22	0.224	-16.72	0.000	15.24
	MF	0.886	25.03	0.113	-17.18	0.001	20.72	0.918	27.48	0.082	-15.39	0.000	24.15
	FF	0.871	28.35	0.129	-17.45	0.000	23.13	0.966	39.53	0.034	-16.50	0.000	38.50
R95PT	NF	0.775	21.83	0.219	-11.54	0.006	14.87	0.717	20.46	0.275	-11.45	0.007	12.12
	MF	0.778	18.24	0.216	-10.21	0.006	12.40	0.780	22.75	0.217	-12.73	0.003	15.69
	FF	0.727	17.53	0.265	-12.21	0.008	10.01	0.914	27.69	0.084	-11.24	0.002	24.93
SDII	NF	0.818	11.88	0.102	-6.61	0.079	12.03	0.358	9.67	0.438	-7.39	0.204	10.95
	MF	0.635	10.39	0.281	-8.03	0.084	15.32	0.795	14.95	0.071	-5.48	0.134	23.44
	FF	0.883	16.50	0.114	-8.53	0.003	21.85	0.970	20.30	0.016	-9.81	0.014	39.00
PRCPTOT	NF	0.782	19.12	0.217	-12.82	0.001	9.02	0.738	20.25	0.254	-14.59	0.007	0.24
	MF	0.885	18.64	0.112	-13.09	0.004	4.97	0.915	26.09	0.085	-12.30	0.000	11.50
	FF	0.918	23.94	0.082	-10.97	0.000	14.34	0.995	38.44	0.005	-8.60	0.000	19.97

Remark: NF: near future, MF: middle future, FF: far future

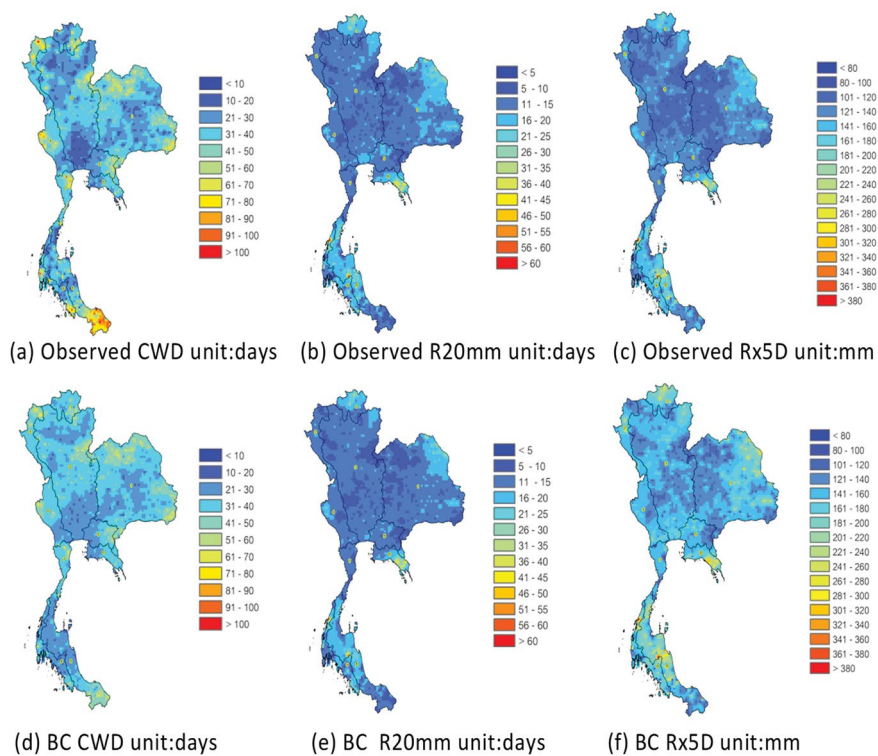


Figure 3. Comparison of CWD, R20mm and Rx5D between observed and bias corrected indices

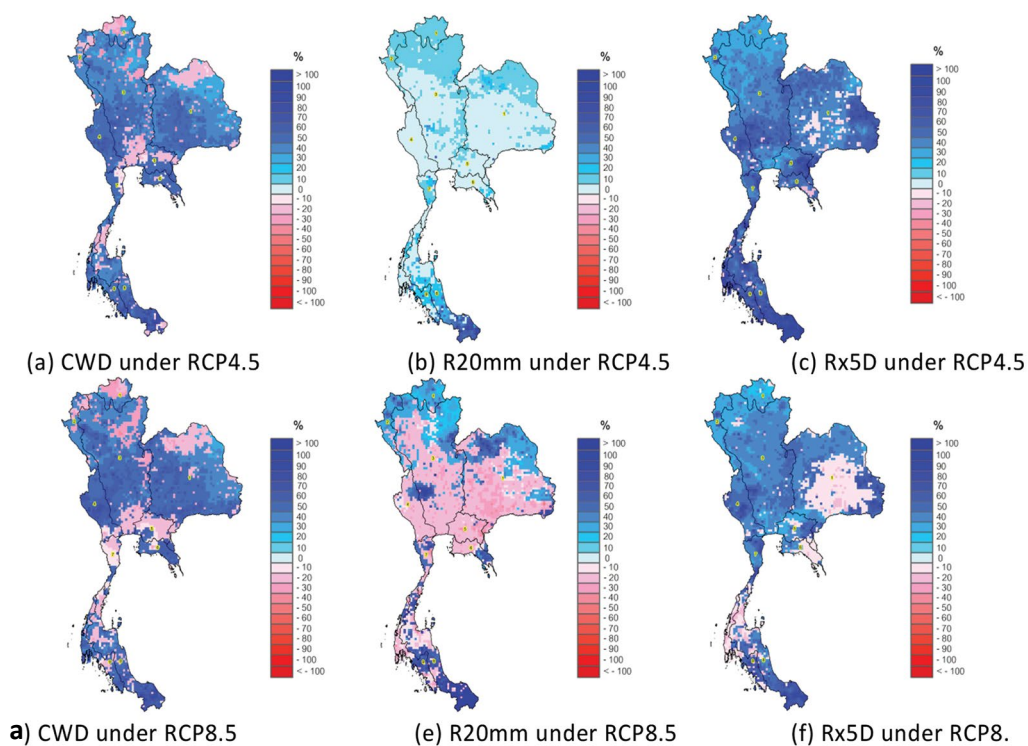


Figure 4. Changes in mean of CWD, R20mm and Rx5D indices in near future period

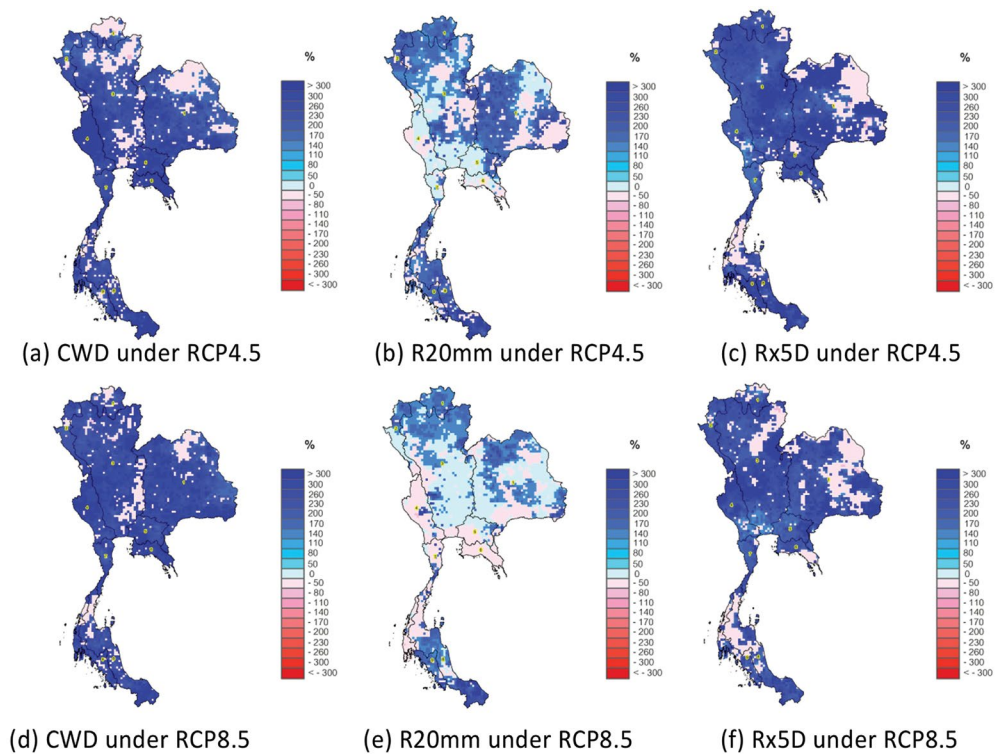


Figure 5. Changes in standard deviation of CWD, R20mm and Rx5D indices in near future period

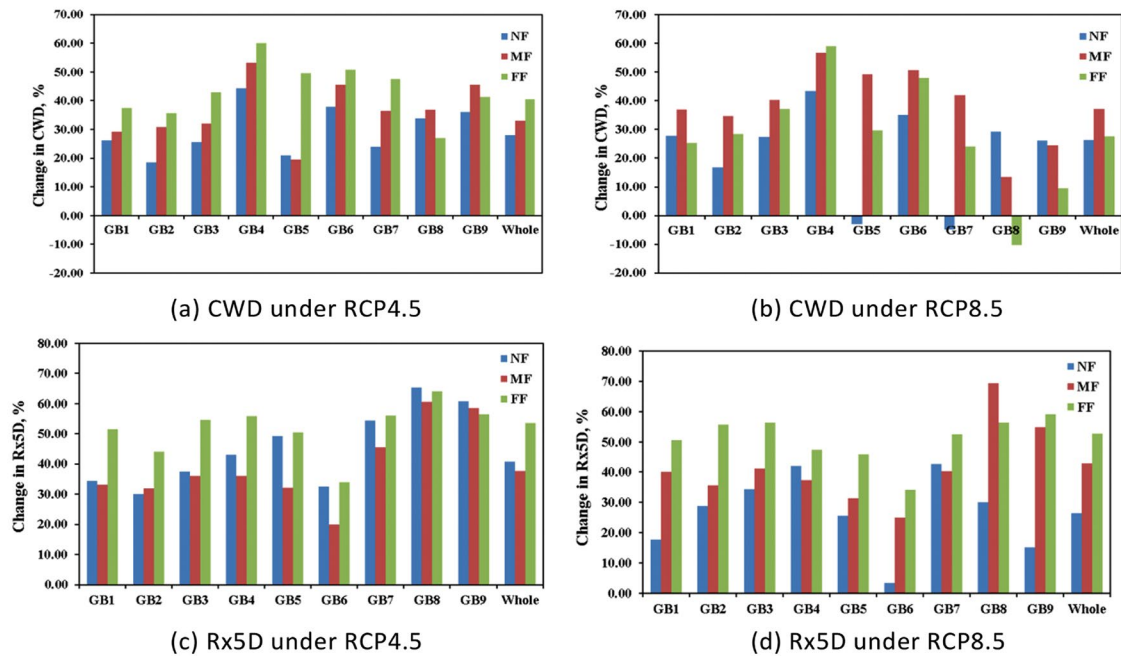


Figure 6. Changes in mean of CWD and Rx5D indices in all periods in 9 group river basins

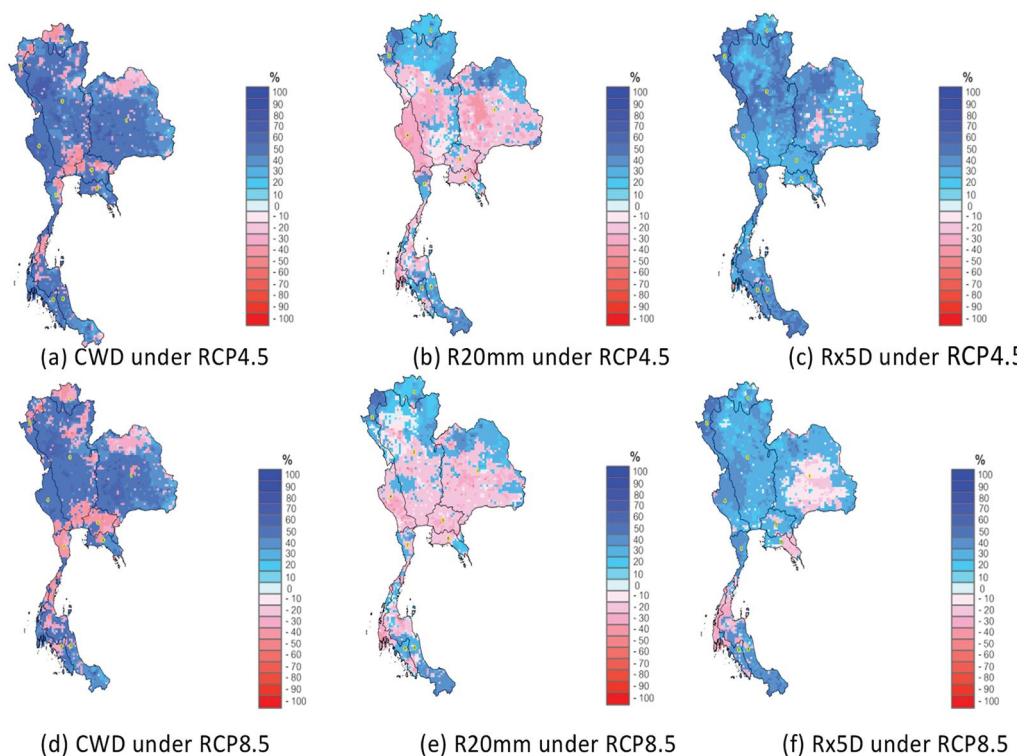


Figure 7. Consistency in mean of CWD, R20mm and Rx5D indices in near future period

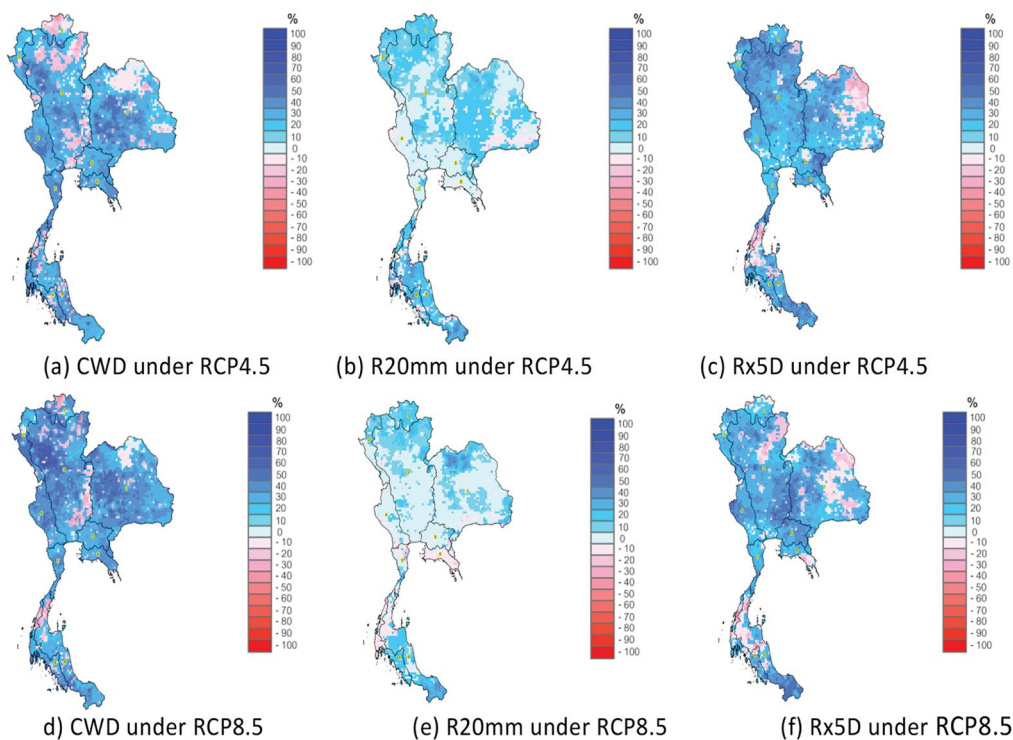
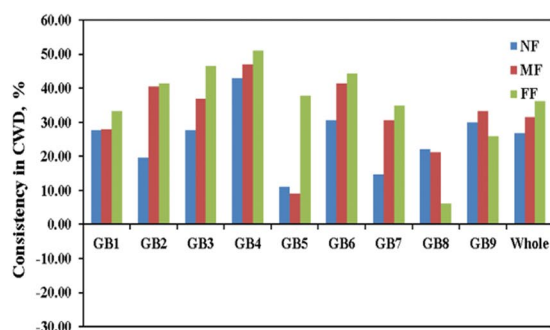
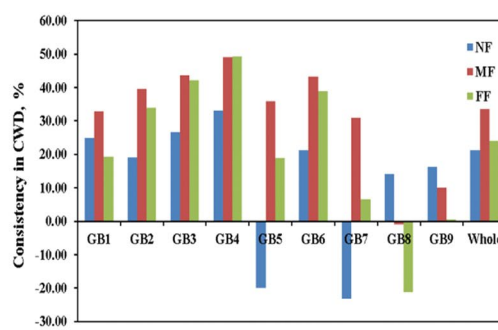


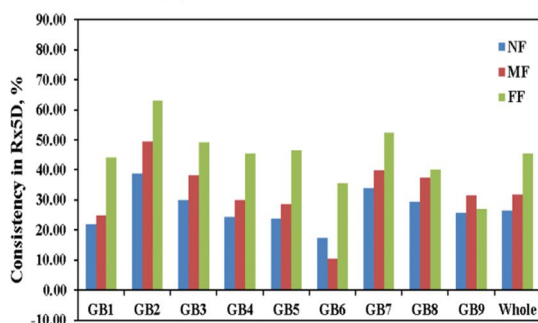
Figure 8. Consistency in standard deviation of CWD, R20mm and Rx5D indices in near future period



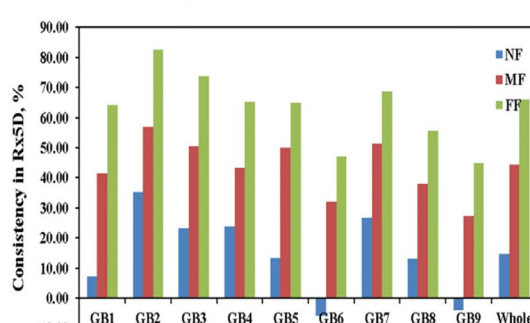
(a) CWD under RCP4.5



(b) R20mm under RCP8.5



(c) Rx5D under RCP4.5



(d) Rx5D under RCP8.5

Figure 9. Consistency in mean of CWD and Rx5D indices in near future period in 9 group river basins

Acknowledgement: The authors gratefully acknowledge the contributions of the Thai Meteorology Department and APEC Climate Center for CMIP5 GCM precipitation data distribution and many thanks to Hydro-Informatics Institute (HII) for supporting the computing facilities for this manuscript.

References

1. Pao-Shin, C., Den-Jing, C., Pay-Liam, L., *Trends in precipitation extremes during the typhoon season in Taiwan over the last 60 years.*
2. Kiktev, D., Sexton, D. M. H., Alexander, L., & Folland, C. K. (2003), *Comparison of modeled and observed trends in indices of daily climate extremes.* *Journal of Climate*, 16(22), 3560–3571. [https://doi.org/10.1175/1520-0442\(2003\)016<3560:COMAOT>2.0.CO;2](https://doi.org/10.1175/1520-0442(2003)016<3560:COMAOT>2.0.CO;2)
3. K. Kamiguchi, A. Kitoh, T. Uchiyama, R. Mizuta, A. Noda. *Changes in precipitation-based extremes indices due to global warming projected by a global 20-km-mesh atmospheric model SOLA*, 2 (2006), pp. 64-67, 10.2151/sola.2006-017.
4. Kharin, V. V., Zwiers, F. W., Zhang, X. B., & Hegerl, G. C. (2007), *Changes in temperature and precipitation extremes in the IPCC ensemble of global coupled model simulations.* *Climatic Change*, 119(2), 345–357. <https://doi.org/10.1007/s10584-013-0705-8>.
5. Rusticucci, M. et al., (2010), *An intercomparison of model-simulated in extreme rainfall and temperature events during the last half of the twentieth century. Part 1: mean values and variability.* *Clim. Change*, 98(3-4), 493-508, doi: 10.1007/s10584-009-9742-8.
6. Atsamon, L., Patama, S., (2016), *Long-term trends and variability of total and extreme precipitation in Thailand.* *Atmospheric Research*, 169, 301-317. <http://dx.doi.org/10.1016/j.atmosres.2016.05.016>.

7. Wang, F., Yang, S., Higgins, W., Li, Q.P., Zuo, Z.Y., (2014), *Long-term changes in total and extreme precipitation over China and the United States and their links to oceanic atmospheric features*. *Int. J. Climatol* 34 (2), 286–302.
8. Hyunrok Lee and Sang-Cheol Kim, New CLICK (CLIK3.0) *Climate Information toolkit User manual*, APEC Climate Center, Draft ver.1, 2014.10.
9. Agha Kouchak, A. (2013). *Extremes in a changing climate: Detection, analysis and uncertainty*. Dordrecht: Springer.
10. Zhang, X., et al., (2011), *Indices for monitoring changes in extremes based on daily temperature and precipitation data*. *WIREs Clim. Chang.* 2 (6), 851–870. <http://dx.doi.org/10.1002/wcc.147>.
11. Klein Tank, A.M.G., Zwiers, F.W., Zhang, Z., (2009), *Guidelines on analysis of extremes in a changing climate in support of informed decisions for adaptation*. WMO-TD No.1500 (56 pp. (WCDMP-72, WMO-TD/No. 1500)).
12. Vuuren, P. D. V., Edmonds J., Kainuma M., Riahi K., Thomson A., Hibbard K., Hurtt G. C., Kram T., Krey V., Lamarque J. F., Masui T., M. Meinshausen, Nakicenovic N., Smith S. J., Rose S. K., *The representative concentration pathways: an overview*, *Climatic Change*, November 2011, Vol. 109, Issue 1, pp 5–31.
13. Binaya Kumar Mishra, Srikantha Herath, *Assessment of Future Floods in the Bagmati River Basin of Nepal Using Bias-Corrected Daily GCM Precipitation Data* March 2014 *Journal of Hydrologic Engineering* 20(8): 05014027 DOI: 10.1061/(ASCE)HE.1943-5584.0001090.
14. Mishra, B. and Herath, S. (2011), *Climate projections downscaling and impact assessment on precipitation over upper Bagmati River Basin, Nepal*. *Proc., Int. Conf. on Addressing Climate Change for Sustainable Development through Up-Scaling Renewable Energy Technologies*, Institute of Engineering, Tribhuvan Univ., Kathmandu, Nepal, pp. 275–281.
15. Groisman PY, Knight RW, Easterling DR, Karl TR, Hegerl GC, Razuvaev VN (2005), *Trends in intense precipitation in the climate record*. *J Clim* 18:1326–1350.
16. Lomax, Richard G. (2007), *Statistical Concepts: A Second Course*. p. 10. ISBN 0-8058-5850-4.
17. Fisher, R. A., and F. Yates: *Statistical Tables for Biological, Agricultural and Medical Research*. 6th Ed. Oliver & Boyd, Edinburgh and London 1963. X, 146 P. Preis 42 s net <https://doi.org/10.1002/bimj.19710130413>.
18. Wang, G., (2005), *Agriculture drought in a future climate: results from 15 global climate models participating in the IPCC 4th assessment*. *Clim. Dynam.*, 25, 739–753.
19. Kim, D.-W., and H.-R. Byun, (2009), *Future pattern of Asian drought under global warming scenario*. *Theor. Appl. Climatol.*, 98, 137–150.
20. Willmott, C.J. *Some comments on the evaluation of model performance*. *Bulletin of the American Meteorological Society* 1982; 63: 1309–1313.
21. Willmott, C.J., Ackleson, S.G., Davis, R.E., Feddema, 938 J.J., Klink, K.M., Legates, D.R., et al. *Statistics for the evaluation and comparison of models*. *Journal of Geophysical Research: Oceans* 1985; 90: 8995–9005.
22. Willmott, C.J., Matsuura, K. *Advantages of the mean absolute error (MAE) over the root mean square error (RMSE) in assessing average model performance*. *Climate research* 2005; 30: 79–82.
23. Yapo P. O., Gupta H. V., Sorooshian S., (1996), *Automatic calibration of conceptual rainfall-runoff models: sensitivity to calibration data*. *Journal of Hydrology*. v181 i1–4. 23–48.
24. Sorooshian, S., Q. Duan, and V. K. Gupta. (1993), *Calibration of rainfall-runoff models: Application of global optimization to the Sacramento Soil Moisture Accounting Model*, *Water Resources Research*, 29 (4), 1185–1194, doi:10.1029/92WR02617.
25. Roebber, Paul J. (1998), *"The Regime Dependence of Degree Day Forecast Technique, Skill, and Value"*, *American Meteorological Society -- Weather and Forecasting*, 13 (3): 783–794,

Bibcode:1998WtFor..13..783R, doi:10.1175/1520-0434(1998)013<0783:TRDODD>2.0.CO;2.

26. Murphy, Allen H. (1988), *"Skill Scores Based on the Mean Square Error and Their Relationships to the Correlation Coefficient"*, *American Meteorological Society -- Monthly Weather Review*, 116 (12): 2417–2424, Bibcode:1988MWRv..116.2417M, doi:10.1175/1520-0493(1988)116<2417:SSBOTM>2.0.CO;2.

IMPACT ASSESSMENT OF CLIMATE CHANGE ON INDUSTRY AND TRADE IN BINH THUAN PROVINCE

Mai Van Khiem, Le Anh Ngoc, Vo Thi Nguyen, Huynh Thi My Linh

Viet Nam institute of Meteorology, Hydrology and Climate Change

Received: 15 January 2019; Accepted: 26 february 2019

Abstract: *This paper presents the results of assessing the impacts of climate change (CC) on industry and trade in Binh Thuan province. Assessing the impacts of climate change at the present and in the future. The temperature and rainfall scenarios used are RCP4.5 and RCP8.5. Flooded scenario for both the present and the future is calculated with 20% flood frequency. Evaluation results show that CC impacts on the fields of Industry and Trade as: electricity production, seafood processing, minerals processing, factories, industrial clusters, traditional craft villages, trade centres, supermarkets, markets, petroleum stores, warehouses.*

Keywords: *Climate change impact, industry and trade, Binh Thuan Province.*

1. Introduction

The climate of Binh Thuan province has typical characteristics of the monsoon tropical climate. Binh Thuan is a coastal province with an area of 7,943.9km², a population of 1,230,417 thousand people [7].

The meteorological and hydrological factors change due to the impacts of climate change. Both rainfall and temperature tend to increase compared to previous years. Specifically, in 33 years (1984-2017), the annual average temperature at Phan Thiet station increased by 0.213°C/decade and the annual rainfall increased by 1.6mm/year. According to satellite observation data, in the period of 1993-2013 the sea level tends to increase by 42mm/decade [1].

Based on the results of climate trend assessment and climate change scenarios for Binh Thuan province, this study assesses the impact of climate change on industry and trade in the fields of electricity production, seafood processing, minerals processing, factories,

industrial clusters, traditional craft villages, trade centres, supermarkets, markets, petroleum stores, warehouses. The results of climate change impact assessment would contribute to build action plan to respond to climate change for industry and trade sector in Binh Thuan.

2. Data and methodology

2.1. Data

The temperature and rainfall scenarios are RCP 4.5 and RCP8.5, based on the approach of climate change scenarios of the Ministry of Natural Resources and Environment in 2016. Flooded scenario for both the present and the future is calculated with 20% flood frequency.

Climate change scenarios for Binh Thuan Province are based on results of the completed projects Technical Consultancy for present and future climate data and analyses for water management in Luy River Basin, Bac Binh District, Binh Thuan Province.

The collected map includes: map of Binh Thuan province, industry and trade status in 2016 and development plans for Binh Thuan industry and trade in the period of 2016 - 2020, vision to 2030 [2-3].

Corresponding author: Le Anh Ngoc
E-mail: leanhngoc.sihymecc@gmail.com

2.2. Methodology

Assessing the impact of climate change on the industry and trade of Binh Thuan province including: qualitative and quantitative

Evaluation based on scenarios of temperature, rainfall, flood calculation according to CC scenarios.

The methods used to assess impacts include:

- Numerical modelling method: using models to predict future impacts through extrapolation of the observed climate factors in the past.
- Extrapolation of historical data: used in statistical research of past data on impacts of climate change on economic and social sectors.
- Expert method: analytical methods on the opinions of experts on the impact of climate change on the object under

consideration, through interviews or conferences and seminars.

- Impact assessment map: overlapping administrative and hydrological maps of VN2000 reference system, results of climate change scenarios of MONRE, flooding scenario of 20%.

3. Results and discussion

3.1. Evaluate the impact of flooding

Overlaying the current flooded map in 2016 (Figure 1) and Binh Thuan province industry and trade status in 2016 map. The results show that the flood area is from 0.1 to 1.3% compared to natural land area. Districts have large flooded areas such as Phan Thiet (14.2%), Bac Binh (3.2%), Ham Tan (2.3%) (Table 1).

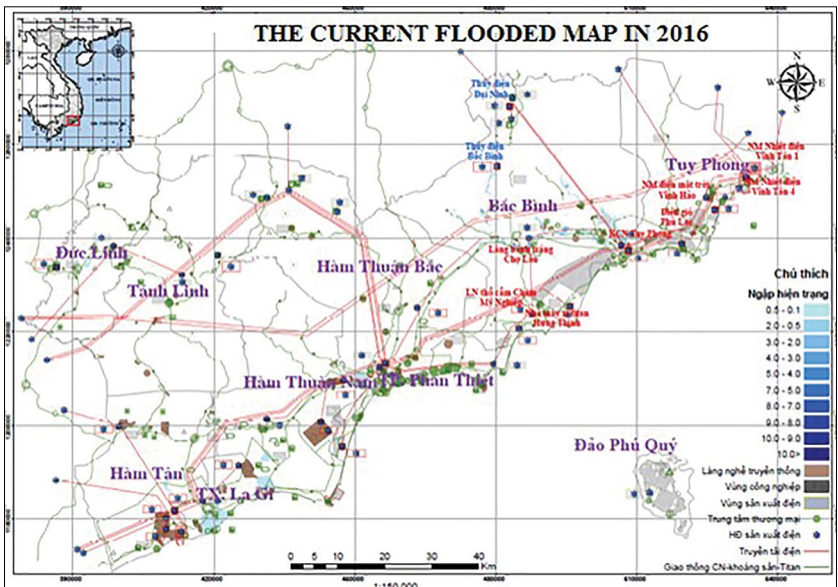


Figure 1. The current flooded map in 2016

Table 1. Total current flooded area in 2016

District	Flooded area (ha)	Natural land area (ha)	Rate (%)
Bac Binh	5,906	186,882	3.2
Tuy Phong	91	79,385	0.1
Duc Linh	649	53,491	1.2
Ham Thuan Bac	1,248	117,442	1.1
Ham Thuan Nam	380	135,044	0.3
La Gi	1,428	106,279	1.3
Phan Thiet	3,010	18,541	14.2
Ham Tan	224	21,168	1.0

Up to 2030, the flood area is up to 1.5%, compared to natural land area. There are

several districts with large flooded areas such as Phan Thiet (14.9%), Bac Binh (3.2%).

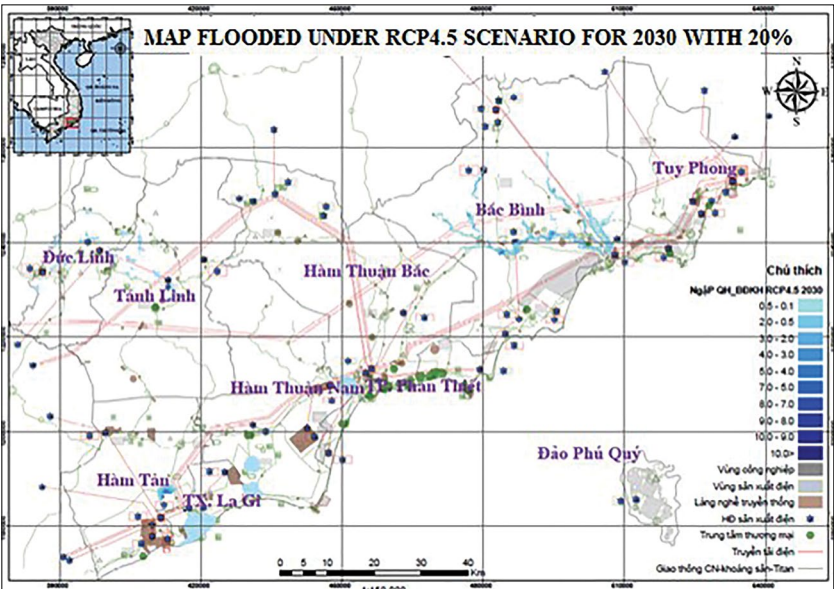


Figure 2. Map flooded under RCP4.5 scenario for 2030 with 20% flood frequency

Table 2. Total flooded area under RCP4.5 scenario for 2030 with 20% flood frequency

District	Flooded area (ha)	Natural land area (ha)	Rate (%)
Bac Binh	4,566	186,882	2.4
Tuy Phong	1	79,386	~0
Duc Linh	802	53,491	1.5
Ham Thuan Bac	856	117,442	0.7
Ham Thuan Nam	409	135,044	0.3
LaGi	1304	106,279	1.2
Phan Thiet	2766	18,541	14.9
Ham Tan	221	21,168	1.0

Overlaying map of flooded under RCP8.5 scenario for 2030 with 20% flood frequency with the planning and development of Binh Thuan province industry and trade in the period of 2016-2020, vision to 2030 (Figure 3). The results show that the flood area is from 0.1 to 1.5% compared to natural land area. Districts have large flooded areas such as Phan Thiet (14.9%), Bac Binh (3.1%) (Table 3).

The area is severely affected by flooding: Vinh Tan (Tuy Phong), Bac Binh hydropower, Song Luy hydropower, Hoa Minh wind power, Hoa Thang wind power and Phan Ri Thanh wind power. Plants that are not affected by flooding are: Dai Ninh hydropower, Phu Lac wind power,

Phong Dien 1.

Main roads through Tuy Phong industrial park; Cham brocade weaving village in Phan Thanh, Binh Duc pottery village in Phan Hiep commune, rice paper village of Lau market will be deeply inundated.

3.2. Evaluate the impact of temperature variation

Under RCP4.5 scenario, the results predict that the annual average temperature of Binh Thuan province will increase from 0.6 to 0.8°C in the early 21st century (2016-2035) in comparison with the base period (1986-2005) (Table 4).

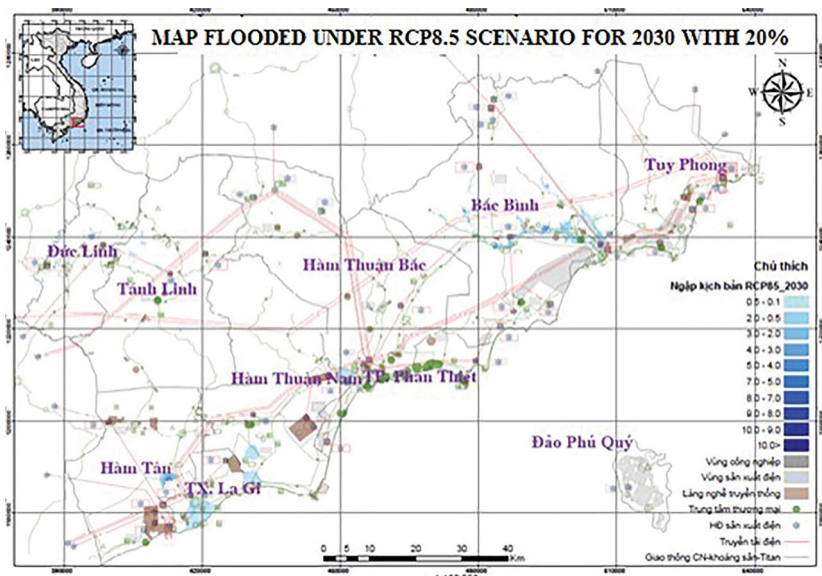


Figure 3. Map flooded under RCP8.5 for 2030 with 20% frequency

Table 3. Total flooded area under RCP8.5 for 2030 with 20% frequency

District	Flooded area (ha)	Natural land area (ha)	Rate (%)
Bac Binh	5,798	186,882	3.1
Tuy Phong	69	79,386	0.1
Duc Linh	802	53,491	1.5
Ham Thuan Bac	418	135,044	0.3
Ham Thuan Nam	1,314	106,279	1.24
La Gi	2,776	18,541	15
Phan Thiet	222	21,168	1
Ham Tan	824	75,309	1

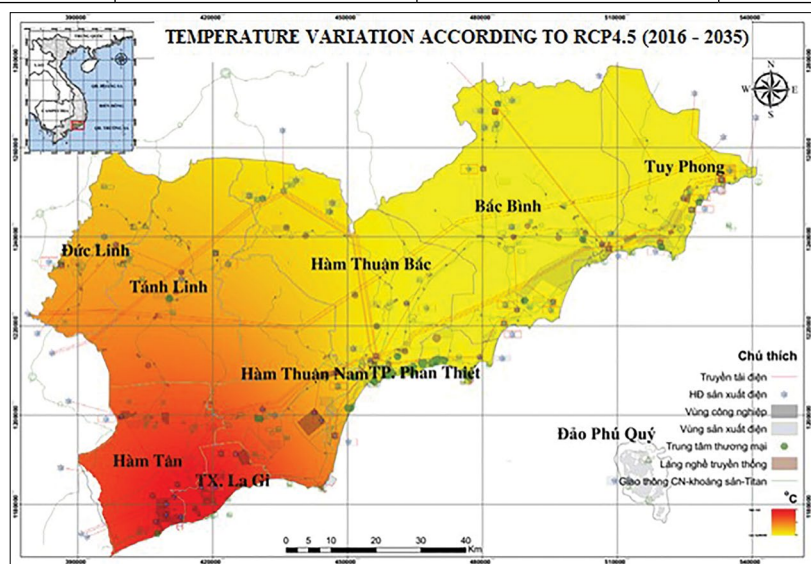


Figure 4. Map of temperature variation according to RCP4.5 scenario in the beginning of the century (2016-2035)

Table 4. Temperature variation according to RCP4.5 scenario in the beginning of the century (2016-2035)

District	Temperature variation (°C)
Phan Thiet	0.7
La Gi	0.6
Tuy Phong	0.6
Bac Binh	0.6
Ham Thuan Bac	0.6
Ham Thuan Nam	0.6
Tanh Linh	0.7
Ham Tan	0.8
Duc Linh	0.6

Under RCP8.5 scenario, the annual average temperature of Binh Thuan province will increase from 0.7 to 0.8°C in the early 21st century (2016-2035), compared to the base period (1986-2005) (Table 5).

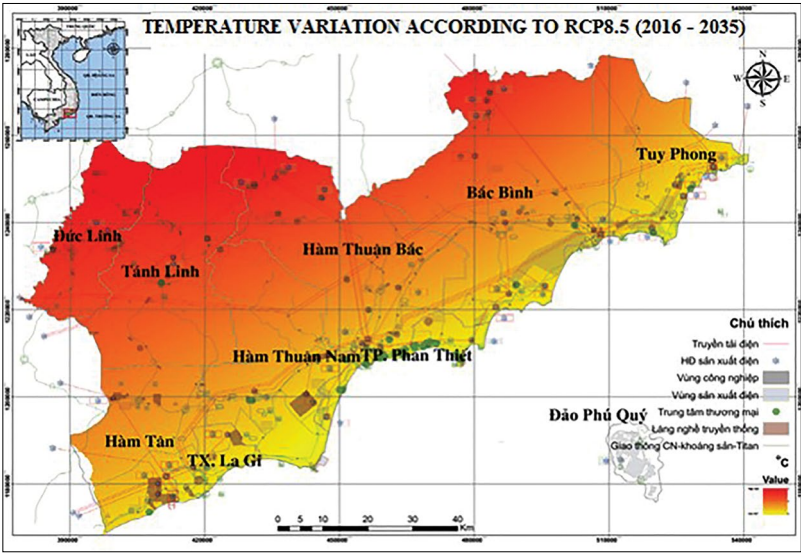


Figure 5. Map of temperature variation according to RCP8.5 scenario in the beginning of the century (2016-2035)

Table 5. Temperature variation according to RCP8.5 scenario in the beginning of the century (2016-2035)

District	Temperature variation (°C)
Phan Thiet	0.7
La Gi	0.6
Tuy Phong	0.6
Bac Binh	0.6
Ham Thuan Bac	0.6
Ham Thuan Nam	0.6
Tanh Linh	0.7
Ham Tan	0.8
Duc Linh	0.6

The annual average temperature in the region such as Tanh Linh, Duc Linh, Ham Thuan Bac, Bac Binh and Tuy Phong quickly increased. These areas concentrated factories, substations, power stations, power transmission lines and auxiliary works of the electricity projects of Binh Thuan province. Hence, increasing temperature will reduce the efficiency of electricity generation, leading to a decrease in power output. Adverse effect on the cooling system of thermal power plants and the range of cooling water quality standards. The increase in temperature accompanied by increased evaporation leads to changes in water reserves and flow into hydroelectric reservoirs. Rising temperatures also reduce the steam turbine thermal cycle performance, causing fuel waste.

Binh Thuan province has fishing centres including: Phan Thiet, La Gi, Phan Ri; in which Phan Ri and Phan Thiet fishing port area under the scenarios of temperature change are strongly influenced by rising temperatures. The change in temperature also affects aquaculture areas, impacts on marine ecosystems, changes in species and marine fish resources.

Titanium mineral processing area in Luong Son, Bac Binh district will be affected by rising temperatures and drought. Increased temperatures, prolonged drought increase cooling costs for processing plants and processing lines.

Vinh Tan thermo-power, Song Binh, Thang Hai 3, Dong Ha and Nam Ha industrial complexes are strongly affected by temperature rise. Increasing temperature also reduces the quality of life of workers, fire, equipment and equipment to reduce quality and longevity.

3.3. Rainfall impact

Under RCP4.5 scenario, the average annual rainfall of Binh Thuan province, except Bac Binh and Ham Thuan Bac districts, will increase from 0.7 to 15% in the early 21st century, compared to the base period (1986-2005) (Table 6).

Under RCP8.5 scenario, the average annual rainfall of Binh Thuan province, except Ham Thuan Bac district, will increase from 2 to 13% in the early 21st century compared to the base period (1986-2005) (Table 7).

Hydropower plants (Dan Sach, Kao Et, Thac Ba, Dan Sach 2, 3, Bom Bi, Song Dinh, Ham Thuan, Da Mi, La Ngau) in the southern districts such as Duc Linh, Tanh Linh, Ham Thuan Bac and Ham Thuan Nam will be affected by rainfall increase. Cost of repair, maintenance, inspection due to prolonged heavy rains cause rust, degradation, flooding is likely raised.

In Ham Thuan Bac district, heavy rainfall combined with flooding of Quao River cause local flooding in Ham Thang, Ham Chinh, Thuan Hoa, Ham Liem and Ham Tri communes which lead to seafood processing damage. In the context of climate change, many extreme phenomena occur such as heavy rain, storms, the exploitation of seafood, especially the offshore fishing is extremely dangerous and difficult. Increasing labour cost, repairing ships, fuel costs, equipment, and difficulties in transportation. Increased rainfall, sudden change in salt concentration caused the death of many species of shellfish and shrimp in Binh Thuan province.

In Suoi Nhum titanium exploiting mine, the collapse of mining pits due to heavy rain has frequently happened. If the waste water treatment system in the mines of inferior titanium mining is polluted in excess of the permissible level, it will be mixed with rainwater flowing into the river, dispersing radioactive substances in the waste water of mining. The impact on the environment is huge.

The main roads through large industrial zones such as Tuy Phong, Bac Binh 1, La Gi, Tan Binh 1, Nam Cang, Phu Hai, Mui Ne, Sung Nhon, Hong Liem Nghia Hoa, Tan Lap, heavy rain will flood deeply, causing damage. Increasing rainfall is the cause of food production. Wet conditions make it harder to store ingredients as food. Plants must increase costs in protection, build stormwater drainage systems.

4. Conclusion

Based on above mentioned data and approach on climate change scenarios for Binh Thuan Province as well as provincial planning of industry and trade, there are some conclusions about the impact of climate change on the fields of Industry and Trade, as follows:

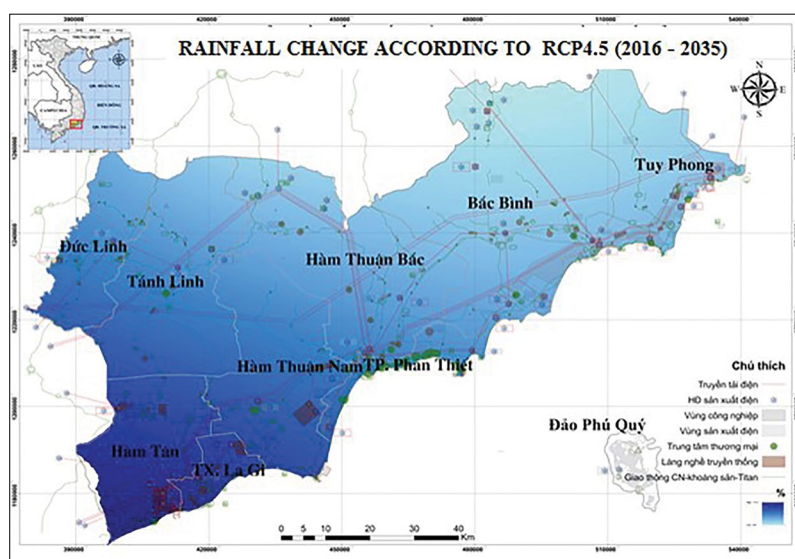


Figure 6. Rainfall change under RCP4.5 scenario for the period 2016-2035

Table 6. Rainfall change under RCP4.5 scenario for the period 2016-2035

District	Rainfall change (%)
Phan Thiet	10.7
La Gi	6.5
Tuy Phong	2.7
Bac Binh	-1.7
Ham Thuan Bac	-1.9
Ham Thuan Nam	0.7
Tanh Linh	2.2
Ham Tan	15.6
Duc Linh	2.6

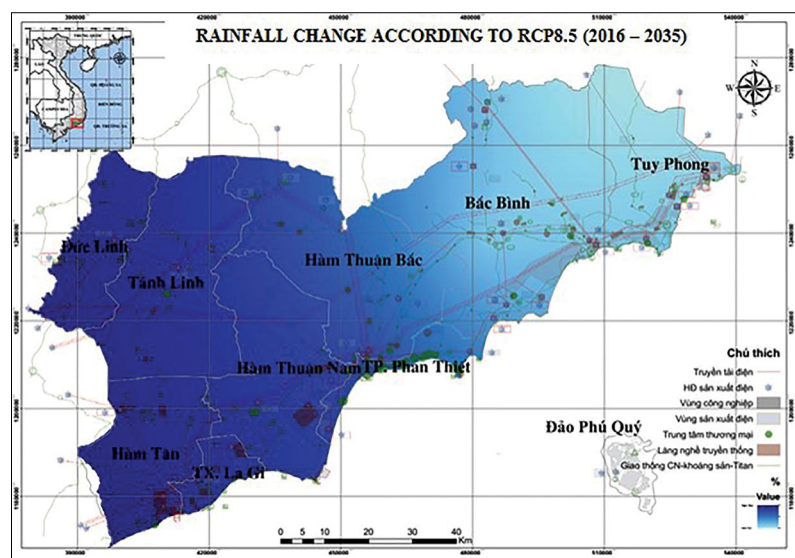


Table 7. Precipitation variation according to RCP8.5 scenario for the period 2016-2035

Table 7. Precipitation variation according to RCP8.5 scenario for the period 2016-2035

District	Rainfall change (%)
Phan Thiet	10.3
La Gi	6.2
Tuy Phong	6.0
Bac Binh	0.0
Ham Thuan Bac	-0.5
Ham Thuan Nam	2.0
Tanh Linh	3.1
Ham Tan	13.3
Duc Linh	2.6

Power production: climate change may lead to increase costs for power production activities during operation, cooling and maintenance. In addition, electric poles, transformer stations, power transmission lines, etc. are overloaded, degraded, damaged due to rising temperatures, rain, extreme climate; prolonged flooding can be dangerous due to electrical leakage.

Seafood processing: changes in temperature and precipitation would impacts on marine ecosystems, loss of diversity and reduction of seafood exploited for processing.

Mineral exploitation and processing: Heavy rain can cause underground mines of titanium to be flooded, makes the equipment damaged.

Heavy rain also is likely to break pits, spill ore and make environmental incidents.

Factories, industrial clusters, traditional craft villages: Roads may be flooded due to heavy and prolonged rain. Heavy rain and prolonged heat could affect the manual production of traditional villages and reduce the number of tourists coming here. Temperature increases, prolonged heat is likely to make fire risk.

Trade centres, supermarkets, markets, petroleum stores, warehouses: Increasing temperature negatively tends to affects the sustainability of buildings, increase electricity consumption and raise cooling costs in trade centres, supermarkets and markets, respectively. The rise in temperature may increases the risk of fire in petroleum stores and warehouses.

Acknowledgement: *This study was carried out and completed thanks to the support of the project Developing action plans to respond to climate change for construction, transportation, industry and tourism sectors and districts in Binh Thuan province*

References

1. Department of Planning and Investment, (2017), *Project "Integrated management of water resources and urban development in relation to climate change in Binh Thuan"*.
2. Department of Industry and Trade, (2017), *Report on implementation of 2017 tasks and orientation for 2018 of Industry and Trade sector*.
3. Department of Industry and Trade, (2012), *Development planning for Industry and Trade in Binh Thuan province to 2020, vision to 2030*.
4. Ministry of Natural Resources and Environment, (2016), *Update results of climate change, sea level rise scenarios for Viet Nam*.
5. Ministry of Industry and Trade, (2010), *Ministry of Industry and Trade's Action Plan to Respond to Climate Change*.
6. 6 Ministry of Industry and Trade, (2010), *Green growth action plan of Industry and Trade sector in the period of 2015-2020*.

IMPACT OF ENSO ON WATER DISCHARGE AND SEDIMENT LOAD IN LOWER MEKONG RIVER

Dang Thi Ha

School of Maritime Economics and Technology, Ba Ria - Vung Tau University

Received: 3 November 2018; Accepted 25 December 2018

Abstract: *The Mekong River is the second largest river basin in Southeast Asia and strongly influenced by climate change. This paper was based on high temporal resolution of water discharge and suspended sediment concentration at Can Tho and My Thuan stations during the 2009-2016 period, showed that the water discharge and sediment supplies by the Mekong strongly varied, and influenced by ENSO events (El Nino Southern Oscillation). Our results obtained showed that during the La Niña event (2010-2011), water supply increased by about 30% and the sediment supply by 55%. In contrast, during the El Niño event (2015-2016) the water supply decreased by 20% and the sediment supply by 50%. Finally, the present water discharge of the Mekong River to the sea can be estimated to be $400\text{km}^3/\text{yr}$, $\pm 100\text{km}^3/\text{yr}$ and the present sediment supply to the sea can be estimated to be $40\text{ Mt}/\text{yr}$, $\pm 20\text{ Mt}/\text{yr}$, depending on ENSO events.*

Keywords: *Mekong; river discharge; sediment; ENSO; El Niño; La Niña*

1. Introduction

The Mekong River is the second largest river basin ($795 \times 103\text{km}^2$) after the Yangtze River ($1.8 \times 106\text{km}^2$) and the third in terms of water discharge (after the Ganges-Brahmaputra and the Yangtze Rivers) in Southeast Asia. In recent years, reservoir operation and climate change have strongly affected on hydrological regime of the Mekong River Basin. Many studies have analyzed the impact of climate variability on hydrological conditions in the Mekong River basin and the El Niño Southern Oscillation (ENSO) indices were widely used (e.g. [2,4,5]). They showed that the ENSO phases significantly influence precipitation, runoff, water level and sediment load in the Mekong River basin. Piton and Delcroix [2], based on data from 43 consecutive years of in situ measurement (1960-2002) and seven years of satellite monitoring (1996-2002), demonstrated that El Niño phases were associated to a decrease in rainfall in the middle and lower Mekong basin and to a

reduction of water discharge at the Chroy Chang Var station (located in Cambodia). The discharge reduction reached 34% during the strong 1997-1998 El Niño. On the other hand, higher discharges were observed during La Niña events [8].

The Mekong River originates from the Tibetan plateau and flows through a narrow deep gorge along with the Salween and Yangtze Rivers that together are known as the "Three Rivers Area". The Mekong River then flows through Myanmar, Laos, Thailand, and Cambodia before it finally drains into the sea creating a large delta in Viet Nam (Figure 1). The Mekong flows in the delta through two main distributaries: the Tien River (generally referred to as the Mekong River, in the delta) in its eastern part, and the Hau River (the "second river" in Vietnamese, also known as Bassac River) in its western part.

The river discharge of the Mekong is mostly controlled by the tropical monsoon climate, which has distinct wet and dry seasons. Mean annual rainfall varies from 1,000mm in Thailand to 3,200mm in Laos. In the Mekong River basin, 85% of water discharge occurs

Corresponding author: Dang Thi Ha
E-mail: leha1645@yahoo.com

during the flood season and 15% occurs in the low flow season. The discharge is the largest from August-September and the smallest in April-May [7].

This paper is based on the recent extensive dataset of hourly water discharges and twice-daily sediment concentrations, from 2009 to 2016 at 2 strategic sites

(Can Tho and My Thuan gauging stations-Figure 1), supplied by the Viet Nam Institute of Meteorology, Hydrology and Climate change (IMHEN). The aim of this study is to analyse the influence of climatic variability on water discharge and sediment flux in the Lower Mekong River.

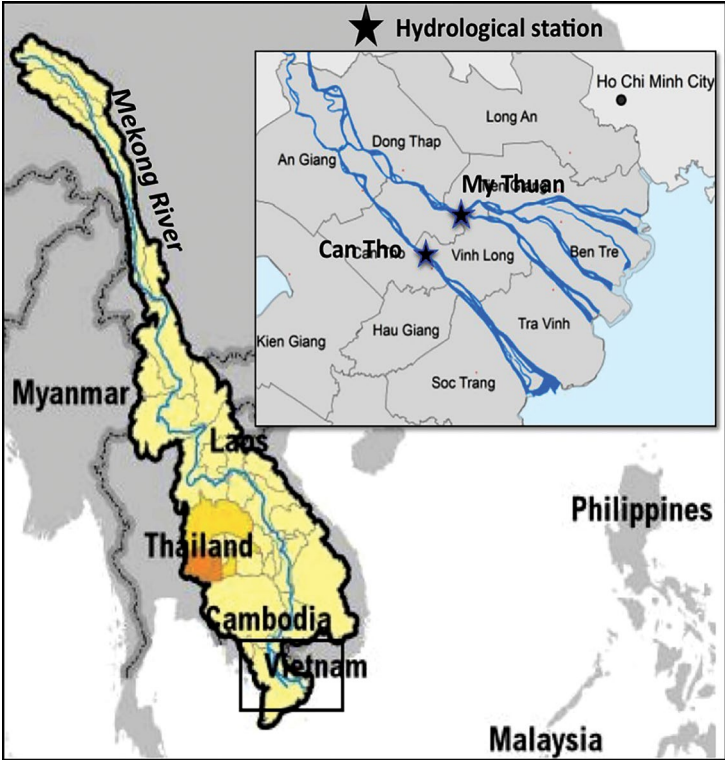


Figure 1. Hydrological network of the Mekong River Basin

2. Data collection and treatment

The sediment flux in ebb tide and flood tide conditions were calculated following:

$$Q_{s,e} = Q_e \times C_{av,e} \quad \text{and} \quad Q_{s,f} = Q_f \times C_{av,f}$$

where Q stands for the water supply during an ebb or flood period, Qs for the suspended sediment supply during this period, Cav for the average suspended sediment concentration, and subscripts e and f stand for ebb and flood, respectively.

The monthly net sediment flux (Qs j, in Mt/month) of month j was then computed from the contributions of all ebb tides and flood tides of the month:

$$Qs_j = \sum_{i=1}^{i=n} Qs_{.ei} - \sum_{i=1}^{i=n} Qs_{.fi}$$

where n stands for the number of days in month j, and the annual sediment flux (Qs_a, in Mt) from:

$$Qs_a = \sum_{j=1}^{12} Qs_j$$

For the information of climatic variations, in particular to assess the impact of ENSO on the water and sediment supplies, different indexes were considered, provided by the National Oceanic and Atmospheric Administration (NOAA, e.g. Sea Surface Temperature - SST, Southern Oscillation Index - SOI,...) and the Southern Oscillation Index (SOI) was often used [1,2,6]. Prolonged periods of negative SOI values coincide with abnormally warm ocean waters across the eastern tropical Pacific typical of

El Niño episodes, whereas prolonged periods of positive SOI values coincide with abnormally cold ocean waters across the eastern tropical Pacific typical of La Niña episodes. Sustained positive SOI values above about +8 indicate a La Niña event while sustained negative values below about -8 indicate an El Niño.

In this paper, the data of SOI was

downloaded from the website <https://www.cpc.ncep.noaa.gov/products/precip/CWlink/MJO/enso.shtml> [5]). The Figure 2 displays the ENSO events using monthly SOI anomalies. Based on time series of SOI anomaly between 2009 and 2016 in Figure 2, we observed one obvious El Niño event (2010-2011) and one obvious La Niña event (2015-2016).

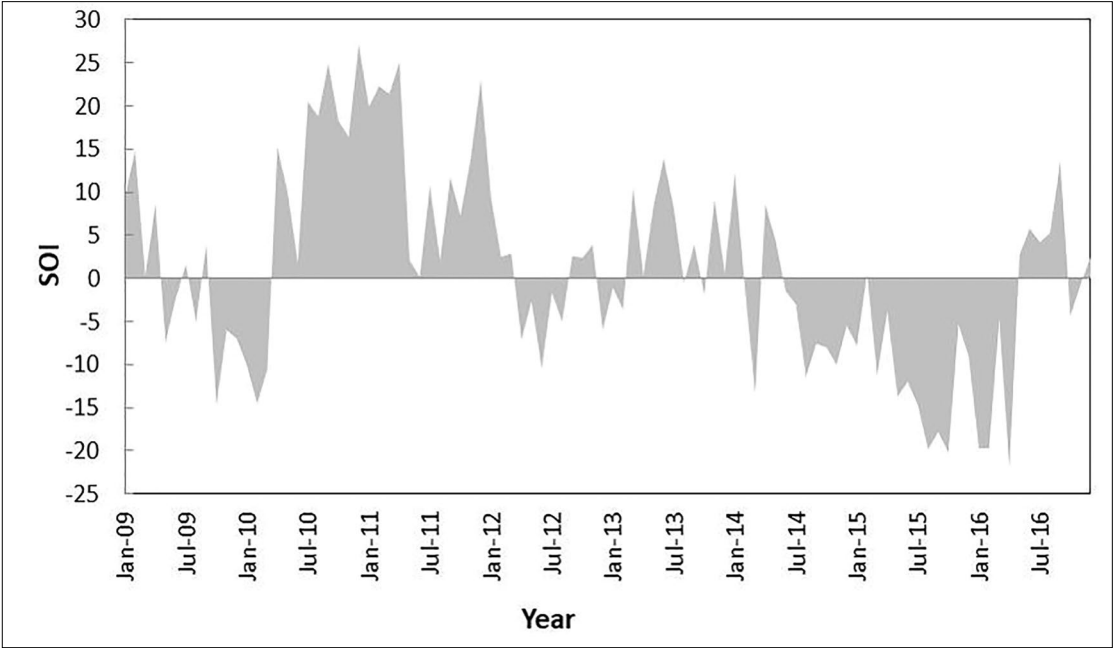


Figure 2. Time series of SOI anomalies. Positive SOI values above about +8 indicate a La Niña event while negative values below about - 8 indicate an El Niño

3. Results and Discussions

3.1. Monthly Averages and Annual Variations of Flux - in and flux Out in the Estuaries

The monthly and yearly values of sediment flux flowing seaward (flux-out) and landward (flux-in) at CanTho and MyThuan stations were calculated over the eight-year monitoring period (2009-2016) and are presented in Figures 2 and 3. We observed that the monthly evolution of sediment flux flowing seaward and landward at both stations experienced strong seasonal variations (Figure 2). At the Can Tho station, the monthly sediment flux-out ranged between 0.14 and 10.5 Mt/month (average value of 1.5 Mt/month) with the highest value observed in rainy season. The highest values of sediment flux-in were observed in dry season with individual values

varying from 0.01 to 0.45 Mt/month (average value of 0.16 Mt/month). A similar evolution of sediment flux-in and-out was observed at the My Thuan station (Figure 3).

The trend to a decrease in the yearly flux flowing out (Figure 4) should be analyzed with care, since the study period encompassed an excess of discharge at the beginning of the study period with the La Niña event of 2010-2011, and ended with a deficit of discharge associated to the El Niño event of 2015-2016. The trend is almost nil at Can Tho, while a short increase in landward sediment flux was observed at My Thuan station, showing slight impact by the ENSO variation in My Thuan (Figure 4). The difference in the trends between the two stations may be partly explained by other factors than El Niño, such as sand mining activities [1, 3].

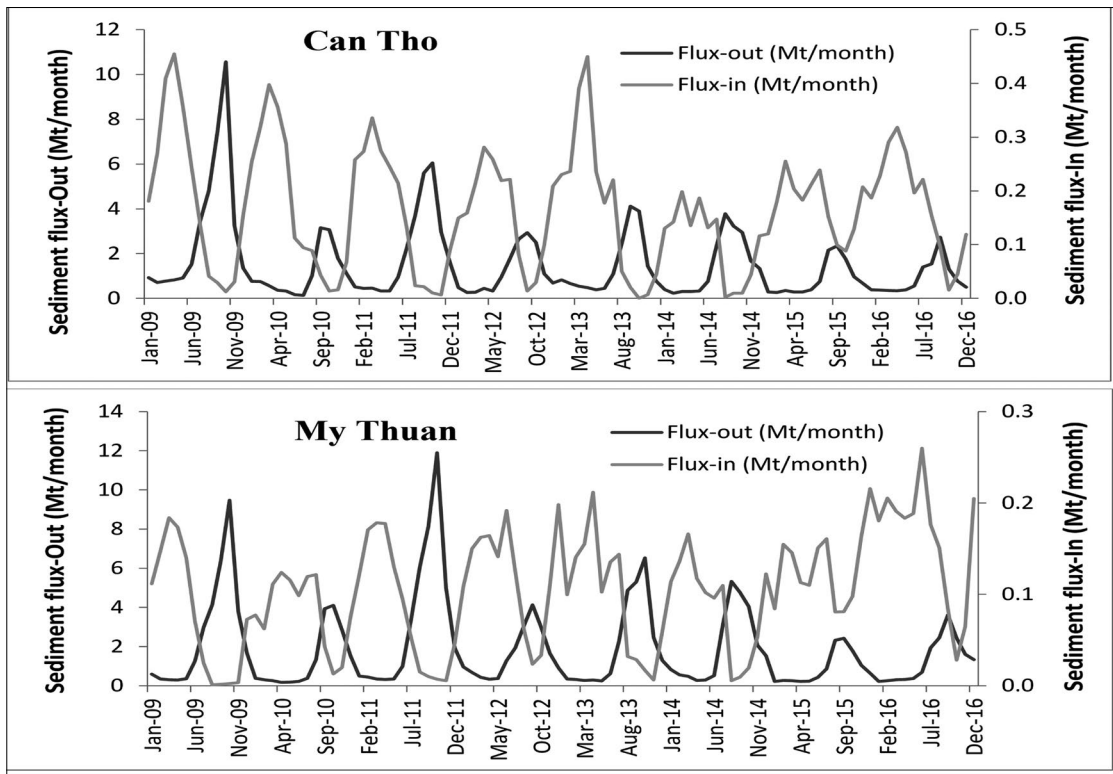


Figure 3. Evolution of monthly sediment fluxes oriented seaward and landward at Can Tho and My Thuan stations for the period 2009-2016

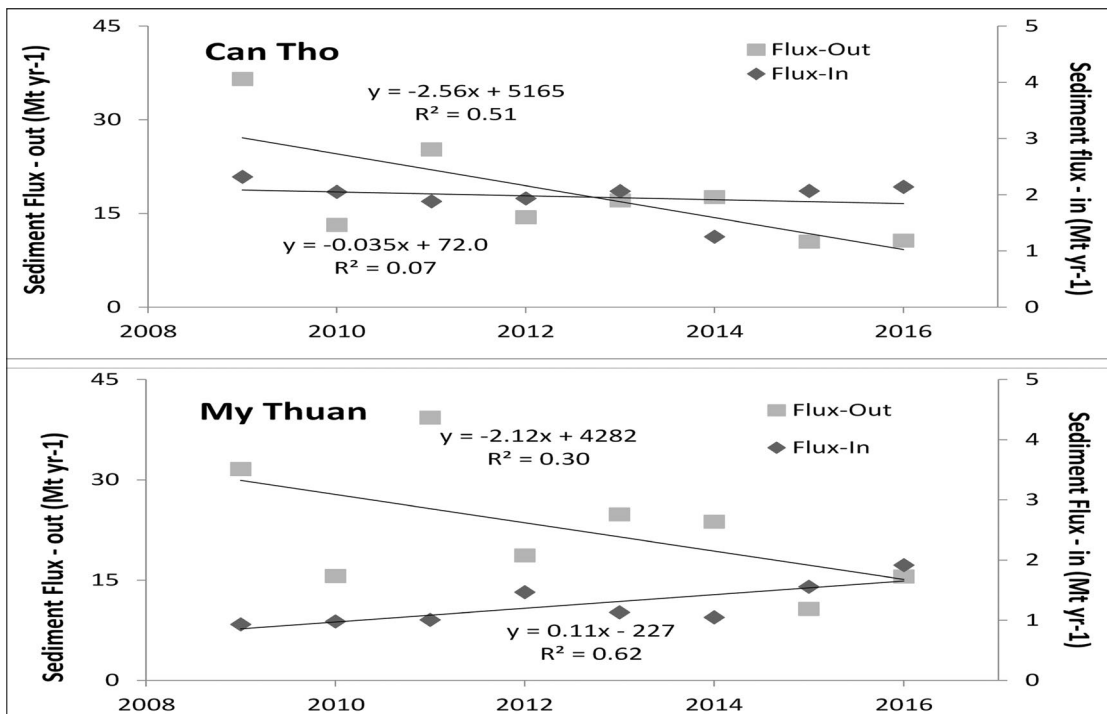


Figure 4. Evolution of annual sediment fluxes oriented seaward and landward at Can Tho and My Thuan stations for the period 2009-2016

3.2 Influences of ENSO on Seasonal and Annual Sediment Supply

In order to assess the influence of ENSO on suspended sediment fluxes at monthly and annual scales, we compared the monthly and yearly values of 2010-2011 (affected by the 2010 La Niña, Figure 2), 2015-2016 (affected by the strong 2015 El Niño, Figure 2), to the ones averaged over 2009 and 2012-2014. The monthly values are presented in Figure 5, and the yearly averaged values, per period, for Q and Qs, are given in Table 1.

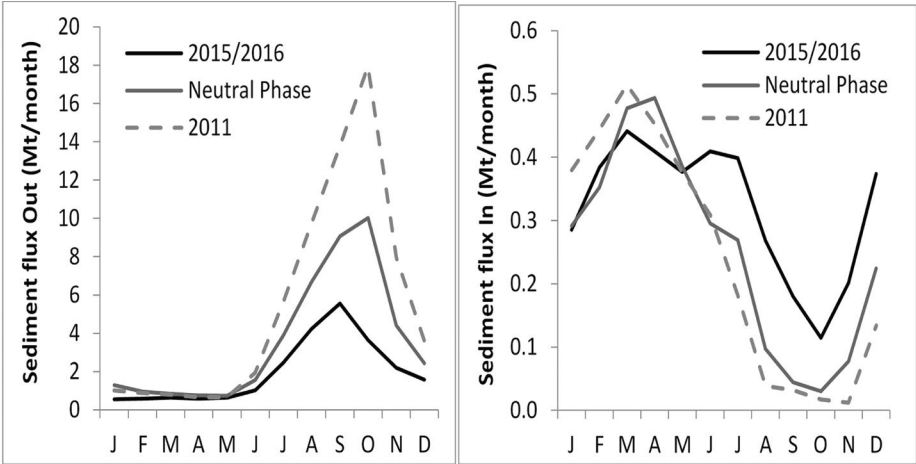


Figure 5. Monthly evolution of the sediment flux-out and flux-in of the Mekong River

Table 1. Average yearly water and sediment discharges at Can Tho and My Thuan stations during different ENSO stages over the 2009-2016 period. (* in km³/yr; ** in Mt/yr)

Period	Can Tho			My Thuan			Can Tho + My Thuan		
	Flux In	Flux Out	Total	Flux In	Flux Out	Total	Flux In	Flux Out	Total
Q 2010-2011 (La Niña)*	47.9	290.2	242.3	36.7	307.9	271.2	84.6	598.1	513.5
Q 2015-16 (El Niño)*	70.7	221.1	150.4	57.1	221.6	164.5	127.8	442.7	314.9
Q 2009,2012-2014 Neutral phase*	54.4	245.2	190.8	40.4	245.6	205.2	94.9	490.9	396.0
Qs 2011 (La Niña)**	1.88	25.25	23.37	1.01	39.33	38.32	2.89	64.58	61.69
Qs 2015-16 (El Niño)**	2.11	10.58	8.47	1.74	13.13	11.39	3.84	23.70	19.86
Qs 2009,2012-2014 neutral phase**	1.93	19.77	17.85	1.11	22.91	21.80	3.04	42.68	39.65

- In 2015-2016 (affected by El Niño of 2015), the flux of water flowing to the sea of the Mekong River (Can Tho + My Thuan) decreased by ~10% and the flux of water entering in the estuaries increased by more than 34%. Globally, the net seaward flux of water decreased by 20.5%. The sediment supply by the river decreased by ~45% and the sediment flux inland increased by 26%, providing a net decrease of sediment supply to the sea by 50%.

The flux back to the estuaries evolves the opposite of the flux seaward. The effect of ENSO on the sediment fluxes (in and out) is mainly sensitive in flood season (Figure 5).

In conclusion, the water flux to the sea was 396km³/yr, and the sediment supply to the sea was 39.65Mt/yr in average over the neutral years. La Niña was seen to increase the water supply by almost 30% and the sediment supply by 55%. El Niño was seen to decrease the water supply by 20% and the sediment supply by 50%.

4. Conclusions

The benefit of regular measurements at each flood and ebb stages from 2009 to 2016 is to provide, for the first time, an estimate of both

sediment fluxes flowing seaward and landward in the estuaries. Our results showed that during 2009-2016 period at both stations measured, the monthly sediment flux flowing seaward was very high in rainy season. In contract, the highest values of monthly sediment flux landward were observed in dry season. The present water discharge of the Mekong River to the sea can be estimated to be 400km³/yr, ± 100km³/yr depending on ENSO, and the present sediment supply to the sea can be estimated to be 40Mt/yr, ± 20Mt/yr, depending on ENSO.

In added, we observed that the water discharge and annual sediment supplies by the Mekong strongly influenced by ENSO events. In fact, the water supply increased by almost 29.6% and the sediment supply by 55.6% due to La Niña event of 2010-2011; the water supply decreased by about 20.5% and the sediment supply by 50% due to El Niño event of 2015-2016. However, we noted that the long-term observation (>10 years) is needed in order to deeply analyse the impacts of the climatic change on the hydrological regime in the lower Mekong River.

References

1. Anthony, E.J.; Brunier, G.; Besset, M.; Goichot, M.; Dussouillez, P.; Nguyen, V.L. *Linking rapid erosion of the Mekong River delta to human activities*. *Sci. Rep.* 2015, 5, 14745, doi:10.1038/srep14745.
2. Kondolf, G.M.; Schmitt, R.J.P.; Carling, P.; Darby, P.; Arias, M.; Bizzi, S.; Castelletti, A.; Cochrane, T.A.; Gibson, S.; Kummu, M.; et al. *Changing sediment budget of the Mekong: Cumulative threats and management strategies for a large river basin*. *Sci. Total Environ.* 2018, 625, 114-134, doi:10.1016/j.scitotenv.2017.11.361.
3. Ogston, A.S.; Allison, M.A.; McLachlan, R.L.; Nowacki, D.J.; Stephens, J.D. *How tidal processes impact the transfer of sediment from source to sink: Mekong River collaborative studies*. *Oceanography* 2017, 30, 22–33, doi:10.5670/oceanog.2017.311.
4. Piton, V.; Delcroix, T. *Seasonal and interannual (ENSO) climate variabilities and trends in the South China Sea over the last three decades*. *Ocean Sci. Discuss.* 2018, doi:10.5194/os-2017-104.
5. Sea Surface Temperature (SST). Available online: <https://www.cpc.ncep.noaa.gov/products/precip/CWlink/MJO/enso.shtml> / (accessed on 20 December 2017).
6. Wang, H.; Saito, Y.; Zhang, Y.; Bi, N.; Sun, X.; Yang, Z. *Recent changes of sediment flux to the western Pacific Ocean from major rivers in East and Southeast Asia*. *Earth-Sci. Rev.* 2011, 108, 80–100, doi:10.1016/j.earscirev.2011.06.003.
7. Wang, J.J.; Lu, X.X.; Kummu, M. *Sediment load estimates and variations in the lower Mekong River*. *River Res. Appl.* 2011, 27, 33-46, doi:10.1002/rra.1337.
8. Xue, Z.; Liu, J.P.; Ge, Q.A. *Changes in hydrology and sediment delivery of the Mekong River in the last 50 years: Connection to damming, monsoon, and ENSO*. *Earth Surf. Proc. Land.* 2011, 36, 296–308, doi:10.1002/esp.2036.

FLOODING IMPACTS ON RICE CULTIVATING AREA UNDER CLIMATE CHANGE IN TRA VINH PROVINCE

Mai Van Khiem⁽¹⁾, Tran Tuan Hoang⁽¹⁾, Phan Thi Diem Quy⁽¹⁾
Huynh Thi My Linh⁽¹⁾, Ho Cong Toan⁽¹⁾, Pham Thanh Long⁽¹⁾, Nguyen Thi Thu Hang⁽²⁾

⁽¹⁾Viet Nam Institute of Meteorology, Hydrology and Climate Change

⁽²⁾Sai Gon University

Received: 7 January 2019; Accepted: 11 February 2019

Abstract: Climate change (CC) and sea level rise (SLR) are a challenge for many ecosystems, biodiversity and environmental resources, greatly influencing human social life. In this paper, we assess the impact of flooding in the rice cultivating area under climate change and sea level rise by 2100 in Tra Vinh province, through gathering and inheriting database methods, model (MIKE FLOOD) and geographic information system. The results indicated that Cau Ke and Chau Thanh districts have flooded areas on rice growing land larger than other districts. The results obtained in this study can be used to provide options for crop improvement, food security in the region and contributing to the local sustainable development.

Keywords: Climate change, sea level rise, rice cultivation area, Tra Vinh, MIKE FLOOD

1. Introduction

Rice cultivation in Viet Nam was closely associated with the rural population and traditional farmers. Long-term flooding greatly affects cultivated land, rice production, affecting the food security of the province in particular and the Mekong Delta region in general. Under the scenario of climate change and sea level rise for Vietnam to be built and announced in 2016, about 38.9% of the Mekong Delta area will be at risk of flooding if sea level rises by 100cm. Tra Vinh province alone will have a risk of flooding of 21.3% compared to the natural area of the province [1].

Tra Vinh is adjacent to Ben Tre, Vinh Long and Soc Trang provinces; located between Tien River and Hau River (Figure 1). Tra Vinh provincial centre is 130km from Ho Chi Minh City and 100 km from Can Tho city. Tra Vinh province has 1 city, 1 town and 07 districts. Natural land area of Tra Vinh is 235,826ha [2]. Every year, the rice cultivation area of Tra Vinh is quite large. According to Tra Vinh Statistical Office, the total area of 2016 rice cultivation is 234,247ha [6].

The advantage of the province is wet rice agriculture, the annual area of rice cultivation in Tra Vinh province faces many problems of natural disasters such as drought, saline intrusion, especially inundation. Flooding causes much damage to rice as well as damaging crops, reducing rice productivity. In addition, flooding also causes epidemics to reduce both yield and quality of rice.

In the context of climate change that is increasingly harsh and unpredictable, studies of sea level rise causing flooding on rice are essential.

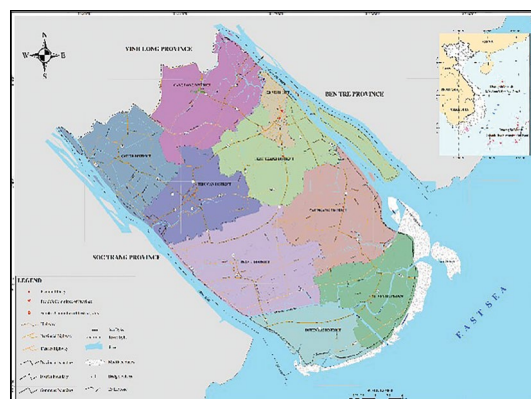


Figure 1. Administrative map of Tra Vinh province

Corresponding author: Pham Thanh Long
E-mail: longpham.sihymete@gmail.com

2. Methodology

(1). Methods of gathering and inheriting databases

This method is implemented on the basis of inheriting, analysing, and synthesizing relevant sources of documents, materials, and data in a selective way. After that, assessed according to the requirements and purpose of the study. In this study, the gathered and inherited sources of documents and data include: flow and water level data provided by the Southern Regional Hydrometeorological Center; Hydraulic diagram and river section are measured and collected from research projects and projects directly implemented by the Sub-Institute of Hydro Meteorology and Climate Change.

(2). Model method

The modelling method is widely used in flood simulation and mapping. In particular, the one-way hydraulic model combines GIS such as MIKE 11, ISIS, VRSAP, HydroGIS, integrated 1-way and 2-way or 2-way (full 2D) models such as MIKE FLOOD (MIKE 21 and MIKE 11 integration), MIKE 21, SOLBECK, TELEMAC [3]. In this article, MIKE FLOOD model was used in linking MIKE 11 HD and MIKE 21 FM modules.

MIKE 11 model is a one-way hydraulic model, in which the hydrodynamic module is a central part, simulating the dynamic process along the unstable flow length with the combination of equation continuous and momentum equations (Saint-Venant equations):

The continuity equation [4]:

$$B \frac{\partial h}{\partial t} + \frac{\partial Q}{\partial x} = q$$

The momentum equation [5]:

$$\frac{\partial Q}{\partial t} + \frac{\partial}{\partial x} \left(\alpha \frac{Q^2}{A} \right) + gA \frac{\partial h}{\partial x} + g \frac{Q|Q|}{AC^2R} = 0$$

MIKE 21 FM model includes:

The continuity equation [5]:

$$\frac{\partial h}{\partial t} + \frac{\partial hu}{\partial x} + \frac{\partial hv}{\partial y} = hS$$

The shallow water equation [6]:

$$\frac{\partial hu}{\partial t} + \frac{\partial hu^2}{\partial x} + \frac{\partial huv}{\partial y} = f\bar{v}h - gh \frac{\partial \eta}{\partial x} - \frac{h}{\rho_0} \frac{\partial p_a}{\partial x} - \frac{gh^2}{2\rho_0} \frac{\partial \rho}{\partial x} +$$

$$\frac{\tau_{xx}}{\rho_0} - \frac{\tau_{bx}}{\rho_0} - \frac{1}{\rho_0} \left(\frac{\partial S_{xx}}{\partial x} + \frac{\partial S_{xy}}{\partial y} \right) + \frac{\partial}{\partial x} (hT_{xx}) + \frac{\partial}{\partial y} (hT_{xy}) + hu_s S$$

$$\frac{\partial hv}{\partial t} + \frac{\partial huv}{\partial x} + \frac{\partial hv^2}{\partial y} = -f\bar{u}h - gh \frac{\partial \eta}{\partial y} - \frac{h}{\rho_0} \frac{\partial p_a}{\partial y} - \frac{gh^2}{2\rho_0} \frac{\partial \rho}{\partial y} +$$

$$\frac{\tau_{yy}}{\rho_0} - \frac{\tau_{by}}{\rho_0} - \frac{1}{\rho_0} \left(\frac{\partial S_{yx}}{\partial x} + \frac{\partial S_{yy}}{\partial y} \right) + \frac{\partial}{\partial x} (hT_{xy}) + \frac{\partial}{\partial y} (hT_{yy}) + hv_s S$$

(3) GIS method

Map tools such as Mapinfo and ArcGIS are used to extract the results of the model, serve the management and exploitation of information and overlap to build flood risk maps.

3. Input data for models

Based on data from the river network throughout the lower Mekong Delta River (see Figure 2) in the project "Update climate change scenarios in Tra Vinh province under the 2016 scenario according to the Ministry of Natural Resources and Environment", we used to calibrate and validate hydraulic models for Tra Vinh province. After achieving the good results, we extracted separate river, cross-sections and boundary data for Tra Vinh province (see Figure 3).

Model input data for river network in Mekong Delta River, include:

- Documents on the design of irrigation works, irrigation systems in the lower Mekong area of the Southern Institute of Water Resources Research from 2002 to the present and have been provided by Departments of Tra Vinh province.

- Boundary conditions: water level and discharge in 2016 were collected from Southern Regional HydroMeteorology Center

- Climate change and sea level rise scenarios have been used in this study was the set of "Climate change and sea level rise scenarios for Vietnam" newest update of 2016 of Ministry of Natural Resources and Environment.

- Hydraulic diagram of river network in Mekong Delta River including: main rivers and canals such as Tien river, Hau river, Vam Nao river, Co Chien river and other small river branches have been set up based on satellite maps and hydrological maps of the Mekong Delta River region with 1,116 branches. The

number of points calculated in the model were about 13,000 points. River sections: about more

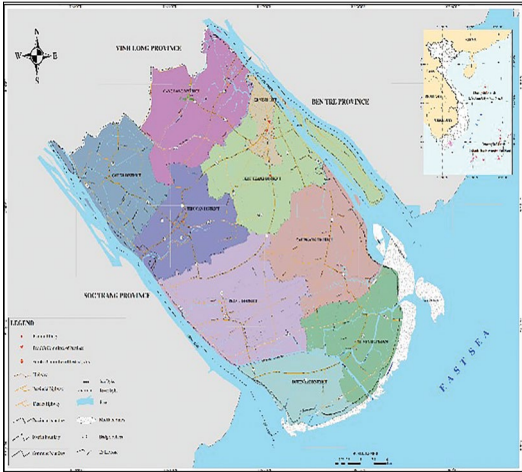


Figure 2. Hydrodynamic diagram of river network in Mekong Delta River

- Hydraulic modules are built based on 2 main flow profiles in Tan Chau and Chau Doc in 2016. Other discharge margins without other rivers or small canals starting in the field are priced value of 0 m3/s. There for, hydraulic diagram including real measured datas in Tan Chau and Chau Doc Stations in 2016.

- Data of water level in coastal estuaries is taken as downstream boundary used in the model is the actual data measured in 2016 at coastal stations such as Vam Kenh station (Tieu gate), Binh Dai station (Dai gate), An Thuan (Ham Luong gate), Ben Trai (Co Chien gate), and My Thanh station (My Thanh, Dinh An gates) and Tran De station (Tran De gate).

- The system of checking water level data includes data at hydrological stations such as Vam Nao, My Thuan, My Tho (Tien river), Can Tho, Dai Ngai, Tran De (Hau river) or Cho Lach station, Tra Vinh (Co Chien river) and My Hoa (Ham Luong river) are collected at the Hydrological Meteorological Station in the Southern region in 2016, serving for model calibration and validation. This set of data ensures reliability and accuracy for model calculation and correction.

Input data for river network is calculated for Tra Vinh province:

- The boundaries have been used in the river network of Tra Vinh province include the upper boundary which is the data of water

than 5,000 sections across the Mekong Delta river system.

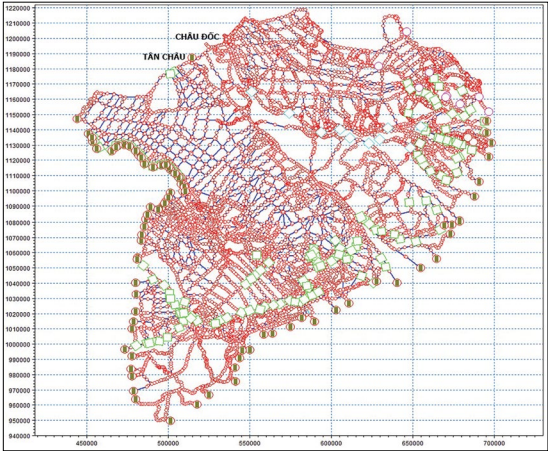


Figure 3. The river network uses flood calculation for Tra Vinh province

level and flow extracted from the Mekong Delta River network (downscaling), including the boundary of Can Tho, My Thuan (water level data and flow data). Downstream boundaries were downstream water level in 2016 at hydrological stations such as Ben Trai station and Tran De station. Figure 3 shows the river network of Tra Vinh province extracted from river network of Mekong Delta River region.

- Topography has been used in flood calculation for Tra Vinh province was Digital Elevation Models (DEM) topography data of Viet Nam Ministry of Natural Resources and Environment (MONRE), with dimensions of 10x10 meter (see Figure 4).

- Topographic data have been used to construct the topography and calculate for the MIKE FLOOD model and the MIKE 21FM model, as follows: topographic data has been extracted from 1: 200,000 map of the Vietnamese People’s Navy, published in 2009; in addition, the study area topography has been also measured during the 2016 survey in the project “Climate Change Adaptation in the Mekong Delta in Tra Vinh Province (Tra Vinh AMD Project)”. It included 78,489 elements and 39,678 nodes (see Figure 5)

- River network in MIKE 11HD model was linked to topography of MIKE 21FM in MIKE FLOOD model by lateral link (see Figure 6).

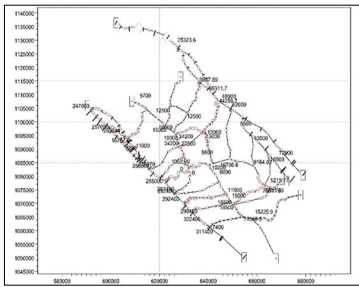


Figure 4. DEM topography data for Tra Vinh province

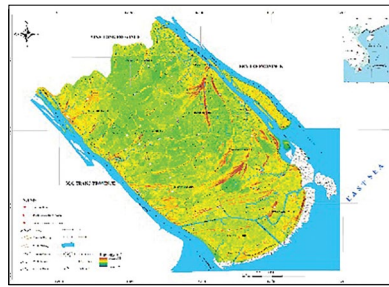


Figure 5. Topography data in MIKE 21FM model

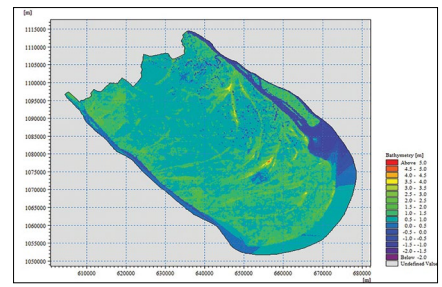


Figure 6. Lateral link between MIKE 11HD model and MIKE 21FM model

4. Results

4.1. Calibration and validation of models

The hydraulic model of saline intrusion calculation has been calibrated, validated based

on the actual measured data at Tra Vinh station in 2016 and 2010. Data were collected from Southern Regional HydroMeteorology Center. Stations location is shown in the Figure 7.

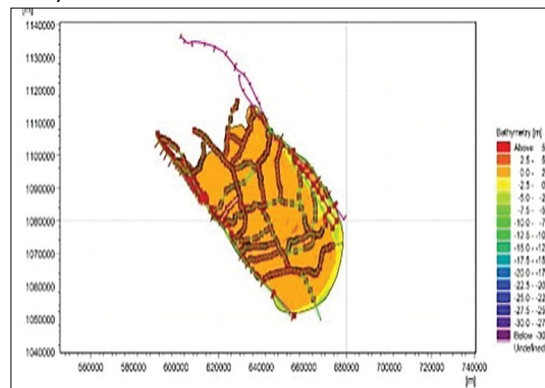


Figure 7. Location map of hydrological stations in Southern of Viet Nam

- Manning roughness coefficient has been adjusted from 30 to 65 depending on the river section;
- Initial conditions: The water level was 0.5m and the flow was equal to 5m³/s for the entire river system;
- Time step for hydraulic calculation (HD) $\Delta t = 5$ minutes.

- Time to calibrate model parameters from July 1, 2016 to July 31, 2016 and validate in the period of July 1, 2010 to July 31, 2010. The results of the water level calculation in the above time were compared with the actual measured data based on the correlation coefficient and the NASH suitability index and the hydraulic model calibration results are shown below.

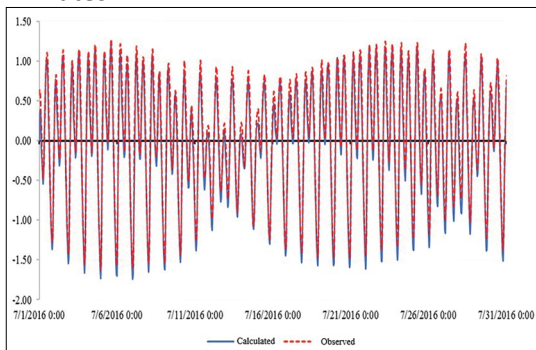


Figure 8a NASH index: 0.97

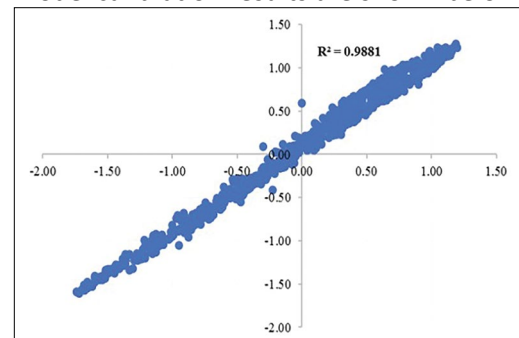
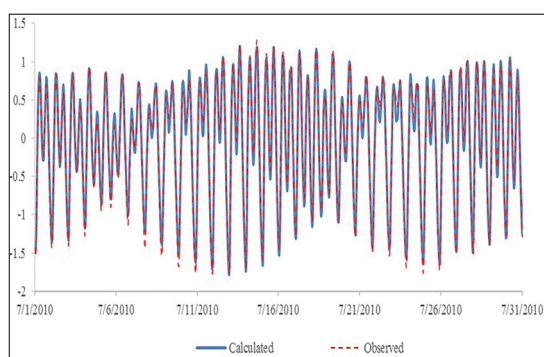
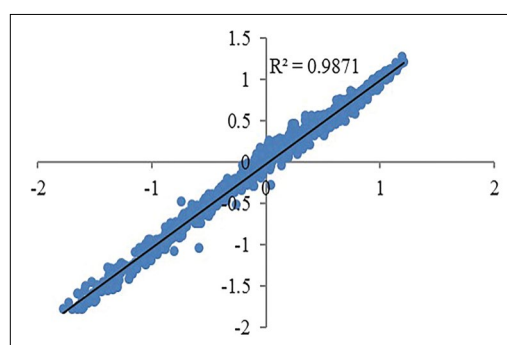


Figure 8b

Figure 8 (a-b): Calibration water level at Tra Vinh Station in July 2016



a) NASH index: 0.92



b)

Figure 9 (a-b). Validation water level at Tra Vinh Station in July 2010

Calculation results and actual measured data of water level satisfying the permissible error limit of value and tidal phase for the NASH coefficient in the range of 0.92-0.97. Thus, the data set used to build the model and the model correction parameter set were reliable.

4.2. Simulation results and updated maps flooded on rice cultivation land for Tra Vinh province

We carried out the calculation and comparison of flooding levels on rice cultivation land in 2016 in the current situation (in 2016)

and climate change scenarios (2025, 2050, 2070, 2100). According to the land use planning map, the area of land for rice cultivation in Tra Vinh in 2016 was about 99,822.47 hectares.

(1). Current status of flooding in 2016

The flooded map of Tra Vinh province according to the current status 2016 is presented in Figure 10.

The total flooded area was 23,497.68 ha, accounting for nearly 10% of the province's natural land area. The total area of flooded rice paddy land was 4,211.11 hectares, accounting for about 4.2% of the province's paddy land.

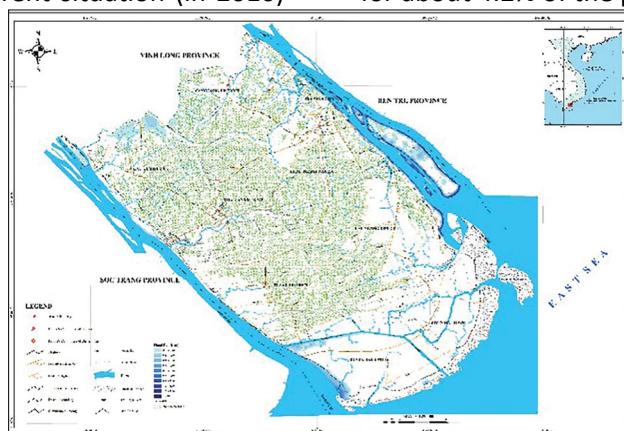


Figure 10. Map flooded in Tra Vinh province in 2016

(2). Forecasting the risk of flooding on rice cultivation land until 2025

To simulated and updated the flood risk map on rice cultivation land in Tra Vinh province until 2025, the study used Sea level rise for Vietnam was published by the Ministry of Natural Resources and Environment in 2016. Accordingly, in 2025, sea level rise will be 0.12m

for RCP4.5 [1]. Flood hazard map of Tra Vinh rice land in 2025 is shown in Figure 11.

The total flooded area will be 26,491 hectares, accounting for about 11.2% of the province's natural land area.

The total area of flooded rice paddy land will be 5,531.7 hectares, accounting for about 5.5% of the province's rice cultivation land.

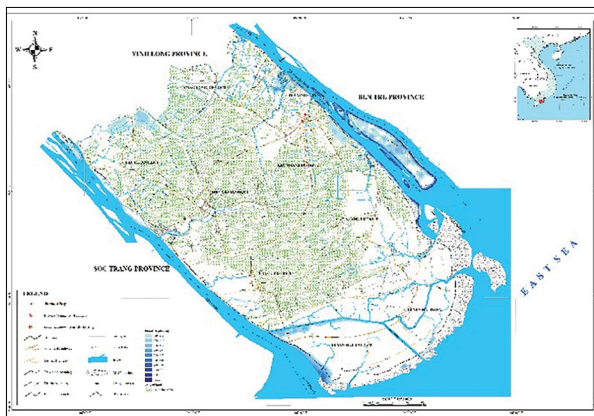


Figure 11. Flood risk map according to scenario RCP4.5_2025 and current status of wet rice cultivation in Tra Vinh province

(3) Forecasting the risk of flooding on rice cultivation land until 2050

To simulated and update the flood hazard map on the rice cultivation land in Tra Vinh province until 2050, the study used Sea level rise for Viet Nam was published by the Ministry of Natural Resources and Environment in 2016. Accordingly, in 2050, sea level rise will be 0.22 m corresponding to RCP4.5 [1]. The risk map of flooding in Tra Vinh rice land in 2050 is shown in Figure 12. The total flooded area will be about 28,762 hectares, accounting for 12.2% of the natural land area. The total area of flooded rice paddy land will be 6,815 hectares, accounting for 6.8% of the province's rice cultivation land area.

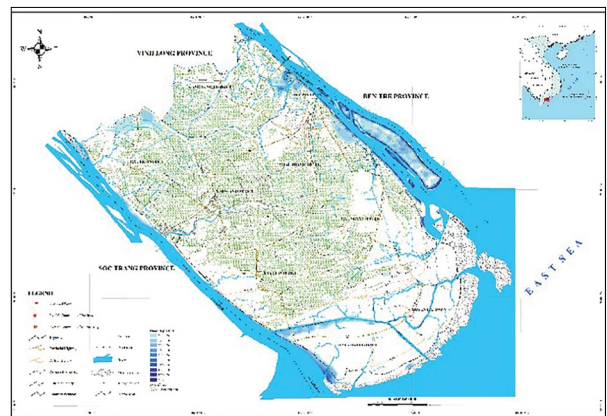


Figure 12. Flood risk map according to scenario RCP4.5_2050 and current status of wet rice cultivation in Tra Vinh province

(4) Forecasting the risk of flooding on rice cultivation land until 2070

To simulated and updated the flood hazard map on the paddy land in Tra Vinh province until 2070, the study used Sea level rise for Viet Nam was published by the Ministry of Natural Resources and Environment in 2016. Accordingly, in 2025, sea level rise will be 0.33 m for RCP4.5 [1]. Flood hazard map of Tra Vinh paddy land in 2070 is shown in Figure 13.

The total flooded area will be 32,101 hectares, accounting for 13.6% of the natural land area. The total flooded area on paddy land will be 8,231 hectares, accounting for 8.2% of the province's rice land.

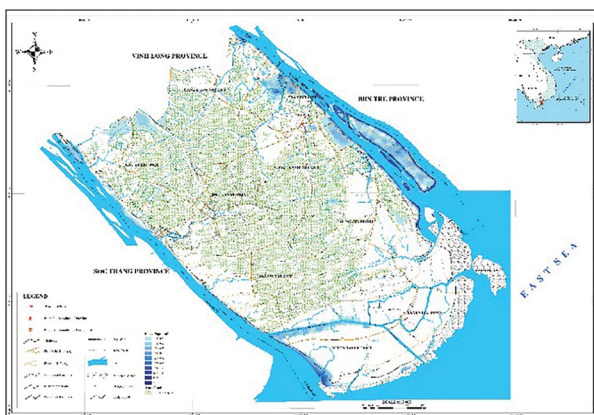


Figure 13. Flood risk map according to RCP4.5_2070 scenario and current status of wet rice cultivation in Tra Vinh province

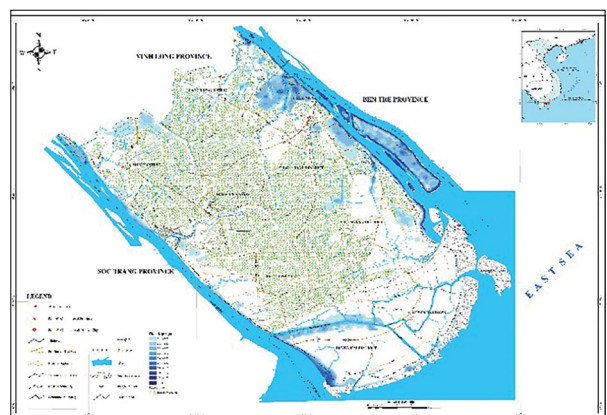


Figure 14. Flood risk map according to RCP4.5_2100 scenario and current status of wet rice cultivation in Tra Vinh province

(5). *Forecasting the risk of flooding on rice cultivation land until 2100*

To simulated and updated the flood hazard map on the paddy land in Tra Vinh province until 2100, the study used Sea level rise for Viet Nam was published by the Ministry of Natural Resources and Environment in 2016. Accordingly, in 2025, Sea level rise will be 0.53m for RCP4.5 [1]. The flood risk map of Tra Vinh rice land in 2100 is shown in Figure 14.

The total flooded area will be 41,159 hectares, accounting for 17.5% of the natural land area. The total area of flooded rice paddy land will be 12,214 hectares, accounting for 12.2% of the province’s rice growing area.

Statistics of the current flooded area in 2016 and the RCP4.5 scenarios in 2025, 2030, 2050, 2100 on the area of rice cultivation and the increase/decrease compared to 2016 is presented in tables 1, 2 , 3, 4 below.

Table 1. *Statistics of flooded areas in Tra Vinh province over the years*

Number	Flooding level (m)	Flooded area (hectares)				
		2016	45_2025	45_2050	45_2070	45_2100
1	0.1-0.2	5,830.61	6,729.02	6,803.48	7,259.09	9,015.82
2	0.2-0.3	2,803.63	3,773.24	4,681.73	4,975.96	6,137.65
3	0.3-0.5	3,026.27	3,482.81	4,127.96	5,482.37	9,070.76
4	0.5-0.6	1301.59	1,301.92	1,254.12	1,367.75	2,132.33
5	0.6-0.7	1,117.84	1,226.62	1,296.25	1,211.78	1,505.16
6	0.7-0.8	1,021.75	1,056.04	1,139.55	1,264.21	1,225.00
7	0.8-1.0	1,390.22	1,632.85	1,822.34	2,048.54	2,331.98
8	1.0-1.2	1,074.83	1,143.94	1,213.14	1,377.83	1,766.99
9	1.2-1.5	1,232.46	1,267.89	1,311.44	1,427.26	1,699.25
10	>1.5	4,698.48	4,876.45	5,112.14	5,686.92	6,274.26
	Total	23,497.68	26,490.77	28,762.16	32,101.71	41,159.21

Table 2. *Statistics difference in flooded area according to the schedule compared to the area flooded in Tra Vinh province in 2016*

Number	Flooding level (m)	Flooded area compared to 2016 (hectares)			
		45_2025	45_2050	45_2070	45_2100
1	0.1-0.2	+898.40	+972.87	+1,428.48	+3,185.21
2	0.2-0.3	+969.60	+1,878.09	+2,172.33	+3,334.02
3	0.3-0.5	+456.54	+1,101.69	+2,456.10	+6,044.49
4	0.5-0.6	+0.33	-47.47	+66.15	+830.73
5	0.6-0.7	+108.78	+178.41	+93.94	+387.33
6	0.7-0.8	+34.29	+117.80	+242.46	+203.25
7	0.8-1.0	+242.63	+432.13	+658.32	+941.76
8	1.0-1.2	+69.11	+138.31	+303	+692.16
9	1.2-1.5	+35.43	+78.98	+194.80	+466.79
10	>1.5	+177.97	+413.66	+988.44	+1,575.78
	Total	+2,993.09	+5,264.47	+8,604.03	+17,661.53

(+: increase: -: decrease)

Table 3. Statistics of flooded areas on rice cultivation land in Tra Vinh province over the years

Number	Flooding level (m)	The area is flooded on the current land for rice cultivation (hectares)				
		2016	45_2025	45_2050	45_2070	45_2100
1	0.1-0.2	2,040.85	2,806.62	2,944.22	3,011.01	4,241.34
2	0.2-0.3	702.57	1,000.42	1,655.20	2,072.49	2,388.25
3	0.3-0.5	371.57	549.81	843.70	1,482.12	3,231.44
4	0.5-0.6	85.29	119.63	184.53	283.93	557.52
5	0.6-0.7	71.95	73.48	103.20	157.96	342.48
6	0.7-0.8	81.14	68.67	69.03	92.51	192.40
7	0.8-1.0	193.55	172.77	164.71	155.99	197.81
8	1.0-1.2	145.87	174.30	198.20	205.19	161.89
9	1.2-1.5	159.21	165.34	183.50	227.34	280.48
10	>1.5	359.10	400.66	468.84	542.76	620.50
	Total	4,211.11	5,531.70	6,815.11	8,231.28	12,214.12

Table 4. Statistics of the difference of flooded area on rice cultivation land according to the schedule compared to the area flooded in Tra Vinh province in 2016

Number	Flooding level (m)	Difference in area flooded on rice cultivation land compared to 2016 (hectares)			
		45_2025	45_2050	45_2070	45_2100
1	0.1-0.2	+765.77	+903.37	+970.16	+2,200.49
2	0.2-0.3	+297.85	+952.63	+1,369.91	+1,685.67
3	0.3-0.5	+178.24	+472.13	+1,110.55	+2,859.87
4	0.5-0.6	+34.34	+99.23	+198.63	+472.23
5	0.6-0.7	+1.53	+31.25	+86.00	+270.53
6	0.7-0.8	-12.47	-12.11	+11.37	+111.26
7	0.8-1.0	-20.78	-28.84	-37.56	+4.26
8	1.0-1.2	+28.43	+52.32	+59.32	+16.02
9	1.2-1.5	+6.12	+24.29	+68.12	+121.27
10	>1.5	41.55	+109.73	+183.65	+261.40
	Total	+1,320.59	+2,604.00	+4,020.17	+8,003.00

(+: increase: -: decrease)

According to the flooded statistics on the natural land of Tra Vinh province, the current situation and climate change scenarios, the total flooded area on natural land gradually increases over the years. In which the total flooded area of the scenario RCP45_2100 is the largest of 41,159.21 hectares, an increase of 17,661.53 hectares compared to the current situation in 2016. The common flood level is from 0.1-0.2 m

for the current situation in 2016, the scenarios RCP45_2025, RCP45_2050, RCP45_2070. For RCP45_2100 scenario, the common flood level is from 0.3 to 0.5 m.

The total flooded area on rice cultivation land also tends to increase, the total flooded area on the rice paddy scenario RCP45_2100 is the largest of 12,214.12 hectares, an increase of 8.003 hectares compared to the current

situation in 2016. In particular, the common flood level on the paddy land from 0.1-0.2m for all years.

5. Concluding

This study has applied the model MIKE FLOOD to simulate the risk of flooding on rice cultivation land in Tra Vinh province according to the 2016 status and the average emission scenarios (RCP4.5) in 2025, 2050, 2070, 2100. From the calculation results, the study has constructed flooded maps on rice cultivation land for Tra Vinh province.

The simulation results, overlapping map and calculating the risk of flooding on rice cultivation land for Tra Vinh province shows: The risk of flooding in 2025 will be about 5,531.7 hectares, accounting for 5.5% of the province's rice cultivation land area; For 2050 will be about 6,815 ha, accounting for 6.8% of the province's rice cultivation land area; For 2070, about 8,231 ha, accounting for 8.2% of the province's rice cultivation land area and in 2100, the risk of flooding will be about 12,214 hectares, accounting for 12.2% of the province's rice cultivation land area. The universal flood level is from 0.1-0.2m, the flood level greater than 1.5m accounts for mainly in the alluvial and canal alluvial areas. According to flooding map then Chau Thanh and Cau Ke districts are the two areas with flooded largest area on rice

cultivation land in Tra Vinh province.

Flooding levels in rice and inundation rates are not high, but they also have a certain effect on the yield and quality of local rice. Flooding can cause root rot, reducing yield. Flooding also causes disease to lower the quality of rice. In addition, flooding due to sea level rise also leads to saline intrusion, narrowing the area of land where rice can be cultivated, greatly affecting production and improving fields due to salinity.

At the same time, Tra Vinh province has the sixth rice output in Mekong Delta River region, contributing to ensuring food security in region. Fluctuations in the and yield and quality of rice in the province will significantly affect the region in particular and Viet Nam country in general.

The updated results of the study are the basis for the agencies and agencies in the province to consider and update flood risks due to climate change, sea level rise ink affecting rice land. Since then they have adjusted, integrated climate change issues, sea level rise to future development programs and plans for the province's wet rice, as well as coordinated with neighbouring provinces in the Mekong Delta River region.

The paper only calculated the impact of flooding in the rice growing area, not yet assessed the effect of each flood level, the time to maintain flooding of rice.

References

1. Ministry of Natural Resources and Environment (2016), *Climate Change and Sea level rise scenarios for Viet Nam*, Ha Noi.
2. Tra Vinh Statistical Office (2017), *2016 Statistical Yearbook*, Tra Vinh.
3. Nguyen Hong Quan (2013), "Some methods to build flooded maps of Long An province in conditions of climate change and sea level rise, *Journal of Science and Technology Development*, Vol 16, No. M1-2013, page 32-39.
4. DHI Water & Environment (2017), *MIKE 11 - A Modelling system for Rivers and Channels Reference Manual*.
5. DHI Water & Environment (2017), *MIKE 21 - Flow model FM*.
6. Department of Agriculture and Rural Development in Tra Vinh province, *2016 summarized report and tasks of 2017 plan of Tra Vinh province*.

CALCULATION OF DESIGNED FLOOD IN WEAK DATA REGION IN VIET NAM USING WIN-TR55 MODEL

Doan Thi Noi⁽¹⁾, Dang Quang Thinh⁽²⁾

⁽¹⁾Faculty of Civil Engineering, University of Transport and Communications

⁽²⁾Institute of Meteorology, Hydrology and Climate Change

Received: 11 February 2019; Accepted: 28 February 2019

Abstract: Road transportation infrastructure is of great importance in the development of a nation. Viet Nam is facing many challenges in developing road infrastructure due to lack of rainfall and flow data required for calculation of designed flood, especially in mountainous areas. Furthermore, many water drainages have been damaged by heavy rain and severely affected by climate change. In this study, the Win-TR55 based on SCS method is employed for calculating storm runoff volume, discharge and hydrograph to estimate designed flood values for small watersheds. In order to use TR55, parameters for calculating designed flood including rainfall, soil type and land use map are required. This program is widely used in many countries, but has not been applied to the small basins in Viet Nam because of data missing. Tong Soong bridge on the National Highway No.31 crossing Dinh Lap district, Lang Son province, Viet Nam was selected as a case study. The study shows a great potential of the Win-TR55 method to estimate the hydrograph for small and medium watershed in Viet Nam.

Keywords: Win-TR55, designed flood, data missing, Tong Soong watershed.

1. Introduction

Determination of design hydrograph is the key information for construction of transportation infrastructure. The size of these infrastructure systems strongly depends on the design hydrograph to make sure they will not be inundated by flood water in the future. There have been many methods developed to construct the hydrograph [1-2]. In general, these methods construct the designed hydrograph from the designed hydrograph based on the rainfall-runoff relationship. They can be classified into three groups. The first method so-called traditional method uses simple equations to formulate the rainfall-runoff relationship (e.g., runoff coefficient). The advantage of this method is that they can provide quick estimate of designed hydrograph.

However, they do not explicitly account for the impact of watershed characteristics such as land use, topography and soil type or watershed conditions such as soil moisture. The second group of methods is based on physically-based hydrological models. These models can well simulate the water dynamics on the watershed but require those data that may be not available in remote regions. The third group of methods uses the conceptual hydrological models. These methods provide relatively accurate estimation of river flow from rainfall with affordable requirement of input data. In these methods, parameters of models are usually estimated from the watershed characteristics using GIS tools. For its accuracy and convenience to estimate, this study uses one of the methods in the third group known as TR55.

In Viet Nam, many studies have been done to develop unit hydrographs. For

Corresponding author: Doan Thi Noi
E-mail: chungnoicg@gmail.com

example, Le Dinh Thanh estimates the portable maximum flood (PMF) from the portable maximum precipitation [4]. Le Van Nghinh documented and applied different methods to calculate designed hyetographs and hydrograph [3]. Ngo Le Long considered the impact of climate change on the estimation of design hydrograph [5]. However, so far there have not been many studies on development of designed hydrograph for small watersheds where the time of concentration is usually less than 10 hours. In these watersheds, using daily rainfall to construct the hydrograph is not suitable due to coarse temporal resolution. Meanwhile, these small watersheds account for up to 70% of drainage structures. In that context, development of designed hydrographs for small watershed is an urgent need.

This study aims at applying the TR55 model based on SCS method to estimate the designed hydrograph for Tong Soong watershed, which is a small mountainous basin in Lang Son province, Northern Viet Nam. In this method, the SCS curve number is employed to estimate runoff and the SCS unit hydrograph is used to estimate the coordinates of hydrograph from runoff.

2. Methodology

This study employed the TR55 software to calculate design hydrographs for small drainage system for Tong Soong watershed. The software was developed in 1998 by the United States Department of Agriculture (USDA, 1999). The TR55 presents simplified procedures for estimating runoff and peak discharges in small watersheds. The model described in TR-55 begins with a rainfall amount uniformly imposed on the watershed over a specified time distribution. Mass rainfall is converted to mass runoff by using a runoff curve number (CN). Runoff is then transformed into a hydrograph by using unit hydrograph theory and routing procedures that depend on runoff travel time through segments of the watershed (USDA, 1999). The software calculates storm runoff volume using the SCS method and constructs hydrograph using tabular hydrograph method.

The SCS method estimated by equation below:

$$Q = \frac{(P - 0.2S)^2}{P + 0.8S}$$

where Q is the runoff; P is the rainfall; S is the potential maximum retention after runoff begin. S is related to the soil texture and land cover conditions of the watershed through curve number (CN) parameter by:

$$S = \frac{100}{CN} - 10$$

CN can be determined from soil type, plant cover type, treatment, impervious areas, interception, hydrologic condition and antecedent runoff condition. CN also depends on whether impervious area is directly connected to the drainage system or whether flow over the previous area before reaching the drainage system.

Next, the hydrograph can be constructed for the watershed using tabular hydrograph method as below:

1) Divide the watershed into subareas with relatively homogeneous watershed characteristics

2) The hydrograph coordinate at time t of a subarea (q) is calculated by:

$$q = q_t A_m Q$$

in which q_t is the tabular unit discharge, which is determined from time of concentration (T_c) and ratio between initial abstraction and rainfall (I_a/P) with $I_a = 0.2S$; A_m is the drainage area of subarea; and Q is the runoff on the subarea.

3) Finally, hydrograph at the outlet of the watershed is obtained from the hydrograph coordinates of subareas and time of travel from each subarea to the watershed outlet.

Clearly, there are three main parameters in the TR55 software including CN, T_c and T_t . In this study, these parameters were estimated from maps of topography, land use and soil type.

3. Study area

In this study, we constructed the design hydrograph for the Tong Soong watershed, which is a small watershed in Lang Son province, Northern Viet Nam (Figure 1). The watershed has an area of around 25km² and a catchment length of 7.14km. Located in a mountainous

region, the watershed topography is quite steep with an average slope of 23.4°, which indicates that the time of concentration of this watershed

is relatively small. More detailed description of the watershed characteristics can be found in Table 1.

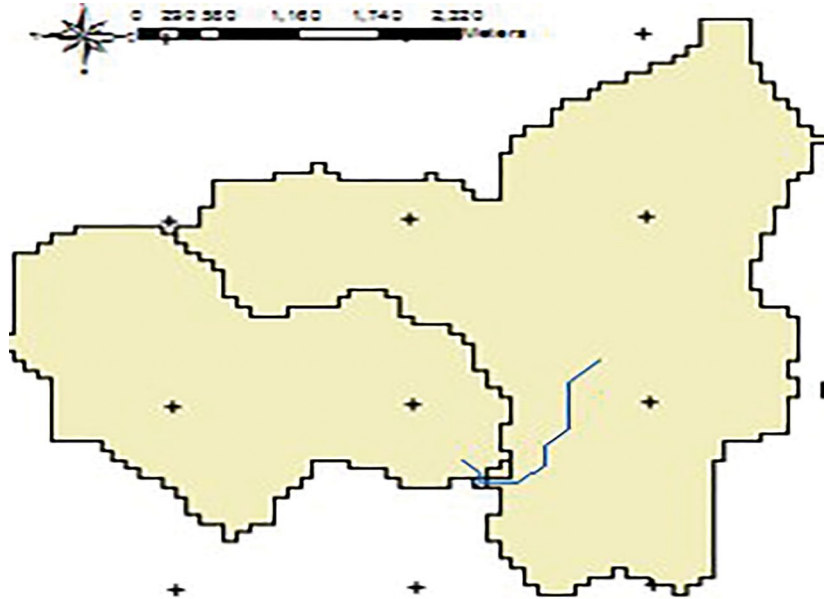


Figure 1. Watershed of Tong Soong Bridge

Table 1. Characteristics of Tong Soong watershed

No.	Characteristic	Symbol	Unit	Value
1	Design probability	P	%	2
2	Catchment area	A	km ²	19.48
3	Main flow length	L	km	1.8
4	Catchment length	Llv	km	7.03
5	Catchment averaged width	B	km ² /km	2.77
6	Catchment roughness			2.00
7	Catchment averaged slope	Sb	%	25.15
8	River bed slope	Sr	%	0.05

4.1 Determination of design hyetographs

In order to develop the design hydrograph for Toong song watershed, we collected hourly data over the period from 1975 to 2016 at Lang Son rain gauge. Subsequently, we determined the main rainfall events occurring over the 1975-2016 period and classified these events into two groups: events with total amount of 24-h rainfall lower than 100 mm (Type I) and events with 24-h rainfall higher than or equal to 100 mm (Type II). Figures 2a and 3a show the 24-hour dimensionless cumulative hyetographs of rain events 24-h rainfall lower and greater

than 100mm, respectively. Based on these hyetographs, we selected the typical hyetograph of each group as shown in figures 2b and 3b. Figures 2c and 3c show the typical incremental hyetographs of each group. It is clearly seen that although the typical hyetographs of two groups are similar, the peak rainfall of type II is much higher than that of type I. Next, the design 24-h rainfall values with return frequencies of 1, 2, 5, 10, 25, 50 and 100 years were calculated based on 24-h rainfall datasets collected in the 1975-2016 period. Finally, the design hyetographs corresponding with the design 24-h rainfall

values were obtained by mapping from two typical hyetographs type I and II. These design

hyetographs were used as the inputs for TR55 to construct the design hydrographs.

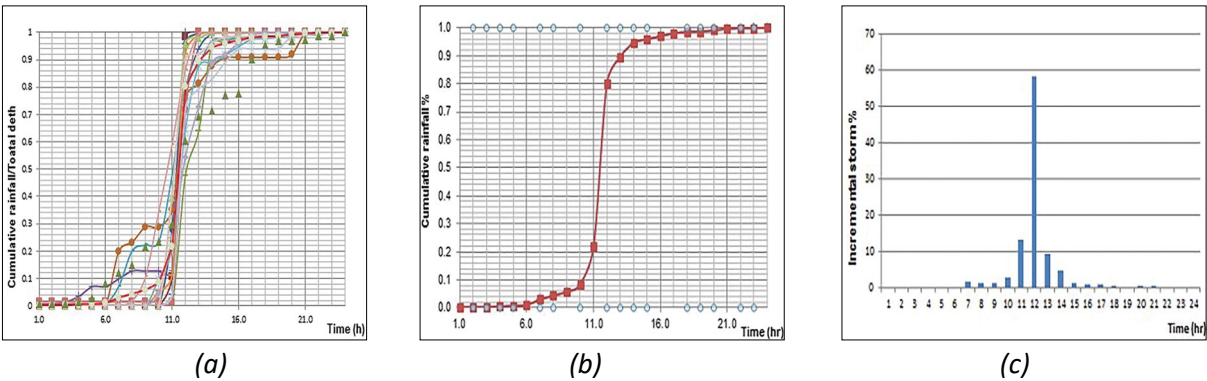


Figure 2. Cumulative dimensionless hyetograph and design hyetograph in Lang Son (type I)

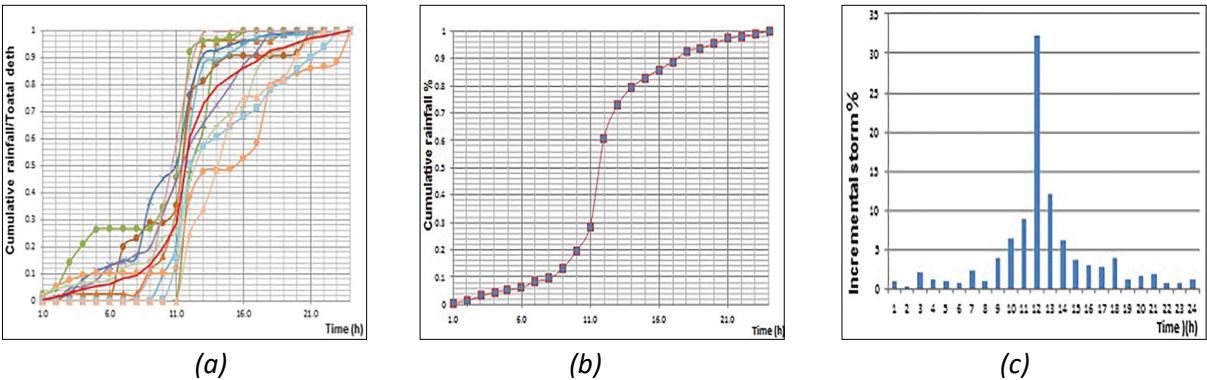


Figure 3. Cumulative dimensionless hyetographs and design hyetographs in Lang Son (type II)

4.2. Land use map and Curve number map

In order to estimate runoff from storm rainfall, the TR55 model uses the curve number (CN) method as mentioned in section 2. Determination of CN depends on the watershed characteristics including soil and land cover conditions, which the model represents as hydrologic soil group, land use, treatment, and hydrologic condition. Given those watershed data, the CN map can be constructed using GIS tools. Figure 4 shows the land cover and CN maps of the Toong song watershed. The figure indicates that there are three regions with CN values of 77, 71 and 70 in which the regions with CN values of 77 and 70 occupy nearly all watershed. Similar to the CN estimation, the time of concentration T_c and time of travel T_t were also calculated by GIS tool from the topography map.

4.3 Determination of design hydrograph

The 1-day hydrograph for the Tong Soong

watershed was constructed from the daily rainfall with return periods of 1, 2, 5, 10, 25, 50 and 100 years using the TR55 method. Figure 5 shows an example of the design hydrograph at the outlet of the watershed corresponding with a return period of 50 years. Table 2 summaries the peak discharge and peak time at sub-basin, reaches and outlet of the watershed.

4. Conclusions

In this study, the TR55 method was explored and applied to estimate the designed hydrographs with return periods from 1 to 100 years. The initial results show that this method is suitable for calculation of designed hydrograph for small and medium watershed. Particularly, the calculation of time of concentration using this method, which accounts for the time traveling both on hill slope and on the river, is more accurate than the traditional methods. The accuracy of runoff simulation using combined GIS and TR55 was

also confirmed in the study of Ramana (2014). The application of the TR55 method shows a great potential to derive hydrographs and develop a database of hyetographs and hydrographs for other mountainous regions having similar conditions in Northern Viet Nam. However, care should be taken as the procedures in TR-55 are simplified by

assumptions about some parameters. These simplifications, however, limit the use of the procedures and can provide results that are less accurate than more detailed methods. The user should examine the sensitivity of the analysis being conducted to a variation of the peak discharge or hydrograph when using the method.

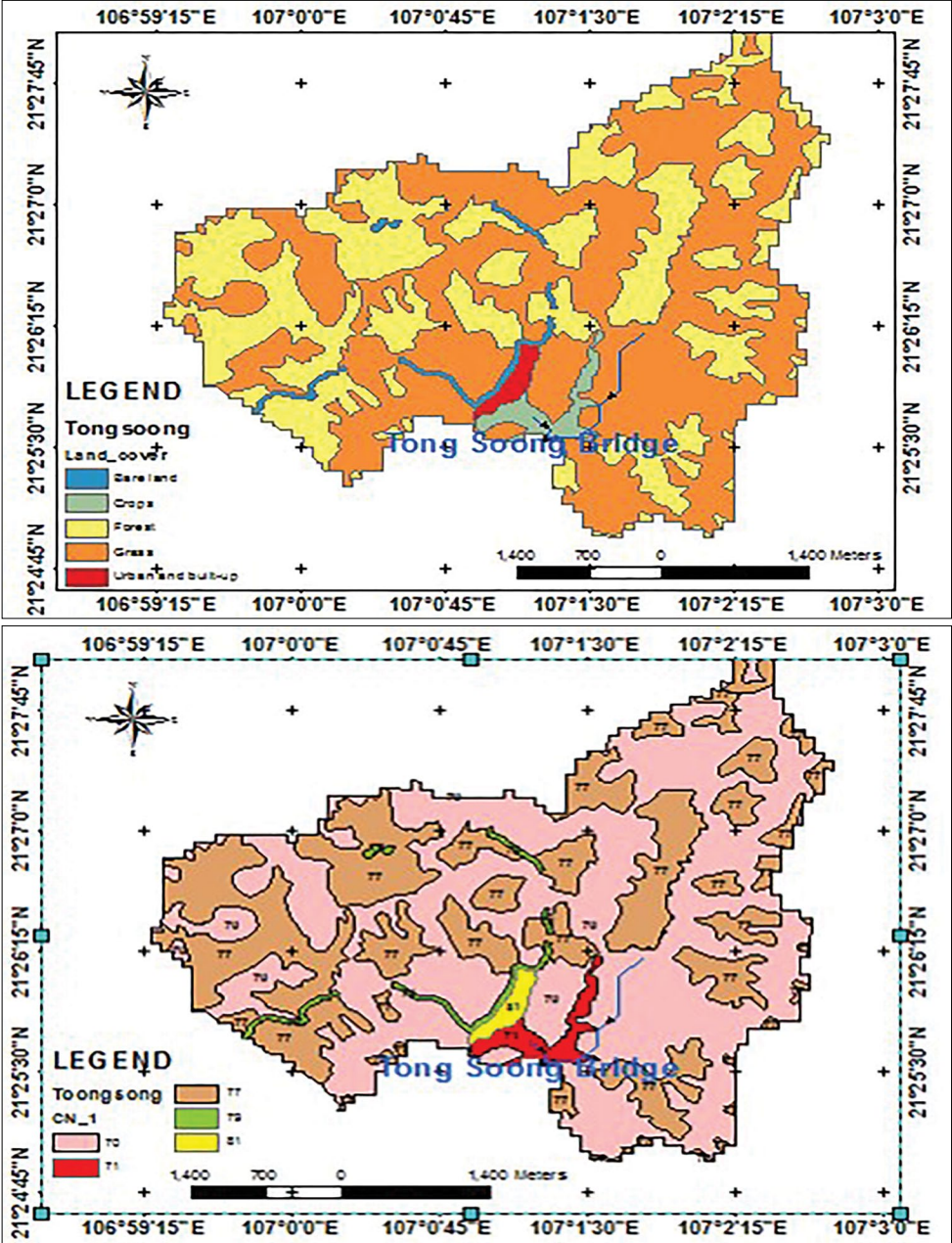


Figure 4. Land cover and Curve number map in Tong Soong

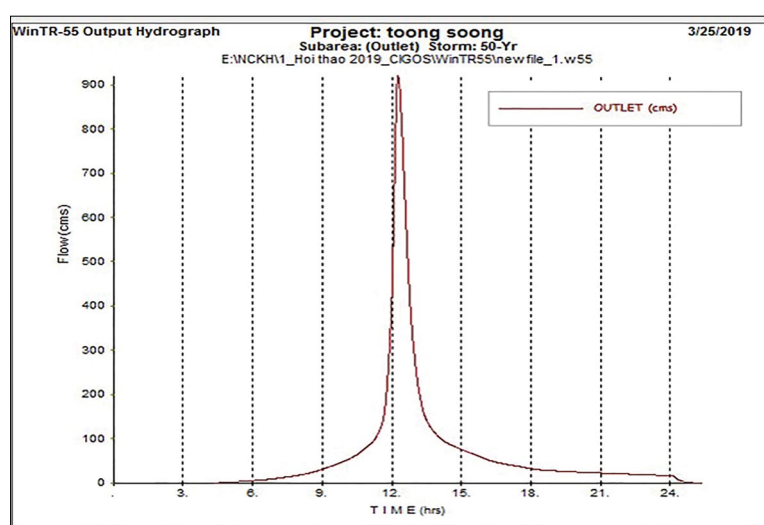


Figure 5. Design hydrograph at Tong Soong watershed

Table 2. Flood peak with different return periods at Tong Soong

Region: lang son Locale:							
Hydrograph Peak/Peak Time Table							
Sub-Area or Reach Identifier	Peak Flow and Peak Time (hr) by Rainfall Return Period						
	2-Yr	5-Yr	10-Yr	25-Yr	50-Yr	100-Yr	1-Yr
	(cms) (hr)	(cms) (hr)	(cms) (hr)	(cms) (hr)	(cms) (hr)	(cms) (hr)	(cms) (hr)
SUBAREAS							
sub 1	75.86 12.16	82.05 12.16	228.38 12.16	306.51 12.15	364.87 12.16	422.24 12.15	72.04 12.17
sub 2	118.94 12.24	128.36 12.23	359.06 12.24	483.43 12.21	574.75 12.23	666.47 12.21	112.36 12.22
sub 3	0.40 12.13	0.44 12.13	1.20 12.12	1.60 12.12	1.90 12.12	2.20 12.12	0.38 12.13
REACHES							
reach 1	75.86 12.16	82.05 12.16	228.38 12.16	306.51 12.15	364.87 12.16	422.24 12.15	72.04 12.17
Down	75.85 12.26	82.02 12.26	227.80 12.23	306.06 12.22	363.75 12.21	421.67 12.22	71.85 12.24
reach 2	118.94 12.24	128.36 12.23	359.06 12.24	483.43 12.21	574.75 12.23	666.47 12.21	112.36 12.22
Down	118.75 12.38	128.27 12.36	358.49 12.30	482.76 12.32	574.12 12.30	665.18 12.31	112.36 12.36
OUTLET	188.93	204.11	575.62	773.54	921.49	1068.16	178.92

References

1. Chow V.T: Applied Hydrology (1988), *In: Hydrology-572 pages*.
2. Chow V.T (1964), *Handbook of Applied Hydrology*.
3. Le Van Nghinh (2000), *Hydrological principles. Agricultural Publishing Inc.*
4. Le Dinh Thanh (1996), *Estimation of PMP and PMF for Vietnam. PhD Dissertation. Hanoi Water University.*
5. Ngo Le Long (2015), *Study on scientific basics for proposing standards of designed flood, sea dykes in the context of climate change, sea level rise in Viet Nam and mitigation measures.*
6. Ramana, G.Venkata, (2014), *Rainfall runoff modelling between TR-55 hydrologic watershed model and overland time of concentration model. A RAMANA, International Journal of Advances in Computer Science and Technology, 3(3).*
7. United States Department of Agriculture, (1999), *Urban Hydrology for Small Watersheds.*

GREENHOUSE GAS EMISSIONS IN AGRICULTURE, BUILDINGS AND WASTER SECTORS IN HO CHI MINH CITY

Le Anh Ngoc⁽¹⁾, Nguyen Van Tin⁽¹⁾, Pham Duc An⁽¹⁾, Vo Thi Nguyen⁽¹⁾, Bao Thanh⁽²⁾

⁽¹⁾Sub-Institute of Hydrometeorology and Climate Change

⁽²⁾Ho Chi Minh University of Natural Resources and Environment

Received: 15 February 2019; Accepted: 2 March 2019

Abstract: Climate change (CC) is a common problem for all people with a strong influence on the world. One of the main causes of climate change is greenhouse gases (GHG). Viet Nam has implemented the National greenhouse gas inventories for five sectors: agriculture, energy, industrial processes, waste, land use change and forestry. Being the biggest economic development centre in Viet Nam, Ho Chi Minh City has emitted numerous amounts of greenhouse gases every year. This paper presents results of GHG calculations in agriculture, waste and buildings in Ho Chi Minh City applying the 2006 IPCC guideline. It is found that greenhouse gases in Ho Chi Minh were about 1.1 million, 3 million and 0.4 million tons of CO₂ equivalent in agriculture, waste and buildings, respectively.

Keywords: IPCC Guideline 2006, greenhouse gas inventory for agriculture, waste, buildings.

1. Overview of agriculture, waste and buildings sectors in Ho Chi Minh City

1.1 Agriculture

Crop Cultivation: Crop structure continues to reduce rice area while increases area of flower, safe vegetables, fodder grass and other annual industrial crops. By 2013, the total area of rice cultivation in the city was about 29,293 hectares. According to the master plan to 2020, rice area will reduce to 3,200 ha.

Livestock: By 2020, the number of dairy cows and pigs are expected at 75,000 heads, 25,600 heads, 800 heads and 275,000 heads, respectively.

Aquaculture: Area of saltwater aquaculture was about 8,460 ha, concentrating mainly in Can Gio and 1,640 ha of freshwater fisheries, mainly in Binh Chanh and Cu Chi Districts. The farming area by 2020 according to the planning has not changed. [2]

1.2 Waste

Three volume of domestic solid waste was

brought to landfills and solid waste treatment plants in the city estimate about 8,300 tons/day.

However, domestic solid waste has not been classified at source, causing great pressure on treatment facilities. Solid waste treatment technology is mainly landfill method (about 75% of the total volume), the rate of solid waste treated by compost processing method was about 15%, the rate of solid waste is treated by burning technology was about 5-10%.

The wastewater sector includes domestic wastewater, medical waste water and industrial wastewater. Regarding domestic wastewater, the amount of urban wastewater was about 2.75 million tons/day, of which 13% was treated. Wastewater from health facilities was around 17,750m³/day, industrial wastewater from 13 industrial parks, 3 export processing zones and 33 production facilities is about 278,191m³/day.

In the situation of increasing waste and impacts of climate change, Ho Chi Minh City needs a master plan to deal with substances of which clearly defining the scale and location of waste treatment facilities. The buildings investment roadmap and technology

Corresponding author: Le Anh Ngoc
E-mail: leanhngoc.sihymecc@gmail.com

in each stage must be specifically set up to keep up with the city's development speed.

1.3. Buildings

Total of high-rise buildings in 2013 in Ho Chi Minh City is 452 piles including 126 projects in district 1, 107 projects in district 7, 66 projects in district 3, 24 projects in district 2. The total electricity consumption for these buildings was 725 million KWH, in which district 1 consumed about 385 million KWH, accounting for 52%. The total electricity consumption for the facilities accounted for 4% of the city's total electricity consumption.

2. Data and research methods

2.1 Database

Table 1. Composition of Domestic solid waste in Ho Chi Minh City

Composition	%
Paper	2.8
Garbage	0
Food	67.9
Wood/ Straw	0.06
Textile	6.4
Skin	2.24
Others	20.6
Total	100

(Source: Department of Solid Waste Management, Department of Natural Resources and Environment of Ho Chi Minh City)

Table 2. Volume of treated domestic solid waste

Types	Volume (tons/year)	Volume (tons/day)	Rate %
Landfill	2,007,135	5,499	80
Burning	146	400	6
Compose	327,040	896	13
Recycle	19,710	54	1
Total	2,499,885	6,849	100

2.1.3. Wastewater

According to survey information of Saigon University, processing technology of EPZs / IPs in Ho Chi Minh City was all Aerotank and SBR forms. These technologies treat wastewater by biological methods

2.1.1. Agriculture

Data in the agriculture sector was collected from the Department of Agriculture and Rural Development of Ho Chi Minh City.

2.1.2. Domestic solid waste

Nowadays, Ho Chi Minh City Urban Environment Company is mainly responsible for collecting the solid waste amount. All domestic solid waste is treated by two main methods, namely burial and compost production, where concentrated in Da Phuoc and Tay Bac Cu Chi treatment areas (Landfill No. 2, Vietstar Company). Of which, burial method accounts for about 85%, whereas compost is about 15%.

under aerobic conditions. Although the centralized wastewater treatment systems of EPZs/IPs are managed and operated relatively methodically, the treatment efficiency has not been as expected, so the group chose MCF = 0.2 to calculate emissions.

Table 3. Wastewater composition of industrial zones and export processing zones in Ho Chi Minh City

No.	KCN-KCX	Actual capacity (m ³ /day)	BOD5	COD	N-Total	TSS	Coliforms
1	An Ha	1,100	51	70	12.6	236	12,000
2	Binh Chieu	350	354	632	114	196	4.6x10 ⁶
3	Cat Lai II	2,400	185	330	18.2	105	9x10 ⁵
4	Vinh Loc	4,600	200	600	60	300	5,000-8,000
5	Hiep Phuoc	3,500	100	400	60	200	-
6	Cu Chi	3,100	60	109	26.8	82	2x10 ⁴
7	Le Minh Xuan	9,800	150	600	60	200	-
8	Linh Trung	2,000	500	800	30	300	104
9	Linh Trung II	1,700	-	225	73.50	122	-
10	Tan Binh	4,200	55-135	105-280	16.27	59	1,500-3,000
11	Tan Phu Trung	2,300	198	325	39.6	215	104
12	Tan Tao	1,500	220	500	40	220	105-106
13	Tan Thoi Hiep	5,000	576	1,384	39.7	300	-
14	Tan Thuan	400	88	135	32.8	92	4.6x10 ⁴
15	Dong Nam	30	Trial operation				
16	Hoa Phu	80	Under buildings				

2.1.3. Buildings

Data for buildings was collected from Department of Construction.

2.2. Methods

2006 IPCC Guidelines for Greenhouse Gas Inventories were applied to calculate GHG for the three sectors in Hochiminh City, as follows:

2.2.1. Agriculture

The method identifies emission of GHG mainly CO₂, CH₄, N₂O through emission factors in each field and industry. These emission factors are included in the IPCC emission calculation formulas for each category of greenhouse gases.

- *Rice Cultivation: Annual CH₄ emission from rice*

$$CH_{4Rice} = A * t * EF_i * 10^{-6} \quad (1)$$

Where: CH_{4Rice} = Annual CH₄ emission from Rice Cultivation (Gg CH₄ yr-1), EF_i: Adjusted daily emission factor for a particular harvested area (kg CH₄ ha-1 day-1), t = Cultivation period of rice (day), A = Annual harvested area (ha yr-1).

- *Livestock:*

In this article, greenhouse gases in livestock generated from the intestinal fermentation of livestock and manure management process were calculated.

Methane Emissions from Enteric Fermentation

$$CH_{4Enteric} = N(T) * EF(T) * 10^{-6} \quad (2)$$

Where: CH_{4Enteric} = Emission factor for Enteric Fermentation (Gg CH₄ yr-1), N (T)= Number of animals (head), EF(T)= Emission factor for Enteric Fermentation (kg head-1 yr-1).

Table 4. Emission factor for Enteric Fermentation

Category of animal	EF(T) (kg head-1 yr-1)
Dairy Cattle	61
Other Cattle	47
Buffalo	55
Swine	1

Methane Emissions from Manure Management

$$CH_4 \text{ Manure} = N(T) * EF(T) * 10^{-6} \quad (3)$$

Where: $CH_4 \text{ Manure}$ = CH_4 emissions from

Manure Management ($Gg \text{ } CH_4 \text{ yr}^{-1}$), $EF(T)$ =Emission factor for Manure Management ($kg \text{ head}^{-1} \text{ yr}^{-1}$), $N(T)$ = Number of animals (head).

Table 5. The coefficient of methane emission from faeces of some livestock [4]

Category of animal	26°C	27°C	>28°C
Dairy Cattle	28	31	31
Other Cattle	1	1	1
Buffalo	2	2	2
Swine	6	7	7

Direct N_2O Emissions from Manure Management Systems

$$N_2O \text{ (mm)} = NEMMS * EF3(S) * 44/2 \quad (4)$$

Where: $N_2O \text{ (mm)}$ = Annual direct N_2O emissions from Manure Management ($kg \text{ } N_2O$

yr^{-1}), NE_{MMS} =Total nitrogen excretion for the MMS ($kg \text{ N } yr^{-1}$), $EF3(S)$ =Emission factor for direct N_2O -N emissions from MMS [$kg \text{ } N_2O$ -N ($kg \text{ N in MMS})^{-1}$], $44/28$ =conversion of (N_2O -N) (mm) emissions to N_2O (mm) emissions

Table 6. Default values for nitrogen excretion rate in Asia ($kg \text{ n } (1000 \text{ kg animal mass})^{-1} \text{ day}^{-1}$)

Category of animal	Nrate ($kgN/ton/day$)	TAM ($kg/head$)
Dairy Cattle	0.47	350
Other Cattle	0.34	200-275
Swine	0.42	60
Buffalo	0.32	350-550

$$Nex_{(T)} = Nrate(T) * TAM * 10^{-3} * 365 \quad (5)$$

Where: $Nex_{(T)}$ =Annual N excretion per head of species/livestock category ($kg \text{ N animal}^{-1} \text{ year}^{-1}$), $Nrate(T)$ = Default N excretion rate [$kg \text{ N } (1000 \text{ kg animal})^{-1} \text{ day}^{-1}$], TAM = Typical animal mass for livestock category (kg)

Amount of manure nitrogen that is loss due to volatilisation of NH_3 and NO_x

$$V_{\text{olatilization-MMS}} = NE_{MMS} * Frac_{(GasMS)} \quad (6)$$

Where: NE_{MMS} =Total nitrogen excretion for the MMS, $Frac_{GasMS}$ =Fraction of managed livestock manure nitrogen that volatilises (Dairy Cattle =40%, Other Cattle =45%, Buffalo =25%, Swine =45%.)

- Aquaculture:

$$CH_4 \text{ Emission}_{WWflood} = P * E(CH_4)_{diff} * Aflood_{\text{total surface}} * 10^{-6} \quad (7)$$

Where: $CH_4 \text{ Emissions}_{WWflood}$ =Total emission CH_4 from flood surface ($GgCH_4 \text{ yr}^{-1}$); P : time, day yr^{-1} ; $Aflood_{\text{total surface}}$ =Annual flood total surface area (ha).

2.2.2. Domestic solid waste

Formula to calculate greenhouse gas emissions from landfills:

$$Lo = W * MCF * DOC * DOCF * (16/12) * xF \quad (8)$$

Where: Lo = CH_4 generation potential, Gg ; W = mass of waste deposited, Gg ; DOC = degradable organic carbon in the year of deposition, fraction, $Gg \text{ C}/Gg \text{ waste}$; $DOCF$ = fraction of DOC that can decompose (fraction); MCF = CH_4 correction factor for aerobic decomposition in the year of deposition (fraction); DOC , $Gg \text{ F}$ = fraction of CH_4 in generated landfill gas (volume fraction) $16/12$ = molecular weight ratio CH_4/C (ratio).

Formula to calculate greenhouse gas emissions from biological waste treatment by biological method

* CH_4 emissions from biological treatment

$$CH_4 \text{ Emissions} = \sum_i (M_i * EF_i) * 10^{-3} * R \quad (9)$$

Where: $CH_4 \text{ Emissions}$ =total CH_4 emissions in inventory year, Gg ; $CH_4 \text{ } M_i$ =mass of organic waste treated by biological treatment type i , Gg ; EF =emission factor for treatment i , $g \text{ } CH_4/$

kg waste treated; i=composting or anaerobic digestion; R=total amount of CH₄ recovered in inventory year, Gg CH₄.

*N₂O emissions from biological treatment

$$N_2O\ Emissions = \sum_i (M_i \times EF_i) \times 10^{-3} \quad (10)$$

Where: N₂O Emissions=total N₂O emissions in inventory year, Gg N₂O; Mi=mass of organic waste treated by biological treatment type i, Gg; EF=emission factor for treatment i, g N₂O/kg waste treated; i=composting or anaerobic digestion;

Formula to calculate greenhouse gas emissions from burning solid waste by burning method

$$E_{j,f} = M_f * EF_{j,f} \quad (11)$$

Where: E_{j,f}=Gas discharge load j of the type of fuel f used during combustion, (ton); M_f=Fuel consumption type f, (TJ); EF_{j,f}=Gas emission factor default j of f fuel type (ton/TJ); J:Type of exhaust gas; F: The type of fuel used during combustion/firing.

2.2.3. Wastewater

Greenhouse gases in the field of wastewater management in Ho Chi Minh City include emissions from wastewater treatment activities. Formula to calculate greenhouse gas emissions in the field of wastewater management:

Table 7. Total CO₂ emissions in the agricultural sector

Field	2013	2020
Cultivation	243,273	73,125
Livestock	830,662	652,452
Aquaculture	85,274	77,785
Agriculture	1,159,209	803,362

3.2. Greenhouse gas emissions in the waste sector

Solid waste sector

Total emissions in the solid waste sector in Ho Chi Minh City was 2,764,212.52 tons of CO₂, of which emissions mainly from landfills, followed by emissions from biological methods.

Waste water

Total GHG emissions from the wastewater treatment sector in Ho Chi Minh City 143,347.9 tons of CO₂ equivalent, emissions mainly from industrial wastewater emit 81,973 tons of CO₂ (accounting for 57.2%), emissions from

$$CO_2 = Q \times BOD_5 \times B_0 \times MCF \times GWP_{CH_4} \quad (12)$$

Where: Q: wastewater flow (m3/day);

BOD₅: country-specific per capita BOD in inventory year, g/person/day;

B₀ = maximum CH₄ producing capacity, kg CH₄/kg BOD (0,6kgCH₄/kg BOD);

MCF = methane correction factor (fraction)

2.2.4. Buildings

Method of calculating greenhouse gas emissions for energy consumption

$$E_{CO_2} = M * EF_e \quad (13)$$

Where: M: Total of Electric energy consumption (MWH); EF_e: Emission factor of electricity (EF_e= 0.56 TCO₂/MWH from the Department of Meteorology, Hydrology and Climate Change)

3. Results and Discussions

3.1. GHG emissions in Agriculture

According to the calculation results, CO₂ emissions in the agricultural sector in 2013 was about 1.16 million tons of CO₂eq, of which emissions from livestock accounted for the majority. The forecast according to the plan until 2020 emissions will be reduced to about 800 thousand tons of CO₂ equivalent.

untreated domestic wastewater are about 58,945.2 tons of CO₂ (41.1%).

3.3. Greenhouse gas emissions in the buildings sector

Total GHG emissions in 2013 in high-rise buildings in Ho Chi Minh City was 406,294 tons of CO₂, corresponding to electricity consumption of over 700 million KWH. District 1 was the largest emission (53.2%), where most of the office buildings and large commercial centres are located. The second and the third were District 7 and District 3, accounting for 15.8% and 9.1%, respectively.

Table 8. Total CO₂ emissions (tons of CO₂) in the solid waste sector

Treatment	Landfill	Compost	Burning	Total
CO ₂ eq. yr -1	2,750,275	110,610	2,876.52	2,764,212.52

Table 9. Total volume of wastewater in 2016 in Ho Chi Minh City

Type of treatment	CO ₂ eq. yr -1	Rate (%)
Domestic wastewater	58,945.2	41.1
Aerobic treatment	0	0
Untreated	58,945.2	41.1
Medical waste water	2,429.5	1.7
Industrial Wastewater	81,973.2	57.2
Total	143,347.9	100

4. Conclusion

In the context of the developing economy, the calculation of GHG emissions contributes to develop Ho Chi Minh's economy while reducing the risk of climate change in agriculture, waste and buildings sectors based on 2006 IPCC guidelines for GHG Inventory and data from relevant authorities.

In agricultural sector, there was about 1.1 million tons of CO₂ in 2013, in which, the largest emission was from livestock (71.7%), followed by cultivation (21%) and the least emission was from aquaculture (7.4%). Main proposed technical measures to decrease GHG in livestock includes reducing CH₄ emissions from the intestinal tract, add starch to plant fibre in diets, providing MUB nutrition cake (Molasses Urea Block) for dairy cows.

Total emissions in the waste industry in

Ho Chi Minh City were about 3 million tons of CO₂ equivalent, of which 2,863,761 CO₂eq (95,2%) in the solid waste sector and 143,348 CO₂ eq (4,8%) in wastewater treatment. Major actions have been implemented in Ho Chi Minh City for decreasing GHG in solid waste such as encouraging CH₄ fermentation technology with combined with electricity generation, developing policies to support recycling actions or reducing solid waste amount treated by disposal sites or burning.

In the buildings sector, the amount of greenhouse gas emissions was 406,294 tons of CO₂ equivalent from the consumption of more than 700 million KWH for buildings. Some solutions to decrease emissions consist of applying Building Energy Management System in buildings to increase energy savings, using air conditioners and refrigerators with high energy efficiency in households, implementing energy-saving solutions in lighting systems.

References

1. Ministry of Agriculture and Rural Development (2011), *Scheme on GHG emission reduction in Agriculture and Rural Development by 2020*.
2. Le Viet Bao (2014), *Situation of agricultural production in the area of Ho Chi Minh City 2011-2014*, Department of Agriculture and Rural Development of Ho Chi Minh City.
3. Nguyen Van Tinh, Nguyen Quang Trung, Nguyen Viet Anh (2007), "Influence of methane wastewater regime in the field drying periods", *Journal of Science and Technology*.
4. *2006 IPCC Guidelines for National Greenhouse Gas Inventories, Vol4 Agriculture, Forestry and Other Land Use*.
5. *2006 IPCC Guidelines for National Greenhouse Gas Inventories, Vol5 Waste*.

IMPACT OF SATELLITE OBSERVED SST ON INTENSITY AND TRACK SIMULATION OF TROPICAL CYCLONE OVER VIET NAM EAST SEA: A CASE STUDY OF TYPHOON NALGAE (2011)

Nguyen Thi Thanh⁽¹⁾, Nguyen Xuan Hien⁽¹⁾, Hoang Duc Cuong⁽²⁾

⁽¹⁾Viet Nam Institute of Meteorology Hydrology and Climate Change

⁽²⁾The National Centre for Hydro-Meteorological Forecasting

Received: 18 February 2019; Accepted: 1 March 2019

Abstract: Sea surface temperature (SST) is one of the most important thermal factors affecting typhoon. This paper was carried out to examine the impact of satellite observed SST on intensity and track simulation of tropical cyclone over Viet Nam East sea by using the Weather Research and Forecast (WRF) model. We have selected typhoon Nalgae (2011) for studying the SST impact. Three different sets of SSTs were used in this study: (1) SST from GFS analysis is provided for the initial condition and kept unchanged during the 72 hr simulation; (2) SST from Remote Sensing Systems (RESS) is used for the initial condition and kept unchanged during the 72 hr simulation; (3) SST from RESS is updated every 24 h for the initial and boundary conditions. The simulated results show that the using SST from satellite data for both only initial condition case and initial and boundary conditions case significantly improve the simulated intensity of typhoon due to improved simulation of latent heat and heat fluxes.

Keywords: Sea surface temperature, SST, typhoon, tropical cyclone, the Viet Nam East Sea

1. Introduction

It has been recognized that the Sea Surface Temperature (SST) is one of the most important parameters which plays a significant role in the formation and intensification of tropical cyclone [12, 13]. Gray (1968, 1978) noted that the 26°C isotherm deepening to a depth to 60m from the surface is required for the formation of tropical cyclone. SST determines the amount of sensible and latent heat available to the tropical cyclone from the ocean, hence, it is indicative of the intensity of tropical cyclone [12].

Large number of studies [1,5-7,14, etc] found that the intensity of tropical cyclone increases rapidly when it passes through the warm water area due to increasing the sensible and latent heat flux. Shankar et al. (2007) showed that not only the magnitude

of SST but also its gradient affects surface wind and convective activity, which affects the intensity of the tropical cyclone. Studies were also performed to investigate the influence of SST on the movement of tropical cyclone. Wu (2005) studied the effect of symmetric and asymmetric SST distributions on the centre of tropical cyclone on the movement of tropical cyclone. Accordingly, the asymmetric SST distribution over large areas affected the movement of tropical cyclone due to various surface friction and surface heat flux [2]. Recently, results from numerical weather prediction (NWP) model shown that the intensity and track of simulated tropical cyclones vary with the various SST due to the changed resolution of SST fields [11,17,4].

In operational NWP modelling applications, SST field is generally obtained from GFS analysis data of National Centers for Environmental Prediction (NCEP) with

Corresponding author: Nguyen Thi Thanh
E-mail: thanhnt.met@gmail.com

horizontal resolution of $0.5^\circ \times 0.5^\circ$. There is a need for alternative SST datasets, which can give more accurate representation of ocean boundary condition in the NWP model.

Nowadays, SST products are available from microwave (MW) and infrared (IR) sensors. One of these is the SST product from Remote Sensing Systems (RESS), Northern California, American. It is created from Tropical Rainfall Measuring Mission Microwave Imager (TMI), Advanced Microwave Scanning Radiometer (AMSR-E), Advanced Microwave Scanning Radiometer 2 (AMSR2), WindSat and the Moderate Resolution Imaging Spectroradiometer (MODIS) data. This SST data is the daily optimally interpolated product at $9\text{ km} \times 9\text{ km}$ (MW_IR OI SST). Thus, it can be seen that MW_IR OI SST data is higher horizontal resolution than GFS SST data.

The objective of the present study is to investigate the impact of MW_IR OI SST on intensity and track simulation of tropical cyclones by using Weather Research and Forecast (WRF) model.

2. Data, experimental design and methodology

2.1. Data

The MW_IR OI SST is available at website: <http://www.remss.com/>.

The GFS analysis data of National Centres for Environmental Prediction available at $0.5^\circ \times 0.5^\circ$ horizontal resolution and 6 hourly interval has been interpolated to the model

grid for providing the initial and boundary conditions. This data is provided at website: ftp://nomads.ncdc.noaa.gov/GFS/analysis_only/.

In addition, tropical cyclone best track data (including tropical cyclone centre locations and intensities) from IBTrACS (International Best Track Archive for Climate Stewardship) data of National Oceanic and Atmospheric Administration (NOAA) and National Climatic Data Center (NCDC) has been used to verify the model simulated track and intensity from two different experiments. This data is available in the website: <https://www.ncdc.noaa.gov/ibtracs/>.

2.2. Experimental design

The mesoscale model used in this study is the WRF model version 3.6 with two nested domains. The first domain ranges from 0°N – 31°N and 92°E – 130°E with 135×158 grid points, horizontal resolution of 27 km. The second domain ranges from 5°N – 25°N and 100°E – 120°E with 259×250 grid points and horizontal resolution of 9 km (Fig. 1). The physics options of WRF model used the same for both domains, include the Kain–Fritsch 2 cumulus parameterization scheme [10], Thompson microphysics scheme [16], Yonsei State University (YSU) [7] Planetary boundary layer scheme. Long-wave radiation and short-wave radiation are parameterized using RRTMG [8] scheme. Land surface are parameterized using the multi-layer Noah land surface model [3], and for Surface Layer, Revised MM5 Monin–Obukhov scheme [9] is used.

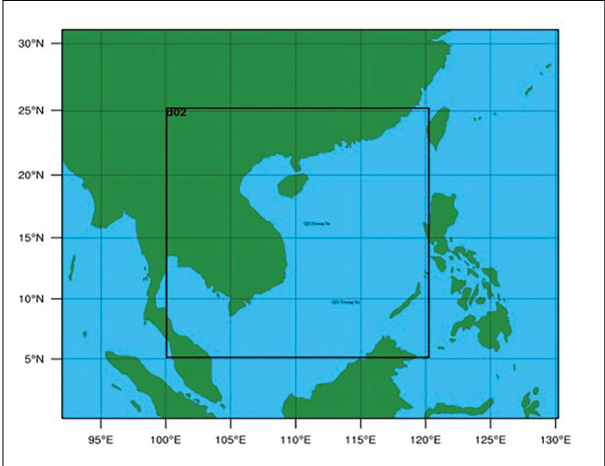


Figure. 1 The WRF model domains for cyclone simulation

Three experiments are carried out: (1) GFS SST is provided for the initial condition and kept unchanged during the 72 hr simulation (GFS); (2) MW_IR OI SST is used for the initial condition and kept unchanged during the 72 hr simulation (SSTVT); (3) MW_IR OI SST is updated every 24 h for the initial and boundary conditions (SSTUP).

2.2. General description of Typhoon Nalgae

Nalgae formed as a tropical depression over the Philippine Sea on September 27, 2011 and moved generally westwards. Within three days, it had strengthened into a severe typhoon. On October 1, Nalgae peaked intensity with an estimated maximum sustained wind of 175km/h, about 300 km northeast of Manila. Then it crossed Luzon and entered the Viet Nam

East sea in the late afternoon. It moved west to west-north-westwards and weakened into a severe tropical storm on October 2. It weakened further into a tropical storm on 4 October and crossed the southern part of Hainan Island that afternoon and weakening into a tropical depression at night. Nalgae moved south-westwards across the southern part of the Gulf of Tonkin on October 5 and dissipated over the seas near Nghe An (Fig. 2). Due to the effect of Nalgae typhoon combined with cold front, the North East, North Central and Mid-Central regions had rainfall and heavy rainfall. The total rainfall of two days from October 4 to October 6 was commonly from 50 to 70mm, especially in the Nghe An - Ha Tinh areas, rainfall measured over 100mm.

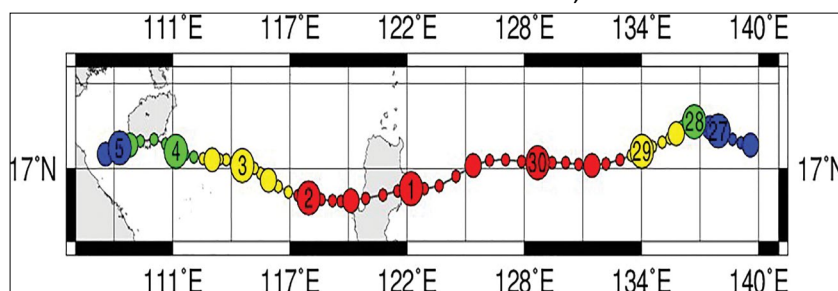


Figure. 2 Best track of Nalgae typhoon

(Source: <http://agora.ex.nii.ac.jp/digital-typhoon/>)

3. Results and discussion

The simulation of Nalgae typhoon for GFS, SSTVT and SSTUP cases were initialized at 00Z on October 2, 2011.

Figure 3 and 4 show the comparison of the GFS SST and the MW_IR OI SST valid for October 2, 2011. Accordingly, MW_IR OI SST

shows colder than GFS SST of 1° to 2°K in the North-eastern part of Viet Nam East sea due to the effect of cold front. On October 3 and 4, MW_IR OI SST shows the effect of cold front on SST field is extended to the southern (Figure 5 and 6). On October 5, the effect of cold front on MW_IR OI SST tends to decrease (Figure 7).

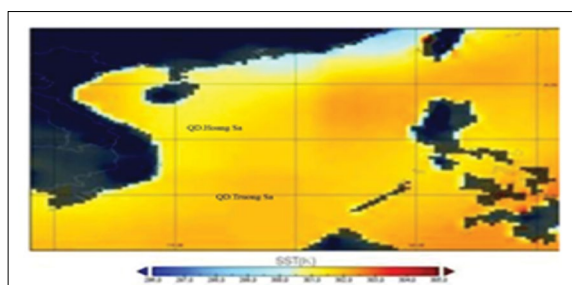


Figure. 3 SST from GFS valid for October 2, 2011

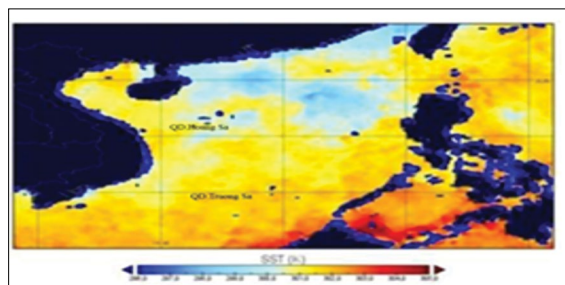


Figure. 4 SST from RESS valid for October 2, 2011

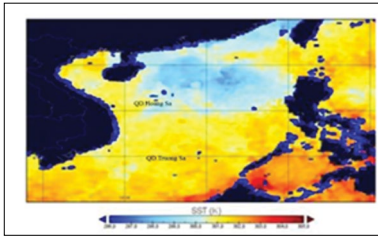


Figure 5. SST from RESS valid for October 3, 2011

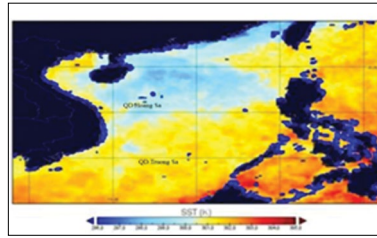


Figure 6. SST from RESS valid for October 4, 2011

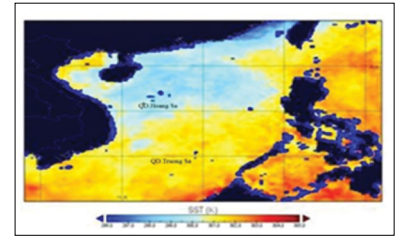


Figure 7. SST from RESS valid for October 5, 2011

Figure 8 shows that there is significant difference in the simulated latent heat fluxes between SSTVT and GFS cases. The 24 hr simulated latent heat flux in SSTVT relatively decreases in both area and magnitude when compared to GFS case. In the centre of Nalgae, the latent heat flux in SSTVT is smaller upto 400 Wm^{-2} than in GFS (Figure 8 a and d). For 48 and 72 hr, the difference in latent heat fluxes between GFS and SSTVT is relatively clear, especially in the southwestern part of the

centre of Nalgae typhoon (Figure 8 b, c and e, f). The simulated latent heat fluxes is not much difference between SSTVT and SSTUP cases for 24 hr, 48 hr and 72 hr simulations (Figure 8 d, e, f and g, h, i).

During the 72 hr simulation, the simulated sensible heat fluxes in SSTVT is also relatively smaller when compared to GFS case and it is not much difference when compared to SSTUP case (Figure 9).

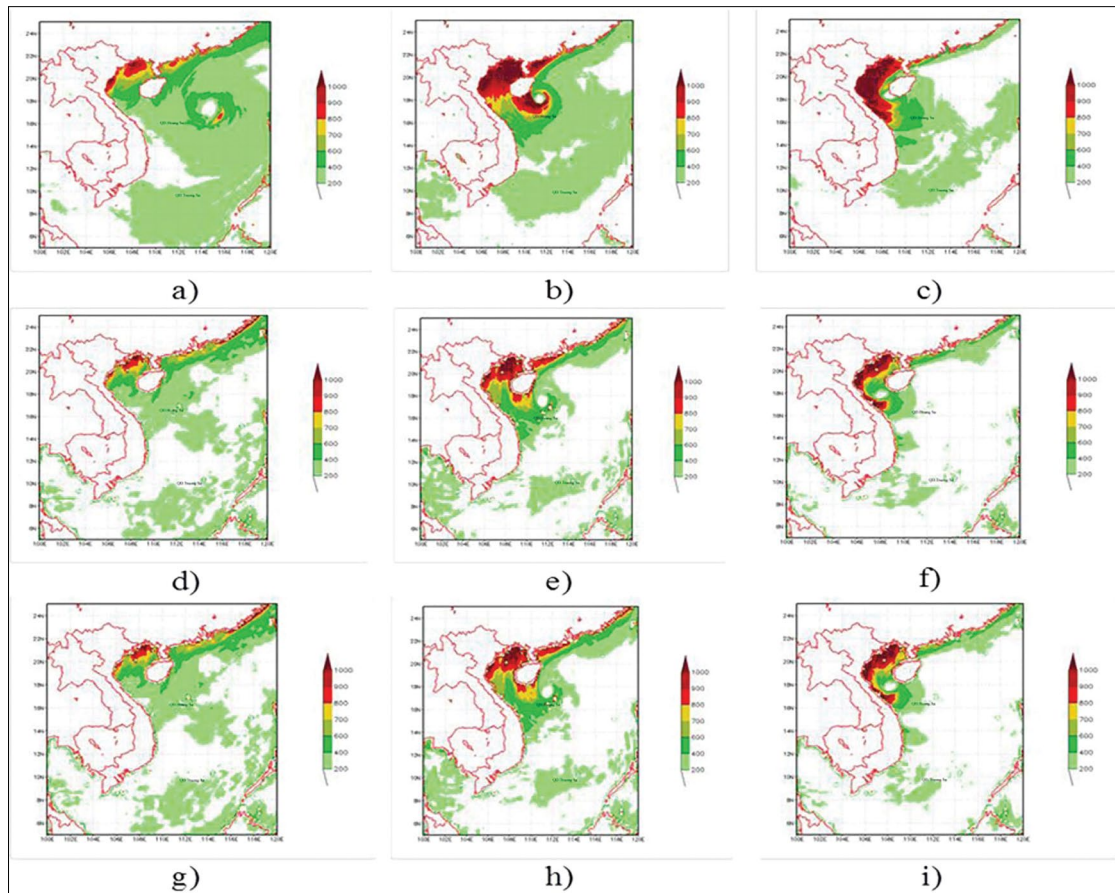


Figure 8. The simulated latent heat flux (Wm^{-2}) after 24 hr (a, d, g), 48 hr (b, e, h) and 72 hr (c, f, i) from 00 Z on July 30, 2013 for: GFS (a,b,c) case; SSTVT (d, e, f) and SSTUP (g, h, i) case

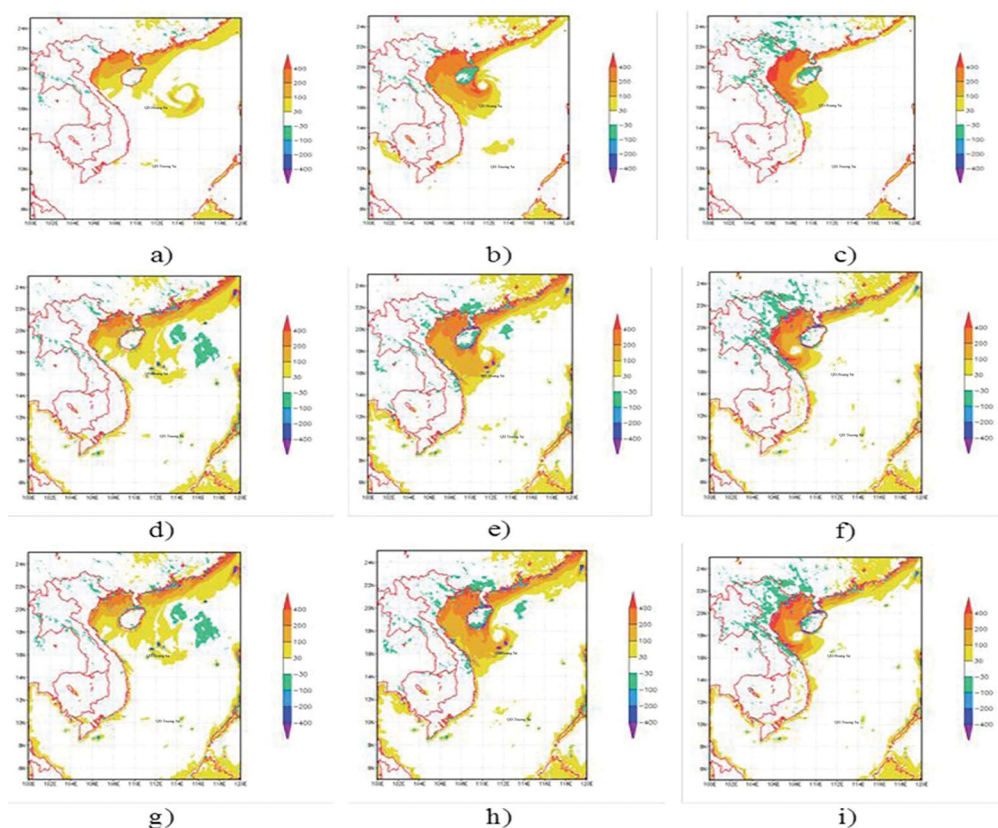


Figure 9. The simulated sensible heat flux (Wm^{-2}) after 24 hr (a, d), 48 hr (b, e) and 72 hr (c, f) from 00 Z on July 30, 2013 for: GFS (a,b,c); SSTVT (d, e, f) and SSTUP (g, h, i) cases

Figure 10 shows the simulated sea level pressure and the wind velocity at 10 m after 24 hr (a, d, g), 48 hr (b, e, h) and 72 hr (c, f, i) from 00 Z on October 2, 2011 for GFS (a, b, c); SSTVT (d, e, f) and SSTUP (g, h, i) cases. The simulated sea level pressures and the wind velocities at 10 m for GFS demonstrate the intensity of Nalgae typhoon is strengthened from 24 hr to 48 hr simulations and significantly decreases at 72 hr simulation (Figures 10 a, b, c). On the Figures 10 d, e, f and g, h, i show the intensity of Nalgae typhoon slight increases from 24 hr to 48 hr simulations and significantly decreases at 72 hr simulation. Figure 10 also shows the simulated sea level pressures increases and the wind velocities at 10 m relatively decreases in both area and magnitude in SSTVT than in GFS. Location of the simulated typhoon centre in SSTVT is slightly shifted toward southwestern when compared to GFS during 72 hr simulation. The

updating of the MW_IR OI SST data makes the cooling of the SST field at active area of the typhoon which leads to decreasing the latent heat flux and the sensible heat flux, therefore, decreases in the intensity and changes in the location of the simulated Nalgae typhoon compared to GFS. Figures 10 also shows there are not much difference in area of the simulated sea level pressures and the wind velocities at 10m between SSTVT and SSTUP cases. However, magnitude of the simulated sea level pressures and the wind velocities at 10 m in SSTVT is slightly smaller than in SSTUP in the North enter of typhoon for 48 hr and 72 hr simulation.

Figure 11 shows the time series of intensity a) Pmin; b) Vmax for Nalgae typhoon simulated from 00 Z on October 2, 2011 by GFS, SSTVT and SSTUP cases and observed by IBTrACS. The Pmin and Vmax are overestimated the IBTrACS observation for three cases, especially after 30

hr simulation. However, SSTVT and SSTUP show significant improvement in Pmin and Vmax simulation when compared to GFS. The Vmax in SSVT is difference upto 3m/s when compared to SSTUP case. However, the Pmin is not much difference between the SSTVT and SSTUP.

Figure 12 shows the observed IBTrACS best track and simulated tracks for Nalgae typhoon

from 00 Z on October 2, 2011 by SSTVT and SSTUP. Accordingly, the simulated track for GFS shifts south-eastward when compared to Best Track. However, the simulated tracks for SSTVT and SSTUP cases slightly shift south-westward when compared to Best Track. The distance error in GFS is significant smaller than the SSTVT and SSTUP cases (Figure 13).

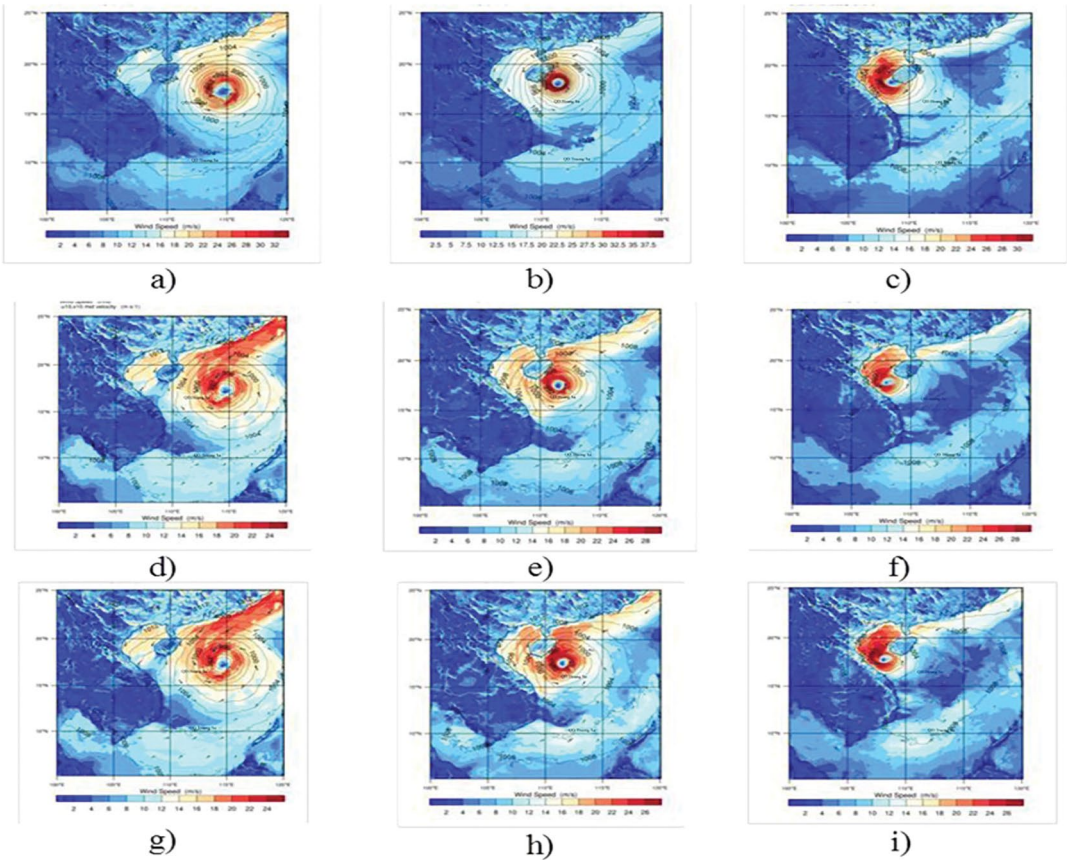


Figure 10. The simulated sea level pressure and the wind velocity at 10 m of Nalgae typhoon after 24 hr (a, d, g), 48 hr (b, e, h) and 72 hr (c, f, i) from 00 Z on October 2, 2011 for: GFS (a, b, c); SSTVT (d, e, f) and SSTUP (g, h, i) cases

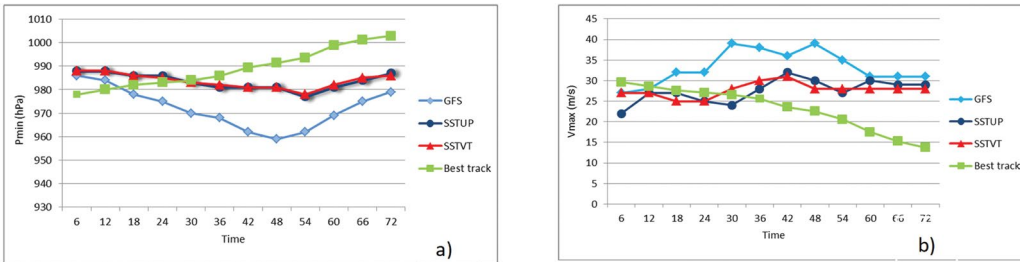


Figure 11. The time series of intensity: a) Pmin; b) Vmax for Nalgae typhoon simulated from 00 Z on October 2, 2011 by GFS, SSTVT and SSTUP cases and observed by IBTrACS (Best Track)

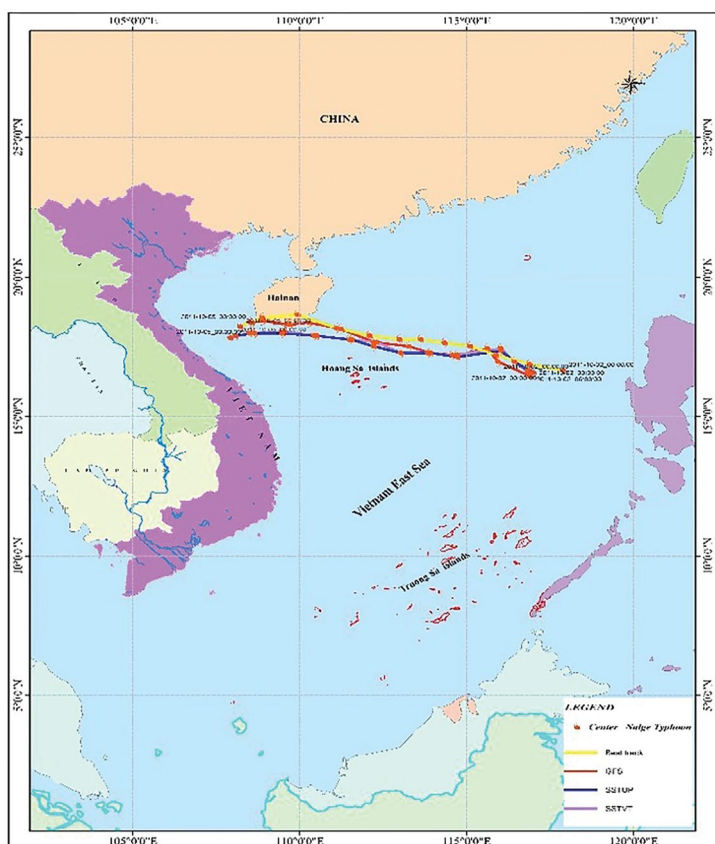


Figure 12. The simulated tracks for Nalgae typhoon from 00 Z on October 2, 2011 by GFS; SSTVT and SSTUP and the observed IBTrACS best track

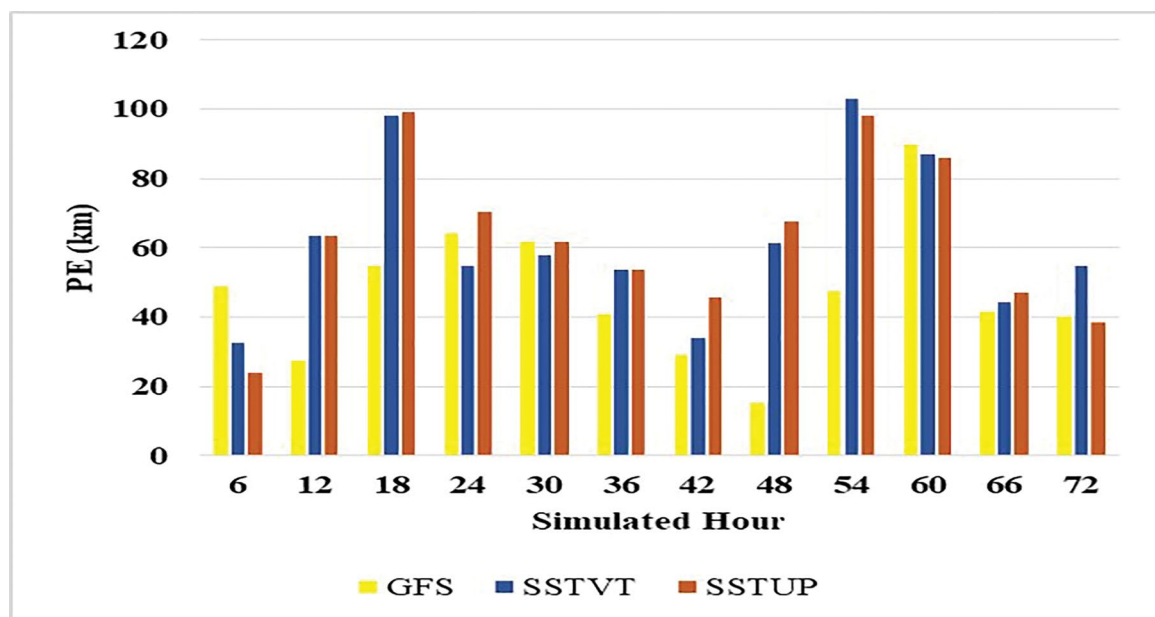


Figure 13. The distance errors (PE) for Nalgae typhoon simulated from October 2, 2011 by GFS; SSTVT and SSTUP cases

4. Conclusion

The present study investigated the effect of SST from satellite data with high resolution of space on intensity and track simulation of typhoon Nalgae (2011). The results demonstrate that the using of SST from satellite data with high horizontal resolution (9x9 km) for both only initial condition case and initial and boundary conditions case plays an important

role to improve the 72 hr simulated intensity of typhoon due to improved simulation of latent heat and heat fluxes. The updating of SST for initial and boundary conditions case is not much difference when compared to only initial condition case. The results also show the using of SST from satellite data does not improve the simulated track of typhoon. The further research is required for more reasonable explanations.

References

1. Bright, R.J, Xie, L. and Pietrafesa, L.J. (2002), *Evidence of the Gulf Stream's influence on TC intensity*, Geophysical Research Letters, 29, 1801.
2. Chang and Madala, R. V. (1980), *Numerical simulation of the influence of sea surface temperature on translating tropical cyclones*. *J. Atmos. Sci.*, 37, 2617–2630.
3. Chen F., Dudhia J. (2001), *Coupling an advanced land surface-hydrology model with the Penn State-NCAR MM5 modelling system*. Part I: Model implementation and sensitivity. *Mon. Weather Rev.*, 129 (4), 569-585.
4. Deepika Rai, S Pattnaik, P. V. Rajesh, and Vivekanand Hazra (2019), *Impact of high resolution SST on tropical cyclone characteristics over Bay of Bengal using model simulations*. *Royal Meteorological Society*, 26 (1), 130-139.
5. Emanuel, K. (2005), *Increasing destructiveness of tropical cyclones over the past 30 years*. *Nature*, 436, 686-688.
6. Hong, X, Chang, S.W, Raman, S, Shay, L.K. and Hodur, R. (2000), *The interaction between Hurricane Opal (1995) and a warm core ring in the Gulf of Mexico*. *Monthly Weather Review*, 128, 1347-1365.
7. Hong, Song–You, Yign Noh, Jimy Dudhia (2006), *A new vertical diffusion package with an explicit treatment of entrainment processes*. *Mon. Wea. Rev.*, 134, 2318-2341.
8. Iacono, M. J., J. S. Delamere, E. J. Mlawer, M. W. Shephard, S. A. Clough, and W. D. Collins (2008), *Radiative forcing by long-lived greenhouse gases: Calculations with the AER radiative transfer models*. *J. Geophys. Res.*, 113, D13103.
9. Jimenez, Pedro A., and Jimy Dudhia (2012), *Improving the representation of resolved and unresolved topographic effects on surface wind in the WRF model*. *J. Appl. Meteor. Climatol.*, 51, 300-316.
10. Kain, John S. (2004), *The Kain–Fritsch convective parameterization: An update*. *J. Appl. Meteor.*, 43, 170-181.
11. Mandal, M., Mohanty, U.C. MOHANTY, Sinha, P, Ali, M.M. (2007), *Impact of sea surface temperature in modulating movement and intensity of tropical cyclones*. *Natural Hazards*, 41, 413-427.
12. Miller B.I. (1958), *On the maximum intensity of hurricane*. *Journal of Meteorology*, 15, 184–185.
13. Palmén E.N. (1948), *On the formation and structure of the tropical hurricane*. *Geophysical*, 3, 26–38.
14. Shay, G, Goni, J. and Black, P.G. (2000), *Effects of a warm oceanic feature on Hurricane Opal*. *Monthly Weather Review*, 128, 1366–1383.
15. Shankar, D., Shetye, S.R., Joseph, P.V. (2007), *Link between convection and meridional gradient of sea surface temperature in the Bay of Bengal*. *Erth Sys Sci*, 116, 385–406.

16. Thompson, Gregory, Paul R. Field, Roy M. Rasmussen, William D. Hall (2008), *Explicit Forecasts of Winter Precipitation Using an Improved Bulk Microphysics Scheme. Part II: Implementation of a New Snow Parameterization*. *Mon. Wea. Rev.*, 136, 5095–5115.
17. Yun, K.S., Chan, J.C.L., Ha, K.J. (2012), *Effects of SST magnitude and gradient on typhoon tracks around East Asia: A case study for Typhoon Maemi (2003)*, *Atmos. Res.*, 109, 36–51.
18. Wu, L., Wang, B. and S. A. Braun (2005), *Impacts of air–sea interaction on tropical cyclone track and intensity*. *Mon. Wea. Rev.*, 133, 3299–3314.

ZONING AGRO-CLIMATIC FACTORS AND EVALUATING ADAPTATION ABILITY OF ARABICA COFFEE IN MUONG ANG DISTRICT, DIEN BIEN PROVINCE

Nguyen Ngoc Anh, Nguyen Huu Quyen, Tran Thi Tam, Duong Hai Yen, Duong Van Kham
Viet Nam Institutes of Meteorology Hydrology and Climate Change

Received: 5 January 2019; Accepted: 18 February 2019

Abstract: *Muong Ang is a mountainous district in the middle of Dien Bien province (the northwest of Viet Nam). Its climatic conditions are quite different compared to the surrounding areas. Specifically, mountainous terrain with a high slope and severe division leads to considerably differentiation in terms of meteorological and hydrological conditions. Muong Ang district is characterised by humid tropical monsoon climate; there are many extreme weather phenomena, e.g. heat wave, unevenly distributed large rainfall, diurnal temperature variation, large seasonal temperature variations. Besides, natural disasters occur quite frequently, such as erosion, landslides, floods and droughts [4]. However, the difference between agricultural meteorology and topography has created a unique landscape in Muong Ang, which is suitable for many kinds of tropical plants with high economic value. Typically, Arabica coffee can adapt very well to the climatic conditions in Muong Ang with high productivity and good quality, which is gradually forming the Muong Ang coffee brand in the domestic and international market.*

In order to confirm the correctness of selecting Arabica coffee to be the main crop in the economic development orientation of Muong Ang district, we need to study the agro-climatic conditions and the agro-climatic zoning of the district and assess the ecological adaptation ability of the coffee in the ecological conditions of Muong Ang, Dien Bien province.

Keywords: *Dien Bien, Arabica coffee, agro-climatic zoning, ecological adaptation, Arabica coffee, Viet Nam.*

1. Introduction

Climate is an irreplaceable component of the living environment. However, the climate is changing towards a detrimental tendency to human and many species. Researching and understanding climate conditions can make the climate invaluable to human life. In relation to agricultural and forestry, the climate is crucially important. Indeed, radiant energy, heat, and water are indispensable climatic factors in creating crop yields and yields. Therefore, the climate is seen as a kind of natural resources. The rational exploitation of climate resource not only provides high and

stable crop productivity but also contribute to protecting the ecological environment. In doing so, it is imperative to study the agro-climatic conditions and the agro-climatic zoning

Muong Ang is a mountainous district in the middle of Dien Bien province (the northwest of Vietnam). The district's climatic conditions are quite different compared to the surrounding areas. Specifically, mountainous terrain with a high slope and severe division leads to considerably differentiation in terms of meteorological and hydrological conditions. Muong Ang district is characterised by humid tropical monsoon climate; there are many extreme weather phenomena, e.g. heat wave, unevenly distributed large rainfall, diurnal

Corresponding author: Nguyen Ngoc Anh
E-mail: nguyenanh.imhen@gmail.com

temperature variation, large seasonal temperature variations. Besides, natural disasters occur quite frequently, such as erosion, landslides, floods and droughts. However, the difference between agricultural meteorology and topography has created a unique landscape in Muong Ang, which is suitable for many kinds of tropical plants with high economic value. Typically, Arabica coffee can adapt very well to the climatic conditions in Muong Ang with high productivity and good quality.

Arabica coffee originates from the highlands of southwestern Ethiopia [10]. It accounts for about 70% of worldwide coffee production. Arabica coffee's optimal temperature range is 18-21°C. It can tolerate mean annual temperatures up to roughly 24°C. The optimal elevation and rainfall for Arabica growth are respectively from 1,300-1,800m (metres above sea level) and from 1,500 to 2,500mm. Coffee can be grown on many different soil types, but the ideal is a fertile, volcanic red earth or a deep, sandy loam. Yellow-brown, high silt soils are less preferred. Avoid heavy clay or poor-draining soils. Coffee prefers a soil with pH of 5 to 6 [4].

In order to confirm the correctness of selecting Arabica coffee to be the main crop in the economic development orientation of Muong Ang district, we need to study the agro-climatic conditions and the agro-climatic zoning of the district and assess the ecological adaptation ability of the coffee in the ecological conditions of Muong Ang, Dien Bien province.

2. Research area

2.1. General geography conditions

The north of Muong Ang district shares the border with Tuan Giao district and part of Muong Cha district. The West is Dien Bien district. The South is Dien Bien Dong district. The East is Tuan Giao district and part of Thuan Chau district (Son La province). Latitude is from 21°24' N to 21°38' N; longitude is from 103°17' E to 103°24' E [10]. Muong Ang terrain is quite complex and divided by high mountain ranges, steep slopes (mostly limestone

mountains scattered throughout the area). Located between limestone mountains are narrow and flat valleys. There is not any big river in Muong Ang. Only 4 streams are running through the district, namely Nam Lan, Nam Lich, Nam Co and Nam Ang.

The district has 44,341.2 hectares of natural area and a population of 46,547 people. The rural population include 41,494 people (accounting for 89.1% of the total population of the district) and mainly ethnic minorities. Mostly ethnic minorities are Thai people (78.1%) and Hmong people (11.8%) [8]. The whole district has 9 communes, 1 town and 139 mountainous villages.

2.2. Agro-climatic characteristics in Muong Ang district

Lighting time

Lighting time is assessed through sunny hours. The total number of sunny hours in Muong Ang district is about 2000 hours. The highest number of sunny hours occurs from March to May (about 200 hours/month). The least sunny month is from June to August (130-140 hours/month) [8]. In general, the number of sunny hours in Muong Ang district is quite high compared to other areas in Dien Bien province and the surrounding areas. This condition favour plants that prefer light such as Arabica coffee.

Temperature

The temperature is crucial to the seasonal structure, the time to plant and harvest Arabica coffee. Monitoring data shows that the average annual temperature in Muong Ang district (collected in Tuan Giao station) is about 21.17°C, the coldest month is December (15.9°C), the warmest month is June and July (25.5-25.8°C). The average temperature in January, February, March, November and December is lower than the annual average temperature (21.7°C) [8]. The remaining months have average temperatures higher than the average annual temperature.

Diurnal temperature variation is considered as an important indicator for climate classification. It has a great impact on the growth of plants, especially on the process

of photosynthesis. Due to its location, located in the mainland, Muong Ang has a wide diurnal temperature variation (averaging about 10°C annually). In the winter (December-March), the diurnal temperature variation is quite dramatic (11-13°C). In summer (June - September), the diurnal temperature variation is about 10.3°C [8].

Absolute minimum temperature

During the winter months, due to the influence of the northeast monsoon, the weather is cold and dry. There often appears sudden weather changes after the cold frontier appearance, the average temperature decreases 3-4°C sometimes 5-6°C. The dry weather at the end of the dry season in the valleys reduces the humidity to below 30%. It is sunny during the light time but it is extremely cold at night time. The strong cooling of the ground facilitates the formation of radiation mist, sometimes frost, especially in the high mountains. Absolute minimum temperature year (-1.2°C) has a great impact on the distribution and growth of Arabica coffee [8].

Rainfall and humidity

The average annual rainfall for many years in Muong Ang district is about 2002mm. Rainfall is unevenly distributed over time and space. Normally, the main rainy season is from April to the end of September. The highest rainfall is distributed in 3 months: June, July and August. It can reach about 200-300mm/month, accounting for 75-92% of the annual rainfall. In the rainy season, the maximum daily rainfall reaches more than 100mm/day, even reaching over 400mm/day [8]. During this period, flooding occurs quite often in low-lying areas. On the sharp slopes of the mountain, it can occur landslides, flash floods, mud and rock floods which results in vegetation loss. The number of rainy days in rainy season is relatively high, about 20 days. The growth of Arabica coffee is badly affected when landslides, floods and flooding occur.

The dry season last for 5 months (November to March) with monthly rainfall under 50 mm/month. However, there are no drought months (rainfall <5 mm/month) [9]. This is a period of

shortage of water for coffee trees.

Average annual relative humidity in Muong Ang district is about 80-90%. It varies differently in terms of space and time. The lowest humid months are February and March (about 80%). The highest humid months are July and August (about 87-91%) [9].

2.3. Types of extreme weather

Heatwave (average daily temperature > 35°C)

The average number of hot and sunny days in the period 1962-2017 usually occurs from March to September. The peak months are April and May. Then the number of days slightly decreases from June to September. The highlands have a much higher number of hot and sunny days than the lowlands. The severity of heatwave in the period 1962-2017 (above 35, 37 and 39°C) tends to increase. The increase in the highlands much higher than that in the lowlands. The number of days with temperature above 35°C increased by 6.4 days/decade in the highlands while one in the lowlands did not increase significantly, only 1.4 days/decade. The number of days with temperature above 39°C has markedly fluctuated by years in the highlands, but the increase is negligible [9].

Extreme cold (average daily temperature ≤ 15°C) and damaging cold (average daily temperature ≤ 13°C)

The cold weather in the period of 1962-2017 usually occurs from November to March. The peak is usually in January and February. The difference between the highlands and lowlands is very small. The highlands appear to be cold more often than the lowlands (about 1 to 2 days). There is a huge fluctuation in the number of extreme cold and damaging cold days in the period 1962-2017. It can reach over 40 days of extreme cold in some years and be only 5 days in some other years. The average number of damaging cold days is about 5 days/year, and up to 12 days/year in some years. In general, extreme cold and damaging cold tend to decrease. However, the number of extreme cold days in the highlands tends to increase slightly, less than 1 day/decade.

Heavy rain (number of days with rainfall greater than 50 mm)

During the period of 1962-2017, heavy rain usually occurred from April to September, peaked in June-August. The lowland areas often have a larger number of rainy days than that in the highlands. The maximum daily rainfall is from 200 to 600mm, usually occurs from May to August (July is the largest value) [9]. The highlands have an average rainfall of 50-200mm. There is a large difference between locations regarding the number of heavy rainy days in the years: the highlands with 10 days, the lowlands with 16 days. In addition, there is a huge variation in extremely high rainfall between years, ranging from 100mm to 600mm [9]. The lowlands often have this value greater than that of the highlands. However, there is no significant difference in relation to extremely high rainfall in the year between high and low areas.

2.4. The other special weather phenomena

Foehn wind effect, fog, hoarfrost, thunderstorm and hail often occur in the district. They significantly affect the life and health of the people in Muong Ang.

Hail appears almost every year in Muong Ang during the end of winter and beginning of summer. It is 0.2-0.6 days occurs hail every year. Hail mainly appears from February to May. Hail damages the coffee gardens that causes broken branches, flowers and fruits, etc. and could completely destroy the crop. Hail is classified as a dangerous weather phenomenon.

Fog often occurs in the district with uneven distribution depending on the local terrain characteristics. The number of foggy days is about 90 days per year and usually occurs during the winter months, especially in December, January and February. This is also a dangerous weather phenomenon because it can cause coffee plants to die.

Muong Ang often appears thunderstorms. Thunderstorms with strong winds often cause significant damage to local people. On average, there are 70-90 thunderstorms each year. Thunderstorms often appear in April - August with about 6-15 days/month

[9]. The thunderstorms here are not serious but can be accompanied by strong winds and hail during the transition period from spring to summer.

It is quite common for the phenomenon of foehn winds. In the lowlands (<500m), there are about 5-30 days of foehn winds per year. The higher it is, the fewer the number of hot and dry days. Hot and dry weather often occurs in the period of February to September, mostly in April and May [9].

3. Data and research methods

3.1. Data

Meteorological data

Meteorological data in Muong Ang district and surrounding areas were collected at 6 meteorological stations including Dien Bien, Tuan Giao, Pha Din, Son La, Song Ma and Lai Chau in the period 1961-2017. The representative data was collected at Tuan Giao station due to the fact that this station shares similar natural conditions to Muong Ang district. The data system is summarized in Table 1 and Figure 1.

Remote sensing data

Muong Ang is one of the mountainous districts of Dien Bien Province. Its terrain characteristics reflect a complex division. A high slope and severe division lead to considerably differentiation in terms of meteorological and hydrological conditions. Therefore, in order to increase the objectivity and scientific foundation for analysis, it needs to supplement the temperature and humidity data interpolated from MODIS and NOAA satellite images in the period of 2000-2018. In addition, data and trends of temperature, precipitation, humidity and atmospheric pressure in the different areas of Muong Ang can be accessed through the website [10].

Survey data on the current state of agricultural production

Field survey to collect documents and data related to agricultural production includes seasonal structure, cultivated area, productivity, output, land use map, soil distribution map, the status quo of natural disasters and epidemics in

Muong Ang district. These documents and data are then used for the assessing and classifying agro-climatic zones in Muong Ang district.

Other data

Documents for establishing single maps,

maps of agro-climatic zones we collected from the national database provided by the Ministry of Natural Resources and Environment - the maps detailed at commune levels with the scale of 1: 25,000.

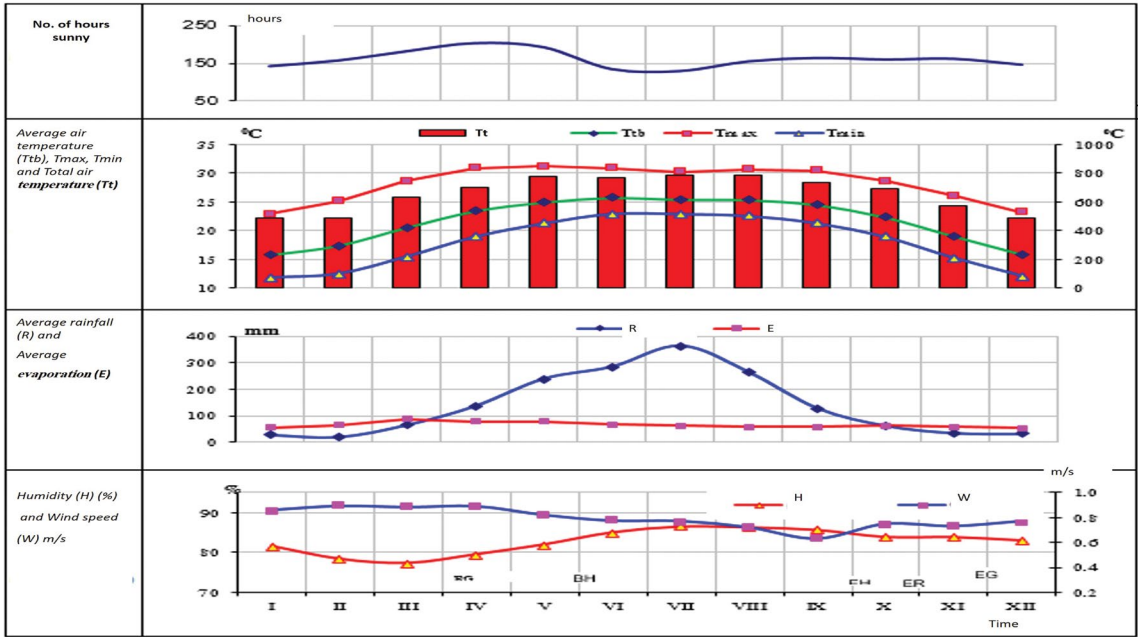


Figure 1. Climate condition graphs of Muong Ang district at Tuan Chau station, 2017.

Table 1. Meteorology climate data in Muong Ang district

Climate factor	Months												Year
	I	II	III	IV	V	VI	VII	VIII	IX	X	XI	XII	
Average temperature	15.7	17.4	20.5	23.4	25.0	25.8	25.5	25.4	24.5	22.4	19.1	15.9	21.7
Temperature range	11.1	12.7	13.2	12.0	9.9	7.9	7.3	8.1	9.1	9.8	10.8	11.1	10.3
Lowest temperature	10	12	14	18	19	22	22	22	20	17	14	10	10
Number of cold days	4.4	2.7	0.4	0.1	0.0	0.0	0.0	0.0	0.0	0.0	0.6	4.4	1.1
Number of sunny hours	141.2	156.8	182.1	204.5	193.6	133.4	127.8	154.3	163.8	159.5	161.5	145.3	1923.8
Average rainfall	29.4	21.3	66.4	137.5	239.6	285.0	363.1	263.0	128.5	63.1	36.0	33.1	138.8
Number of rainy days	18.0	4.5	4.1	7.0	12.6	17.8	21.5	23.8	20.5	13.2	7.7	5.4	-
Relative humidity	82	78	77	80	82	85	87	86	86	84	84	83	83

Source [9]

3.2. Research Methods

3.2.1. Calculating values

The degree of change:

Determining the average value $(\bar{x}), \bar{x} = \frac{1}{n} \sum_{i=1}^n x_i$

Determining the maximum value (Max and Min) by filtering $Max_{xt} = Max(x_1, x_2, \dots, x_n)$; $Min_{xt} = Min(x_1, x_2, \dots, x_n)$; In which t is the time series ($t = 1, 2, \dots, n-1, n$); x_t is a series of data observed over time ($x_t = x_1, x_2, \dots, x_{n-1}, x_n$).

The trend of change

The tendency of changes in past climate factors is often assessed by identifying (a) in the regression line equation:

$X = a_0 + a_1 t$. In which, X is calculated from the series of observational data over time (x_t); t is the time series (can be month, year, decade, etc.), a_0 is the cutting coefficient, a_1 is the corner coefficient. If $a_1 > 0$, the tendency is to increase, if $a_1 < 0$ then the tendency is to decrease.

Revising the reliability of the correlation coefficient

The correlation coefficients is often used in climate research to provide objective conclusions regarding the correlation relationship between variables provided the following formula to revise the reliability of the correlation coefficient [5]:

$$-t_{\frac{\alpha}{2}, n-1} S_r < r_k < t_{\frac{\alpha}{2}, n-1} S_r$$

$$\text{with } S_r = \frac{1}{\sqrt{n}} - t$$

r_k is the correlation coefficient between two chains; S_r is the standard error of the autocorrelation coefficients r_k ; α is the value in the object distribution with $n-1$ degrees of freedom. In climate research, normally α is 0.01 or 0.05 [7].

Interpolation of temperature and rainfall distribution

Based on the average monthly air temperature data in the period 2001-2017 collected at 6 meteorological stations (T_{obs}) and the surface coating temperature value (LST) were analyzed by image data (MOD11A2),

which were set up at the same time and same location. The relationship between T_{obs} and LST with sample size $n = 72$ (12 months \times 6 stations) is used to interpolate the temperature distribution for Muong Ang district and surrounding areas..

Similarly, the total annual rainfall is interpolated. Used data includes the average monthly rainfall value collected 6 stations (R_{obs}) in the period 1981-2017 and the rainfall from the CHIRPS data set (R_{Chirps}).

3.2.2. Method of classifying agro-climatic zones

The agro-climatic zones of Muong Ang district were classified in 5 steps:

Step 1: Determining the partition criteria. The total annual heat index indicates the degree of tolerance of the climate to plants. It also reflects the annual temperature range and related natural disasters (e.g. heat wave, extreme cold). Normally, the total annual temperature is usually proportional to the average seasonal temperature and the number of warm and sunny days while it is inversely proportional to the number of cold days.

Step 2: Determining boundaries between the zones based on the isothermal lines 8500°C (D.V. Kham et al. 2012). The areas with total temperature higher than 8500°C and average elevation under 100m are called 'lowlands'. The areas with total temperature lower than 8500°C and average elevation higher 100m are called 'highlands'. The terms 'low and highlands' are often used by local people. Determining the boundary between sub-zones based on the 2000mm isometric line with the distance between the isosceles lines is 500mm [7].

Step 3: Overlay the maps. The thematic maps (precipitation, temperature, topography, slope, traffic, waterways and administrative boundaries at commune level) are overlapped using GIS technology. The map of agro-climatic zones was established are in lines with the VN2000 reference system, the international UTM projection grid, Ellipsoid WGS84 adapted to Viet Nam [2]. The map was established at the scale 1:50,000.

Step 4: Designing map legend.

Step 5: Edit and finalize the map consulting experts and local officials [1],[7].

3.2.3. Evaluating cultivation potential in agro-climatic zones and sub-zones

The evaluation was based on the instruction of FAO's soil assessment which is coded in the LUSSET model [1],[7]. The model consists of two modules: module 1 is for inputting data related to the plants and soil; module 2 is for processing and outputting data.

Using GIS technology to divide Muong district into land units (LU) with a resolution of 100x100m resulting 44,515 LU. In order to assess the relevance of each LU

regarding the needs of different crops, the information in each identified LU must reflect similar information to the needs of the crops. Climate data including average monthly temperature and monthly rainfall are interpolated for each LU. Slope data is calculated from topographic maps (DEM). Soil data is determined from the soil map and encoded according to the unit system required by the LUSSET model. The identified soil characteristics referencing to ecological requirements of arabica were interpolated for determining suitable areas for Arabica. The outputs of the LUSSET model are integrated with the agro-climatic zones map (Figure 2).

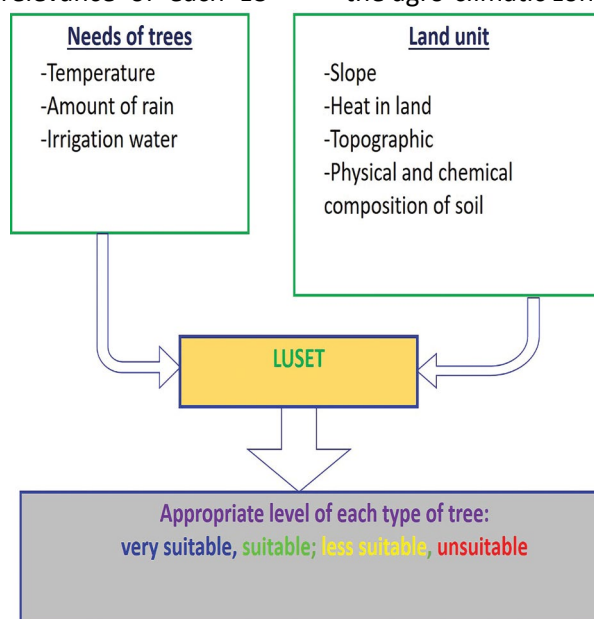


Figure 2. Process of determining the cultivate potential in agro climatic sub-zones, Source [1, 2]

Selecting a calculation method

Select a calculation method

Based on the needs of the crop and the factors related to soil, temperature, and water resources in each LU, the LUSSET model can calculate the suitability (OVS) for each element and integrated elements into index synthesized OVS through 4 methods: Minimum, Maximum, Average and Redundant so that users can choose an appropriate method depending on the purpose of use. Natural disasters often occur in Muong Ang, e.g., heavy rain, flooding, heat wave, droughts, cold and extremely cold

weather. In addition, agricultural production has not been developed. Most of the cultivated area strongly depends on rain. Therefore, the method selected is "Minimum". This is the assessment method with the highest safety level among the four methods. Appropriate index is defined as the lowest score of all factors considered. OVS is calculated according to the formula:

$$OVS = \text{Min} (SF1, SF2, SF3, \dots SFn).$$
 In which: OVS is the appropriate value; SF1, SF2, SF3, ... SFn is the appropriate score (ranging from 0 to 100) of the n selected elements.

The calculation of OVS index is done in 2

steps.

Step 1: Calculating OVS separately for each element (OVSg), OVSg can be soil (slope, soil depth, soil type), temperature (average temperature per month) or water (monthly rainfall, assumed irrigation or not).

$OVSg = f(S1, S2, \dots, Sn).$

S1, S2, ... Sn are the appropriate score of elements in a group; f is a function to calculate the overall suitability (Min function).

Step 2: Calculating the overall fit from three groups of factors (soil, temperature, water).

$OVS = f(Ss, Sh, Sw).$ In which: Ss, Sh, Sw are

OVSg values corresponding to soil, temperature and water element.

The scores and weights in calculating OVS index:

Due to the different ecological characteristics of each crop, the role of each element in the crop is different. Therefore, determining the appropriate score for an element is divided according to the weights from 1 to 3 (1 is the most important, then 2 and 3). This study uses FAO weighting sets [1]. The score for the 4 appropriate levels corresponds to the three weights shown in Table 2.

Table 2. Appropriate levels corresponding to the weight factors [7]

Suitability levels	weight number = 1	weight number = 2	weight number = 3
S1	85	95	100
S2	60	65	70
S3	40	45	50
S4	0	10	15

Combining the appropriate elements and weighting factors to create a value that ranges from 0 to 100. This value is the OVS score of the elements considered for a

particular crop in a LU. Using the minimum method to determine an overall suitable value and then to classify the suitability levels from S1, S2, S3 to N (Table 3).

Table 3. Classification of overall suitability [7]

No	Score	Suitability levels	Legend
1	≥ 85	S1	Very suitable
2	≥ 60 and < 85	S2	Suitable
3	≥ 40 and < 60	S3	Less suitable
4	< 40	N	Not suitable

Calculating the cultivation potential area in the zone and sub-zones: Based on the adaptive conditions of Arabica coffee, the map ecological adaptive ability was built.

Applying GIS technology with Krigging method - distance inversion algorithm (IDW) in spatial interpolation and overlaying information level to establish thematic maps.

4. Results

4.1. Classifying agro-climatic zones in Muong Ang

The climate and agro-climatic climate are decisive in forming agricultural production areas. Therefore, classifying agro-climatic zone

is a scientific basis for rational distribution of crop structure. It helps to classify agro-climatic zones and sub-zones based on climatic features and the conditions of agricultural production. The map of agro-climatic zones is the scientific basis for many purposes. For example, planning agricultural and forestry production; assessing the adaptation of crops in general and Arabica coffee in particular; assessing water resources; assessing the impact of climate change on people's lives and production; helping people identify appropriate cultivation measures; calculating potential yield of crops in regions and sub-regions; determining the structure of crops.

4.1.1. Identifying agro-climatic sub-zones in Muong Ang district

- *Criterion 1:* The first indicator to delineate the agro-climatic sub-regions is the total annual temperature. The total amount of temperature in a year is directly related to the annual average temperature and somehow related to the annual variation of temperature. The annual variation of temperature indicates the thermal season, the growing season of plants. This is the foundation for determining planting/harvesting seasons.

- *Criterion 2:* Total annual rainfall is important to the growth of crops, especially Arabica coffee in Muong Ang where the irrigation water depends mainly on rainwater. This indicator is used to assess the available water supply for agricultural production and then for selecting rational crops structure and proposing appropriate irrigation solutions.

- *Criterion 3:* Temperature decreases with increase in altitude.

- *Criteria 4:* the reduction of rainfall according to the terrain, wind direction, air masses with high moisture content.

Synthesizing the above criteria to classify agro-climatic zones. The results are presented as follows:

- Thermal background of the district is divided into 4 thermal zones as shown in Figure 3:

+ Zone T1 (elevation above 1,500m): Total annual temperature is below 7,000°C, the annual average temperature is below 20°C. This region is located in the northwest of Muong Dang commune, east of Xuan Lao commune, south of Cang Cang commune and Nam Lich.

+ Zone T2 (800-1,500m): Total annual temperature is from 7,000-7,500°C, annual average temperature is from 20- 21°C. This area is mainly concentrated in the northern edge, west and south of the district.

+ Zone T3 (600-800m): Total annual temperature is from 7,500-8,000°C, the annual average temperature is from 21-22°C. This region accounts for the largest portion and is distributed in most communes in the district.

+ Zone T4 (lowlands, valleys along rivers and streams, altitudes from 400-600m): Total annual temperature is from 8,000-8,500°C, the annual average temperature is over 22°C. This area is distributed along the valley of rivers and streams in Ang To, Bung Lao, Xuan Lao and Muong Lan communes.

- The number of sunny days in the district is divided into 4 sub-regions on the map of Figure 4. The map shows that the number of sunny days (over 35°C) with the value over 15 (days) occupies a fairly wide range in the whole district. Overall, Muong Ang receives a large amount of heat, concentrating on the district centre. In the edge of the district, the number of sunny days gradually decreases. This is an important basis for the district to make appropriate crop structure choices.

- The number of cold days in the district is shown in figure 5 with 4 areas. The areas featuring the number of cold days at over 25 days include the highlands of Xuan Lao commune, south of Ang Cang commune, and west and northwest of Muong Dang commune. The remaining areas have a number of cold days less than 15 days.

- The humidity in Muong Ang is presented in Figure 6.

+ Zone R1: Total annual rainfall is over 2,000mm. This area is located in a mountainous area (>1,000m) in the northwest of Muong Dang commune. It is easy to happen flash floods when it has unusually heavy rain. This is a remote area for people to access and develop agriculture and forestry. Therefore, forest in this area is preserved quite well and it is difficult to grow Arabica coffee here.

+ Zone R2: Total annual rainfall from 1,900 to 2,000mm. This area is distributed in mountainous areas with an altitude of 800-1,000m, belonging to communes of Coong Cay, Muong Dang, Ang Nua, Ang Cang and Nam Lich.

+ Zone R3: Total annual rainfall from 1,800-1,900mm. This region is distributed in areas with elevations between 600-800m, belonging to communes in the central area to the west of the district.

+ Zone R4: Total annual rainfall is less than 1800 mm. This region is distributed in eastern communes of the district.

- The annual average number of heavy rainy days in the district is shown in Figure 7. Mostly areas of two communes of Cang Cang and Ang Nua belong to the region with few heavy rainy days (2-3 days). This is a positive indicator for the development of Muong Ang Arabica coffee. Through the map of Figure 7, it is found that the annual average number of heavy rainy days is concentrated in the edge of the district such as the easternmost area of Xuan Lao commune, southwest and south of Phung Cang commune, North and Northwest

of Muong Dang commune. The central part of the district has less rainy days than the outer border.

4.1.2. The map of agro-climatic zones

Most of the district's area is hilly and mountainous in different directions and with highly differentiated elevations. This is the reason why the district has many sub-zones (6 sub-zones) as shown in Figure 3. This map is the final result of the process of researching, analysing and evaluating climate conditions for the purpose of classifying agro-climatic zones of the district.

Temperature variation of the sub-zones is visualized in the diagram in Figure 3,4.

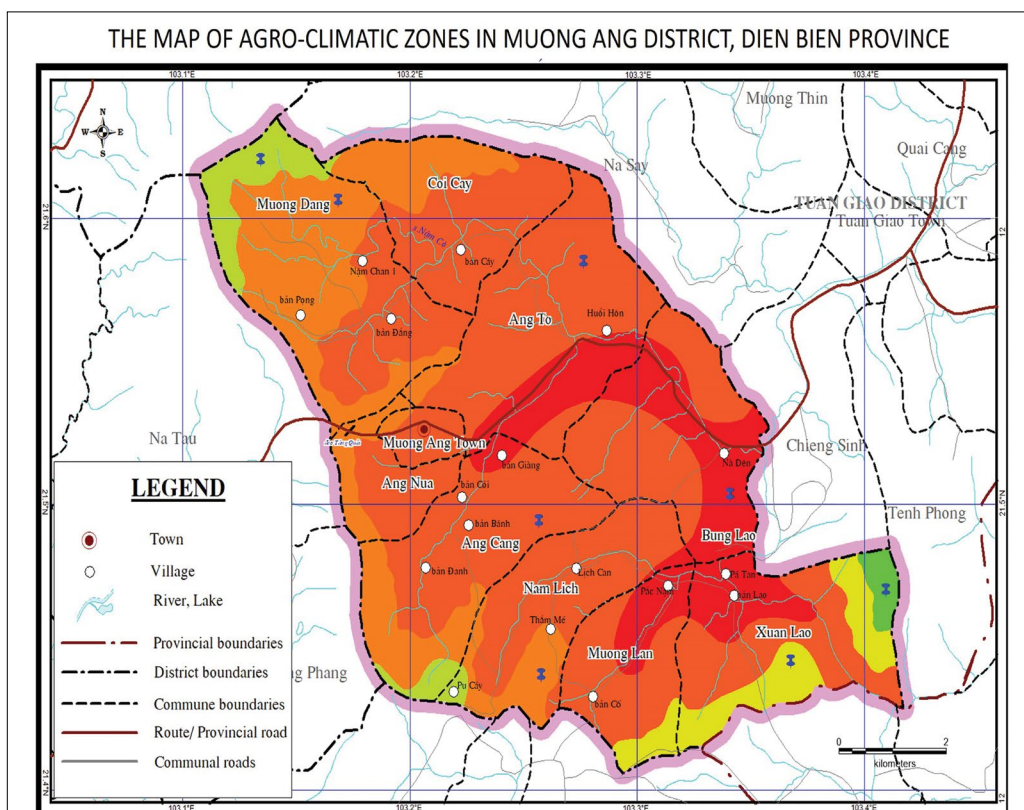


Figure 3. Map of Agro-climatic zoning

The diagram shows that the temperature in the sub-zones is quite consistent and in line with a rule. The sub-zones all reach their maximum temperature in June and minimum in December and January. The temperature differentiation is also consistent with the space distribution of the sub-zones. This explains the correctness of the analysis.

The rainfall of the sub-zones is also quite uniform. Rainfall is highest in July and gradually decreases in November, December, and January. Rainfall is minimum in February.

- Sub-zone 1: the total annual heat below 7,000°C, the annual average temperature is under 20°C; Total annual rainfall is from 1,800-1,900mm. The average number of hot and

sunny days ($T>35^{\circ}\text{C}$) is about 5days per year; the number of extremely cold days ($T<15^{\circ}\text{C}$) is about 45-60 days/year; the number of damaging cold days ($T\leq 13^{\circ}\text{C}$) is about 25-35 days/year; the number of days with heavy rain ($R>50\text{mm}$) is about 3-4 days/year. This sub-zone is distributed at the eastern edge of Xuan Lao commune.

- Sub-zone 2: The total annual heat, temperature and average number of hot sunny days are the same Sub-zone 1; The total annual rainfall is greater than or equal to 1,900mm. the number of extremely cold days is from 30-45 days/year; the number of damaging cold days is about 15-25days/year; the number of days with heavy rain is about 3-4 days/year. This sub-zone is distributed in the northwest of Muong Dang commune and a small part of the mountain area above 1500m in Ang Cang commune and Nam Lich.

- Sub-zone 3: The total annual temperature from $7,000-7,500^{\circ}\text{C}$, the annual average temperature of $20-21^{\circ}\text{C}$; Total annual rainfall is under 1,800mm. The average number of hot sunny days is similar Sub-zone 1. The number of extremely cold days is about 30–45 days/year; the number of damaging cold days is about 15-25days/year; the number of days with heavy rain is about 2-3 days/year. This sub-zone is mainly distributed in the highlands above 800m in Xuan Lao and Muong Lan communes.

- Sub-zone 4: This sub-zone is the same

Sub-zone 3 by heat, temperature, extremely cold days, damaging cold days and heavy rain day. There is a different at the total annual rainfall is from 1,900 to 2,000mm. The average number of hot and sunny days is about 5-10 days/year. This sub-zone is mainly distributed in areas with elevations below 1,000m in the northern edge, west and south of the district.

- Sub-zone 5: The total annual temperature from $7,500-8,000^{\circ}\text{C}$, the annual average temperature of $21-22^{\circ}\text{C}$; Total annual rainfall is from 1,800 to 1,900mm. The average number of hot and sunny days is 10-15 days/year; the number of extremely cold days is about 15-30 days/year; the number of damaging cold days is about 6-15 days/year; the number of days with heavy rain is about 1-2days/year. This sub-zone is mainly distributed in the area of 600-800m belonging to most communes in the district.

- Sub-zone 6: The total annual temperature higher than $8,000^{\circ}\text{C}$, the annual average temperature higher than 22°C . Total annual rainfall is less than 1,800mm. The average number of hot and sunny days is higher than 15 days/year; The number of extremely cold days, damaging cold days and heavy rain day are similar the sub-zine 5. This sub-zone is mainly distributed in areas with elevations below 600m and river valleys in Ang To, Bung Lao, Xuan Lao and Muong Lan communes.

Table 4. The legend for Agro-climatic zone







Region	Sub-region	Symbol	Total heat (oC)	Tavr (oC)	Total rainfall (mm)	Characteristics of adverse weather conditions
Highland	Sub-region 1		< 7000	< 20	1800 - 1900	Hot and sunny day (≥ 35 celsius) appears about 5 days/year for sub-region 1,2,3; 5-10 days/year for sub-region 4; 10-15 days/year for sub-region 5 and over 15 days/year for sub-region 6
	Sub-region 2				≥ 1900	
	Sub-region 3		7000 - 7500	20 - 21	< 1800	Strong cold day (≤ 15 celsius) appears about 60-80 days/year for sub-region 1; 45-60 days/year for sub-region 2; 30-45 days/year for sub-region 3,4 and 15-30 days/year for sub-region 5,6.
	Sub-region 4				1900 - 2000	
Lowland	Sub-region 5		7500 - 8000	21 - 22	1800 - 1900	Harmful cold day (≤ 13 celsius) appears about 35-50 days/year for sub-region 1; 25-35 days/year for sub-region 2; 15-25 days/year for sub-region 3,4 and 6-15 days/year for sub-region 5,6.
	Sub-region 6		> 8000	> 22	< 1800	Heavy rain day (≥ 50 mm) appears about 4-5 days/year for sub-region 1; 3-4 days/year for sub-region 2; 2-3 days/year for sub-region 3,4 and 1-2 days/year for sub-region 5,6.

Figure 1 is a line graph showing the monthly average temperature (t_C) for six different types of greenhouses (TV1 to TV6) from January (I) to December (XII). The temperatures generally follow a seasonal curve, peaking in June (VI) and reaching their lowest points in January (I) and December (XII). TV6 consistently has the highest temperatures, while TV1 has the lowest.

Tháng	TV1	TV2	TV3	TV4	TV5	TV6
I	13.5	14.5	15.5	16.0	17.0	17.5
II	14.5	15.5	16.5	17.0	18.0	19.0
III	16.5	17.5	18.5	19.0	20.0	21.5
IV	19.0	20.0	21.0	22.0	23.0	24.5
V	20.5	21.5	22.5	23.5	24.5	26.0
VI	21.0	22.0	23.0	24.0	25.0	26.5
VII	20.5	21.5	22.5	23.5	24.5	26.0
VIII	20.5	21.5	22.5	23.5	24.5	26.0
IX	20.0	21.0	22.0	23.0	24.0	25.0
X	18.5	19.5	20.5	21.5	22.5	23.5
XI	16.0	17.0	18.0	19.0	20.0	21.0
XII	13.5	14.5	15.5	16.0	17.0	17.5

Through the diagrams in Figures 1, 4, 5 and the map on Figure 3, the high compatibility between the partition results, the actual monitoring data at Tuan Giao station and the information extracted from the website.

ADAPTABILITY DISTRIBUTION OF THE MEDICINAL PLANT *PHYLLANTHUS NIRURI* IN MUONG ANG DISTRICT

LEGEND

- Town
- Village
- River, Lake
- Provincial boundaries
- District boundaries
- Communal boundaries
- Route/ Provincial road
- Communal road

SUITABILITY

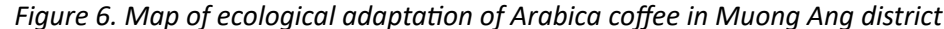
- Very suitable
- Suitable
- Less suitable
- unsuitable

Điển biến lượng mưa trong các tiểu vùng

Tháng	TV1	TV2	TV3	TV4	TV5	TV6
I	40	45	45	45	45	45
II	25	30	30	30	30	30
III	60	75	75	85	75	75
IV	130	160	160	170	160	160
V	210	280	280	300	280	280
VI	260	340	340	360	340	340
VII	340	450	450	470	450	450
VIII	300	380	380	400	380	380
IX	140	180	180	200	180	180
X	50	70	70	80	70	70
XI	40	45	45	45	45	45
XII	40	45	45	45	45	45

4.2. Classifying zones depending on ecological adaptation of Arabica coffee

Ecological and growth characteristics of Arabica coffee are analyzed carefully for interpolating ecological adaptation. The result is shown in Figure 6. The map shows that the coffee can adapt very well in sub-zones 4, 5 and 6. Sub-zones 1, 2 and 3 are not suitable for planting the coffee [4]. Based on the map, data on the area of adaptive levels can be extracted (Table 5 and Figure 7).



The area and productivity of Arabica coffee in Muong Ang are presented in Table 6.

In 2017, after applying the results of scientific research into the production process, the output of Arabica coffee in Muong Ang

increased significantly from 4,965 tons (in 2013) to 7,244.9 tons (in 2017). In the meanwhile, the area for planting decreased slightly. This confirms the effectiveness of agricultural development in the district.

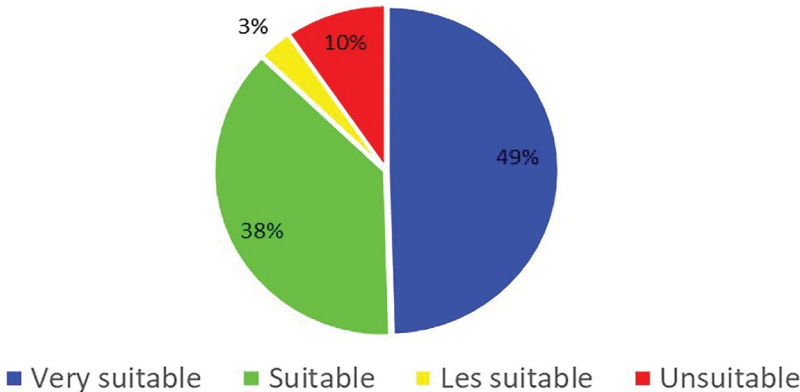


Figure 7. Structural levels of the ecological adaptation of Arabica coffee trees

Table 5. Soil structure by adaptive capacity of Arabica coffee

Levels	Area (ha)	Proportion (%)
Very suitable	21,955.77	49.52
Suitable	16,703.18	37.67
Moderate	1,416.44	3.19
Unsuitable	4,266.06	9.62

Table 6. Area and production of Arabica coffee in Muong Ang district [8]

Year	2013	2014	2015	2016	2017
Planting area (ha)	3,318.2	3,349	3,428	3,449.3	3,311
Area for harvesting (ha)	1,655	1,951	2,999	3,200	3,154.1
Coffee production (ton)	4,965	3,200	5,700	3,094	7,244.9

5. Conclusion and recommendations

The agro-climatic zone of the district is divided into 6 sub-zones based on the criteria of temperature, rainfall, humidity and algorithms and spatial interpolation methods. This research aims at serving the crop selection, planning and, most importantly, socio-economic development planning of Muong Ang district.

The communes selected for the pilot study include Ang Nua and Ang Cang. In which, Ang Nua commune is in sub-zones 4 and 5, Ang Cang commune is located in sub-zones 2, 4 and 5. The area of sub-zone 2 of Ang Cang commune

is quite small. Both communes share quite a similar agro-climatic condition.

Sub-zones 4 and 5 are the most beneficial for growing industrial crops and perennial crops, typical Arabica coffee, citrus fruit, longan, plum and cashew. Annual crops should be corn and peanuts. Rice is slightly adaptable.

Still there exist some shortages in this research:

+ Due to the fact that there is no monitoring station in Muong Ang district, the data for analysis is collected in a neighbouring station (Tuan Giao station) and interpolation data from satellite images and GIS. This affects

the accuracy of the results. However, the result is still acceptable.

+ When establishing ecological adaptation maps of some main trees, it lacks a number of soil criteria such as soil thickness, pH, chemical components in the soil. It is for the reason that there is no available data in the district. However, thanks to other criteria such as temperature, precipitation, humidity, experience and expert knowledge, the findings are highly reliable.

We have some recommendations as follows:

- It is imperative to build a monitoring

station in Muong Ang district. It can be located in Ang Nua commune or Yen Cang commune to monitor and provide data for the whole district serving researching, planning and for other research-related purposes.

- The district should establish a soil map system with a scale of 1: 50,000 or more detailed in order to identify accurately soil characteristics serving agricultural and forestry production.

- Expanding research areas for other communes regarding interdisciplinary development throughout the district.

References

1. Bernardi M., (2000), *Application software developed by FAO for management of soils and crops data*. Software for Agroclimate data management. USDA & WMO.
2. Huard F. and Perarnaud V., (2001), *Agrometeorological database management strategies and tools in France*. WMO & USDA.
3. Jagtap, Shrikant S., (2001), *Planning sustainable agriculture using agroclimatic database*. WMO - CAgM.
4. Mitchell, H. W. (1988), *Cultivation and Harvesting of the Arabica Coffee Tree*. Book.
5. Oldeman L.R., Frere.M (1998), *A study of the agroclimatology of the humid tropics of South East Asia*. FAO/UNESCO/WMO No.597, 230p.
6. Stigter C.J., Das H.P., J.J. Salinger. (2000), *Agrometeorological adaptation strategies to increasing climate variability and climate changes*. WMO-CagM.
7. CARE Viet Nam (2018), *Developing an agro-climatic zoning map in Muong Ang district - Dien Bien province*. PR1711_VNM257 ACIS.
8. Dien Bien's Statistics Department (2018), *Statistical Yearbook of Dien Bien Province*. Statistical Publishing House.
9. General Department of Meteorology and Hydrology (2017), *Set of meteorological and hydrological data*.
10. <https://www.climate.gov/news-features/climate-and/climate-coffee>.
11. <https://www.meteoblue.com>.
12. <http://www.dienbien.gov.vn>.



VIETNAM INSTITUTE OF METEOROLOGY, HYDROLOGY AND CLIMATE CHANGE

No.23 Lane 62 Nguyen Chi Thanh, Ha Noi, Viet Nam

Email: imhen@imh.ac.vn

Website: www.imh.ac.vn